Journal Pre-proofs

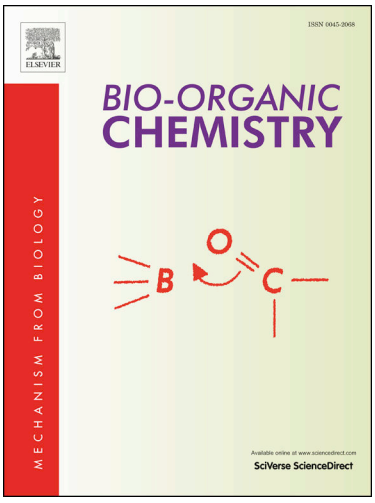

Structure-Based Design of Glycyrrhetinic Acid Derivatives as Potent Anti-Sepsis Agents Targeting High-Mobility Group Box-1

Yuanyuan Wang, Zongmin Yu, Hu Yuan, Hao Chen, Ning Xie, Zhibin Wang, Qingyan Sun, Weidong Zhang

PII: S0045-2068(20)31759-4
DOI: https://doi.org/10.1016/j.bioorg.2020.104461
Reference: YBIOO 104461

To appear in: *Bioorganic Chemistry*

Received Date: 28 April 2020
Revised Date: 15 October 2020
Accepted Date: 2 November 2020

Please cite this article as: Y. Wang, Z. Yu, H. Yuan, H. Chen, N. Xie, Z. Wang, Q. Sun, W. Zhang, Structure-Based Design of Glycyrrhetinic Acid Derivatives as Potent Anti-Sepsis Agents Targeting High-Mobility Group Box-1, *Bioorganic Chemistry* (2020), doi: https://doi.org/10.1016/j.bioorg.2020.104461

Structure-Based Design of Glycyrrhetinic Acid Derivatives as Potent Anti-Sepsis Agents Targeting High-Mobility Group Box-1

Yuanyuan Wang [a,†], Zongmin Yu [c,e,†], Hu Yuan [d], Hao Chen [c,d], Ning Xie [d], Zhibin Wang [c,*], Qingyan Sun [b,*], Weidong Zhang [a,b,c,*]

[a] Interdisciplinary Science Research Institute, Shanghai University of Traditional Chinese Medicine, Shanghai 201203, China.

[b] Shanghai Institute of Pharmaceutical Industry, Shanghai 200040, China.

[c] School of Pharmacy, Second Military Medical University, Shanghai 200433, China.

[d] State Key Laboratory of Innovative Natural Medicine and TCM Injections, Jiangxi 341000, China.

[e] Department of Medical Service Training Center, No.965 Hospital, Joint Logistics Support Force of PLA, Jilin 132011, China.

■ AUTHOR INFORMATION

Corresponding Author

* W.-D.Z. E-mail: wdzhangy@hotmail.com. Phone/Fax: +86-21-81871244.

Q.-Y.S. E-mail: sqy_2000@163.com. Phone/Fax: +86-21-20572000-2030.

Z.-B.W. E-mail: methyl@smmu.edu.cn. Phone/Fax: +86-21-81871213.

Author Contributions

† Y.-Y.W. and Z.-M.Y. contributed equally to this work.

Notes

The authors declare no competing financial interest.

Graphical abstract

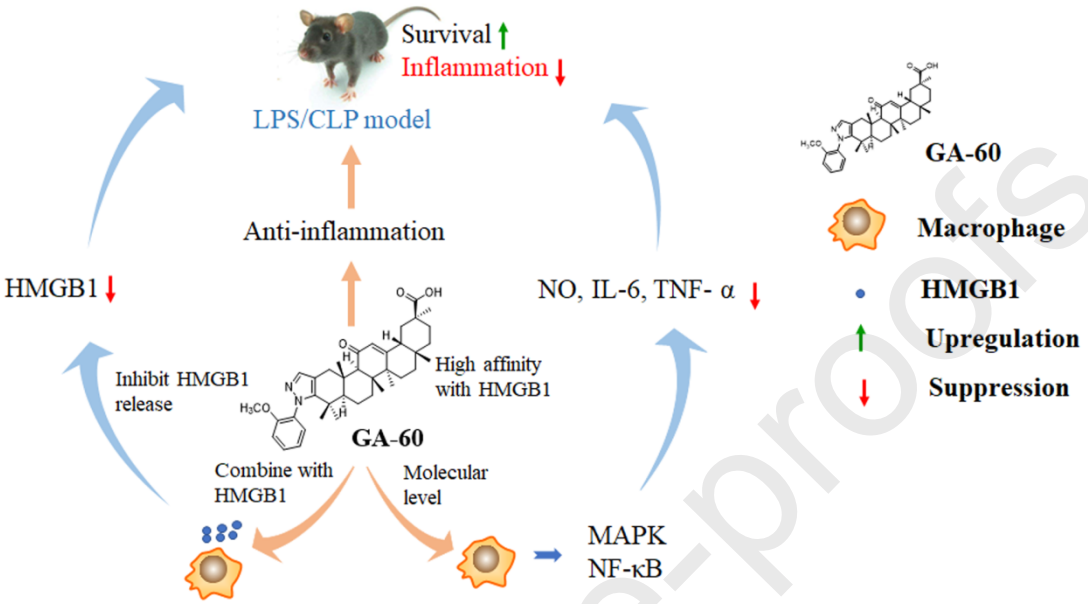

ABSTRACT

Novel Glycyrrhetinic Acid (GA) derivatives with fused heterocycles on A ring were structure-based designed and synthesized. Their potential anti-inflammatory effects were investigated by a classical LPS stimulated macrophage model. Surface plasmon resonance (SPR) was used to verify the binding of GA analogues with HMGB1. A preliminary structure-activity relationship was summarized and an analogue **GA-60** with *ortho*-methoxybenzyl pyrozole showed stronger anti-inflammatory effect and higher affinity for HMGB1 with a K_d value of 12.5 μM. In addition, this compound exhibited excellent inhibitory functions on NO (96%), TNF-α (94%), and IL-6 (100%), by interfering with phosphorylation of p38, ERK, JNK MAPKs, as well as that of NF-κB p65 and IKKα/β. Moreover, **GA-60** extended the survival of either the classic CLP-induced or LPS-induced sepsis mouse models. Molecular modeling predictions further supported these findings, clearly indicating that inhibiting HMGB1 release, using fused heterocyclic GA derivatives, is a promising strategy for treatment of sepsis.

Key words: Glycyrrhetinic Acid; HMGB1; Sepsis; Structure-Based Design, Inflammation

1. Introduction

Sepsis, defined as life-threatening organ dysfunction and caused by dysregulated host response to infection, is one of the most challenging medical conditions worldwide[1]. In 2017, sepsis was diagnosed in about 48.9 million people, ending with death in 11.0 million, accounting for 19.7% of the global mortality[2]. The dysregulated host response is caused by hyperinflammation response and immunosuppressive anti-inflammatory response. As a significant factor of immune imbalance, the hyperinflammatory response always runs through the development of sepsis. International guidelines for treatment of both sepsis and septic shock emphasize that antibiotics should be administered as soon as possible, preferably within one hour, following diagnosis[3].

However, sepsis patients did not benefit from anti-inflammatory therapy targeting early inflammatory factors, such as tumor necrosis factor-α (TNF-α), nitric oxide synthase inhibitor, Toll-like receptor-4 (TLR-4) antagonist, and Interleukin-1 (IL-1) receptor antagonist[4-7]. This is due to the characteristics of these early inflammatory factors, which result in failures. For instance, they reach peak levels within one to four hours, at the start of sepsis, and reverse to the near baseline in eight hours[8]. Treatment targeting these early inflammatory factors is also delayed due to hysteresis diagnoses.

High mobility group box protein 1 (HMGB1), previously described as a nuclear DNA-binding protein, was identified as a late inflammatory mediator of endotoxin lethality in mice in 1999[9]. Studies have demonstrated that HMGB1 levels are significantly elevated during late, compared to early phases of inflammatory cytokines,

like TNF-α and Interleukin-6 (IL-6), and peak plasma concentrations within 16 to 32 hours after sepsis onset. This is always the case whether in experimental sepsis animal models[9, 10] or in patients[11, 12]. In addition, circulating HMGB1 levels do not decline until a week after sepsis[12] and are, therefore, a late predictor of mortality in sepsis.[13, 14] HMGB1, like the activators of lipopolysaccharide (LPS), can also induce proinflammation cytokines to release TNF-α and IL-6 in human monocytes[15]. Massive accumulation of HMGB1, *in vivo,* have been implicated in amplification of the cytokine cascade, stimulation of inflammation eventually mediating injurious inflammatory responses[16]. Furthermore, anti-HMGB1 has been found to increase survival of sepsis even through delayed administration in LPS induced endotoxin[9]. Pre-clinically, administration of neutralizing anti-HMGB1 antibodies improves survival in murine endotoxemia or CLP induced sepsis model and relevant rat sepsis models[10, 17, 18]. Persistent elevation of HMGB1 in plasma provides a wide therapeutic window for development of clinical interventions and emerges as a therapeutic target for sepsis[16, 19].

Natural products play an important role in drug discovery, with nearly half of all new drugs introduced into the market over the past two decades developed from natural products or their derivatives[20-23]. Glycyrrhizic acid (GL), a triterpene glycoside derived from licorice root extracts, possesses a wide range of pharmacological, especially anti-inflammatory properties **(Figure 1**)[24]. Mollica and coworkers [25] were the first to report that GL directly bound (K_d = ~150 μM) and inhibited HMGB1, thus preventing its chemoattractant and mitogenic activities. However, *in silico* docking

studies revealed that the binding portion was represented by the glycyrrhetinic acid (GA) moiety (**Figure 1**), which seemed to interact with specific amino acid residues present in the hydrophobic, shallow pockets of HMGB1. Furthermore, Cavone and co-workers[26] reported that GA impaired antibody recognition of HMGB1, indicating that it directly binds to the protein. Meanwhile, Yamaguchi et al.[27] used the Molecular Operating Environment (MOE) software package to demonstrate that GA possibly inhibits HMGB1 function by non-covalently interfering with Lys90, Arg91, Ser101, Tyr149, Cys230 and Cys231 in the HMGB1-DNA complex. Collectively, these studies suggest that the GA moiety might be the pharmacophore for the inflammatory effects and therefore need to be elucidated.

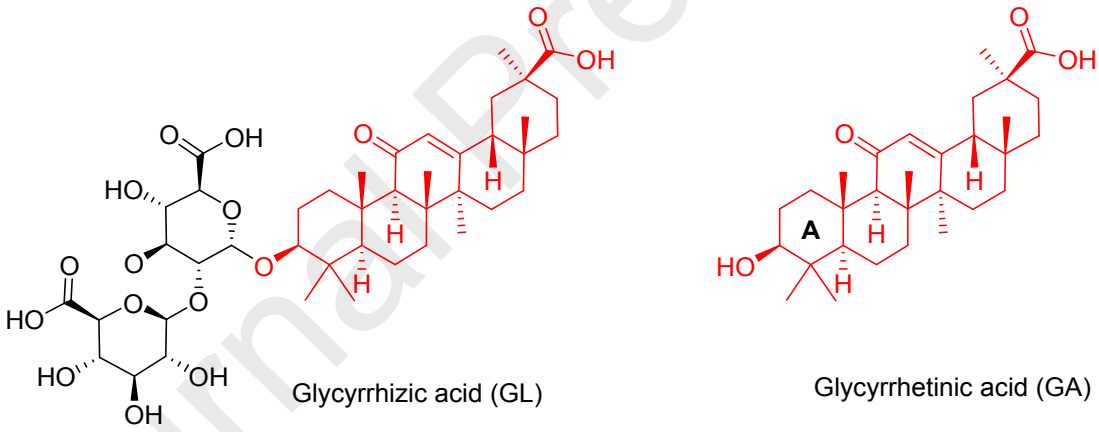

Figure 1. Chemical structures of **GL** and **GA**. The binding moiety with HMGB1 is highlighted in red.

In this article, GA was selected as the lead compound for structural optimization. Three series of analogues were synthesized by structure-based design and optimization on A ring of GA, with different fused heterocycles, including pyrazoles, indoles and isoxazoles. Among them, **GA-60** significantly prolong the survival time of LPS/CLP

induced sepsis mice *in vivo*, showing potential anti-sepsis efficacy. From our results, it is clearly evident that inhibition of HMGB1 release, using GA derivatives, is a promising strategy for treatment of sepsis.

2. Results

2.1 Design rationale

On the basis of reported binding mode of GA and HMGB1[25, 27, 28], the carbonyl group at the C-11 position of GA forms a stable hydrogen-bonding interaction with HMGB1, and the pentacyclic triterpene ring of GA establishes favorable van der Waals interactions with HMGB1. On the other hand, the glycoside moiety of GL does not bind directly to HMGB1[28], indicating the optimization potential of the hydroxyl group of A ring. It is also reported that some of the triterpenic acids with heterocyclic group attached to ring "A" of the steroidal and triterpenic acid skeleton exhibited potent anti-inflammatory activity[29, 30]. Therefore, we firstly positioned the modification strategy on the A ring of GA, based on the predicted binding complex, and performed modification of the fused heterocyclic rings in the derivatives (**Figure 2**).

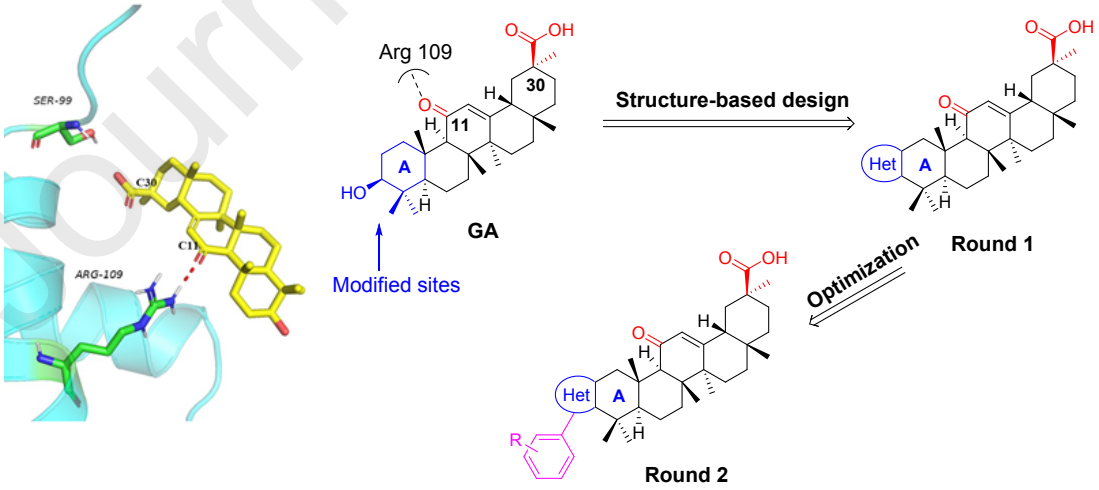

Figure 2. Design strategy of GA analogues.

2.2 Chemistry

All the target compounds were synthesized via the routes shown in **Schemes 1-3**. The key intermediate **GA-2** was produced by treating GA with methyl iodide and potassium carbonate in acetone to form compound **GA-1,** which was then oxidized with pyrindium chlorochromate (PCC) in dichloromethane. Further treatment with NaH (60%) and ethyl trifluoroacetate or ethyl formate converted **GA-2** into crucial intermediates **GA-3** or **GA-4** (**Scheme 1**).

As depicted in **Scheme 2**, compounds **GA-2**, **GA-3** and **GA-4** can further be synthesized into heterocyclic fused GA derivatives. To a solution of **GA-2** in acetic acid was added hydrazine hydrochloride with different N-phenyl substituents at 118 °C for 4 h. After cooling to room temperature, the solvents were removed and the residue was purified by a column chromatography to obtain indole heterocyclic fused GA derivatives (**GA-16~GA-19**). Heating **GA-3** or **GA-4** with hydrazine chloride (or hydrazine hydrochloride with different N-phenyl substituents) in EtOH at 85 °C for 3 h and purifying the mixture with a similar method as the indole heterocyclic fused GA derivatives yielded trifluoromethyl substituted pyrazole heterocyclic (**GA-8~GA-11**) or pyrazole heterocyclic fused GA derivatives (**GA-12~GA-15**). **GA-7** (isoxazole heterocycle fused GA derivatives) was synthesized by reacting **GA-4** with hydroxylamine hydrochloride in anhydrous pyridine. Heterocyclic fused GA derivatives were finally hydrolyzed by NaOH in MeOH to reveal C-30 carboxyl group (**Scheme 3**), affording **GA-20~GA-34**.

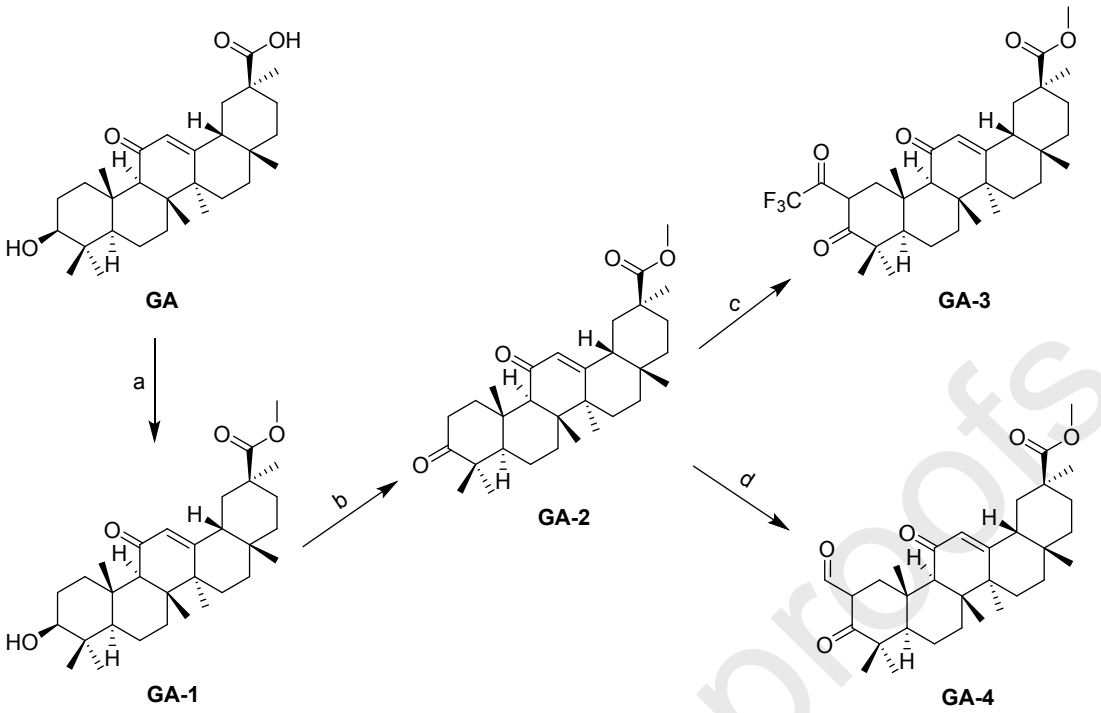

Scheme 1. Synthesis of important intermediates. Reagent and Conditions: (a) CH_3I, K_2CO_3, acetone, r.t., 12 h, 95%; (b) PCC, DCM, r.t., 4 h, 85%; (c) Ethyl trifluoroacetate, NaH, THF, r.t., 8 h, 70%; (d) Ethyl formate, NaH, THF, r.t., 8 h, 80%.

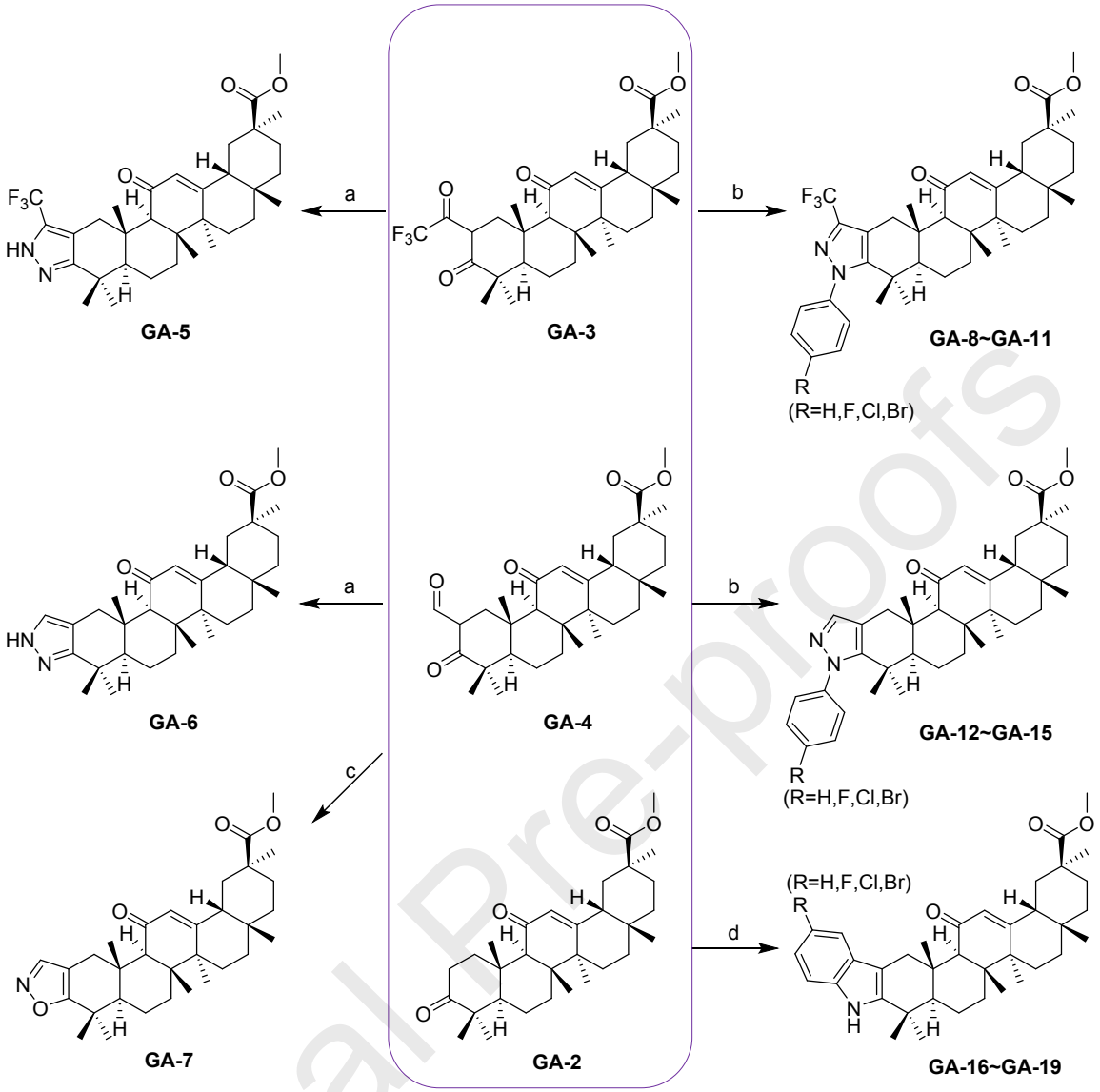

Scheme 2. Synthesis of heterocyclic intermediates. Reagent and Conditions: (a) $NH_2NH_2 \cdot 2HCl$, EtOH, reflux, 3 h, 75%; (b) p-$RPhNHNH_2 \cdot HCl$, EtOH, reflux, 4 h, 70%; (c) $NH_2OH \cdot HCl$, Pyridine, reflux, 5 h, 75%; (d) p-$RPhNHNH_2 \cdot HCl$, CH_3COOH, reflux, 4 h, 80%.

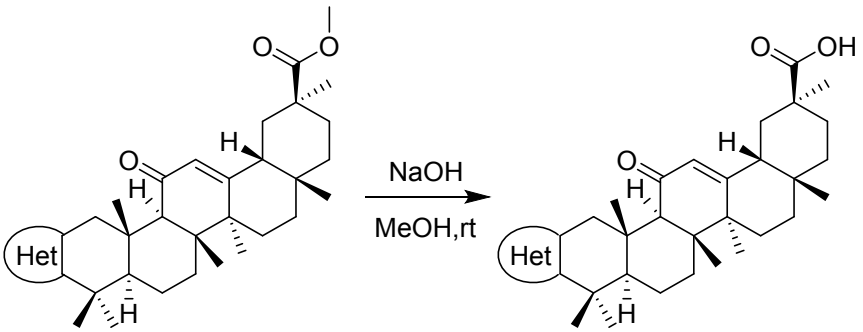

Scheme 3. General formula of hydrolysis reaction.

2.3 Fused hetercylces on ring A of GA exhibit enhanced anti-inflammatory effects

The production of pro-inflammatory cytokines, nitric oxide (NO) induced by LPS is the main cytotoxic and proapoptotic mechanisms[31]. The potential anti-inflammatory effects of GA derivates were evaluated by classical LPS stimulated macrophage model. In RAW264.7 cells, HMGB1 was found to increase at 6-8 hours, reaching the peak at 16-32 hours after LPS stimulation[9]. We choose to evaluate the NO inhibition at 24 hours after LPS stimulation through the Griess assay.

As shown in **Table 1**, GL with the glycoside moiety only had a 55% NO inhibitory activity at 10 μM. GA exhibited 96.9% inhibition of NO. Carbenoxolone (CBX), a commercially available analogue, with a modified hydoxyl group, still showed a 96.2% inhibition. Methyl esterification of the carbonyl group at the C-30 position (**GA-1**) resulted in a decrease in NO inhibition at the same concentration, thereby validating our design hypothesis. Then, as proposed, analogues with fused hetercycles, including pyrazole (**GA-21**), trifluoromethyl pyrazole (**GA-20**), isoxazole (**GA-22**), and indole (**GA-31**), on ring A of GA were synthesized. To our delight, they all exhibited ~100% NO inhibitory activity at 10 μM. Considering HMGB1 also stimulates early inflammatory factors as a late inflammatory cytokines[15], TNF-α and IL-6 inhibition

activities were evaluated by flow cytometry assay to further evaluate GA derivates' anti-inflammatory activities. However, none of the derivatives could inhibit their expressions at 10 μM, except the indole analogue **GA-31** for IL-6 (101% at 10 μM) (**Table 1**). In addition, their cytotoxicities were low (IC_{50} > 50 μM) except CBX.

Table 1. Structure optimization of GA

	Chemical Structure	Cytotoxicity (IC_{50}, μM) [a]	NO inhibition %[b]	TNF inhibition % [b]	IL-6 inhibition %[b]
GL	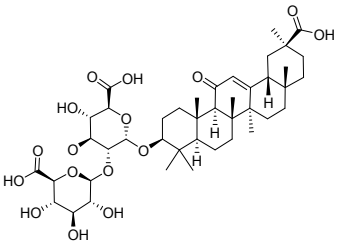	145.59±2.16	54.6%	0	0
GA	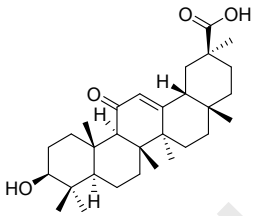	81.87±1.91	96.9%	0	0
CBX	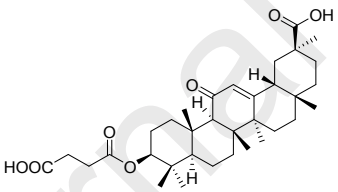	47.58±1.68	96.2%	0	0
GA-1	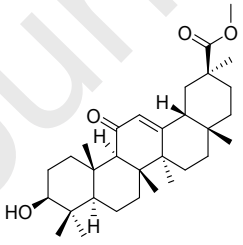	88.39±1.95	75.6%	0	0
GA-20	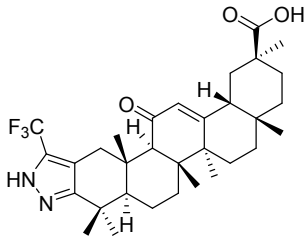	71.34±1.85	100.8%	0	0

GA-21	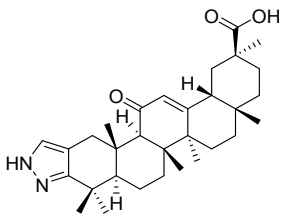	67.34±1.83	100.0%	0	0
GA-22	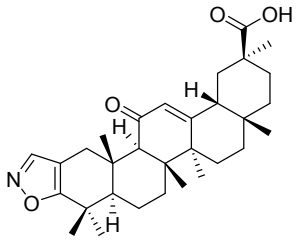	96.51±1.99	99.6%	0	0
GA-31	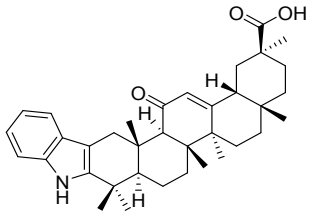	69.82±1.84	100.0%	0	101%

[a]IC_{50}=half maximal inhibitory concentration.
[b] Percent (%) Inhibition of Released Nitric Oxide (NO), Tumor Necrosis Factor (TNF-α), and Interleukin-6 (IL-6) upon treatment with Derivatives (10 μM).

2.4 Further optimizations lead to potent heterocyclic analogues with higher inhibition of NO, TNF-α and IL-6

Next, three hetercylic analogues with 100 % NO inhibition were further optimized except **GA-22** (99.6% NO inhibition). As shown in **Table 2**, introducing a benzyl group (**GA-23**) on the trifluoromethyl pyrazole ring retained the NO inhibition at 10 μM, while the cytotoxicity was slightly increased and still no TNF-α and IL-6 inhibition was observed. Halogenated compounds (fluoro, **GA-24**; chloro, **GA-25**; bromo, **GA-26**) showed no differences with regard to potency, while their cytotoxicities were increased. For the non-trifluoromethyl substituted pyrazole analogues, a totally different result was observed (**Table 3**). Compound **GA-27** with a benzyl ring had 95% NO inhibition and 100% TNF-α and IL-6 inhibition. The cytotoxicity was much higher, indicating an

IC_{50} of 29.29 μM. The *para*-substituted halogenated compounds (**GA-28**~**GA-30**) maintained the potency. Then, the fluoro, chloro, bromo groups were moved to *meta*-, *ortho*-positions of the benzyl rings. Compounds with bromine substitutions showed less potency toward TNF-α and IL-6. For fluorine-substituted (**GA-28**, **GA-52** and **GA-53**) and chlorine-substituted (**GA-29**, **GA-54** and **GA-55**) analogues, *ortho*-substituted compounds (**GA-53** and **GA-55**) showed the best activity in this series, but less activity toward TNF-α. A similar result was recorded for compounds with methoxyl (**GA-58**~**GA-60**) and trifluoromethyl (**GA-61**~**GA-63**) groups. They were less active toward TNF-α. In addition, methyl analogues (**GA-64**~**GA-66**) exhibited higher potency compared with other compounds toward TNF-α. Moreover, the *ortho*-methyl substituted compound (**GA-66**) showed higher TNF-α inhibitory activity (100%) than that of the *meta*-substituted (**GA-65**, 72%) and *para*-substituted analogue (**GA-64**, 56%). Introducing methylsulfonyl (**GA-67**) and sulfamide (**GA-68**) was unfavorable to the activity. We also introduced halogens to the indole compounds, and found that only the compound with a chloro group showed 72% inhibition of TNF-α (**Table 4**). Taken together, **GA-27**, **GA-53**, **GA-55**, **GA-60**, and **GA-66** with *ortho*-substitutions showed more than 90% inhibition of NO, TNF-α and IL-6, with acceptable cytotoxicities, and were selected for further evaluations.

Table 2 Structure optimization of GA-20

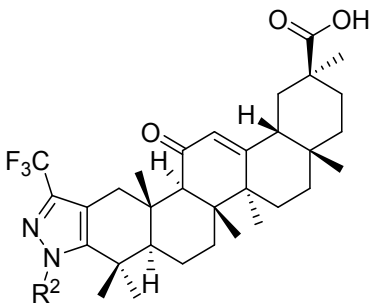

	R^2	Cytotoxicity (IC_{50}, μM) [a]	NO inhibition %[b]	TNF inhibition %[b]	IL-6 inhibition %[b]
GA	/	81.87±1.91	96.9%	0	0
GA-20	**H**	71.34±1.85	100.8%	0	0
GA-23	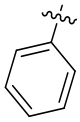	50.77±1.71	101.9%	0	0
GA-24	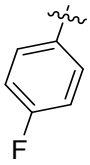	26.52±1.42	101.5%	0	0
GA-25	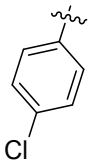	43.37±1.64	96.9%	0	0
GA-36	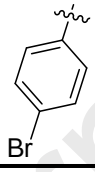	32.10±1.51	100.0%	0	0

Table 3 Structure optimization of GA-21

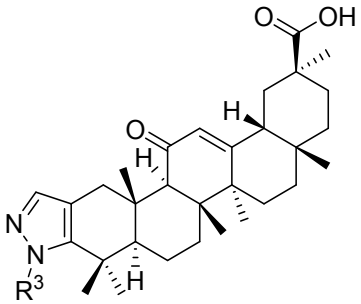

	R^3	Cytotoxicity (IC_{50}, μM) [a]	NO inhibition %[b]	TNF inhibition %[b]	IL-6 inhibition %[b]
GA	/	81.87±1.91	96.9%	0	0
GA-21	**H**	67.34±1.83	100.0%	0	0
GA-27	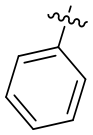	29.29±1.47	95.0%	104%	101%
GA-28	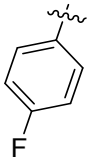	33.73±1.53	102.3%	77.0%	100%
GA-29	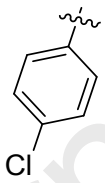	23.96±1.38	98.1%	88.0%	101%
GA-30	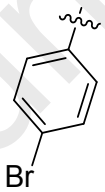	24.90±1.40	100.0%	88.0%	100%
GA-52	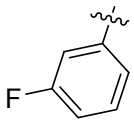	73.49±1.87	102.3%	86.0%	100%
GA-53	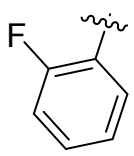	105.39±2.02	98.9%	103.0%	101%
GA-54	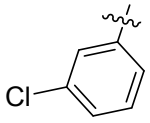	54.93±1.74	102.3%	2.0%	100%

GA-55	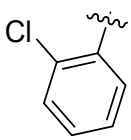	54.21±1.73	102.7%	102.0%	100%
GA-56	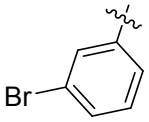	60.06±1.78	103.8%	0	89%
GA-57	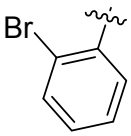	74.78±1.87	98.9%	0	20%
GA-58	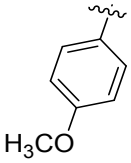	42.13±1.63	102.7%	0	0
GA-59	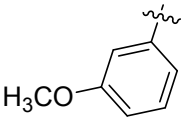	45.04±1.65	100.4%	63.0%	101%
GA-60	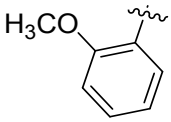	63.94±1.81	96.2%	94.0%	100%
GA-61	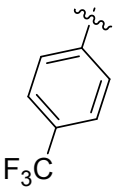	33.87±1.53	101.9%	0	98%
GA-62	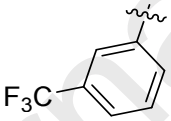	28.26±1.45	101.5%	0	101%
GA-63	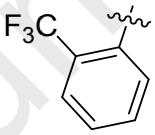	79.88±1.90	103.1%	0	99%
GA-64	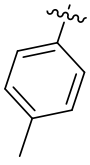	26.61±1.43	101.9%	56.0%	101%
GA-65	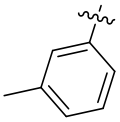	27.88±1.45	101.5%	72.0%	100%
GA-66	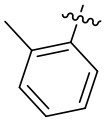	27.21±1.44	101.1%	100.0%	101%

GA-67	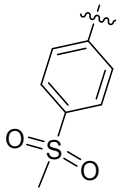	45.39±1.66	99.6%	0	100%
GA-68	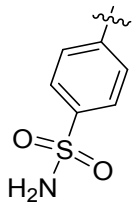	52.17±1.72	95.4%	0	0

Table 4 Structure optimization of GA-31

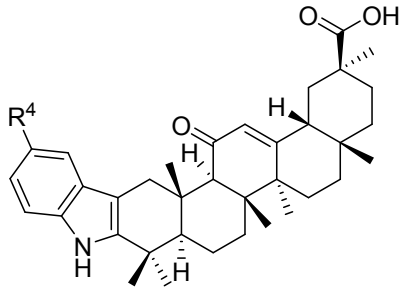

	R^4	Cytotoxicity (IC_{50}, μM) [a]	NO inhibition %[b]	TNF inhibition % [b]	IL-6 inhibition %[b]
GA	/	81.87±1.91	96.9%	0	0
GA-31	**H**	69.82±1.84	100.0%	0	101%
GA-32	**F**	116.76±2.07	101.9%	0	67%
GA-33	**Cl**	49.03±1.69	100.8%	72.0%	101%
GA-34	**Br**	35.87±1.56	95.4%	0	0

2.5 GA-60 shows no apparent cytotoxicity and does not induce apoptosis in the presence of LPS

Since LPS is the main component of the outer membrane of Gram-negative bacteria and exhibits biological toxicity, we hypothesized that it might increase cell cytotoxicity and cover up false positive results. To verify this, we performed cell viability assays in the presence of LPS. Results showed a reduction the relative cell viability of **GA-27**, **GA-53**, **GA-55**, and **GA-66** (10 μM) in the presence of LPS, with only **GA-60** (10 μM) not exhibiting cytotoxicity compared with dimethyl sulfoxide (DMSO) **(Figure 3A**). To validate the result, we evaluated cell apoptosis, in the presence of LPS and found consistent results to those from the cell viability assay (**Figure 3B**). Particularly, **GA-60** did not exhibit apoptosis compared with DMSO. Owing to an outstanding

combination of NO (96%), TNF-α (94%), and IL-6 (100%) inhibition function, **GA-60** was eventually selected as our optimal candidate.

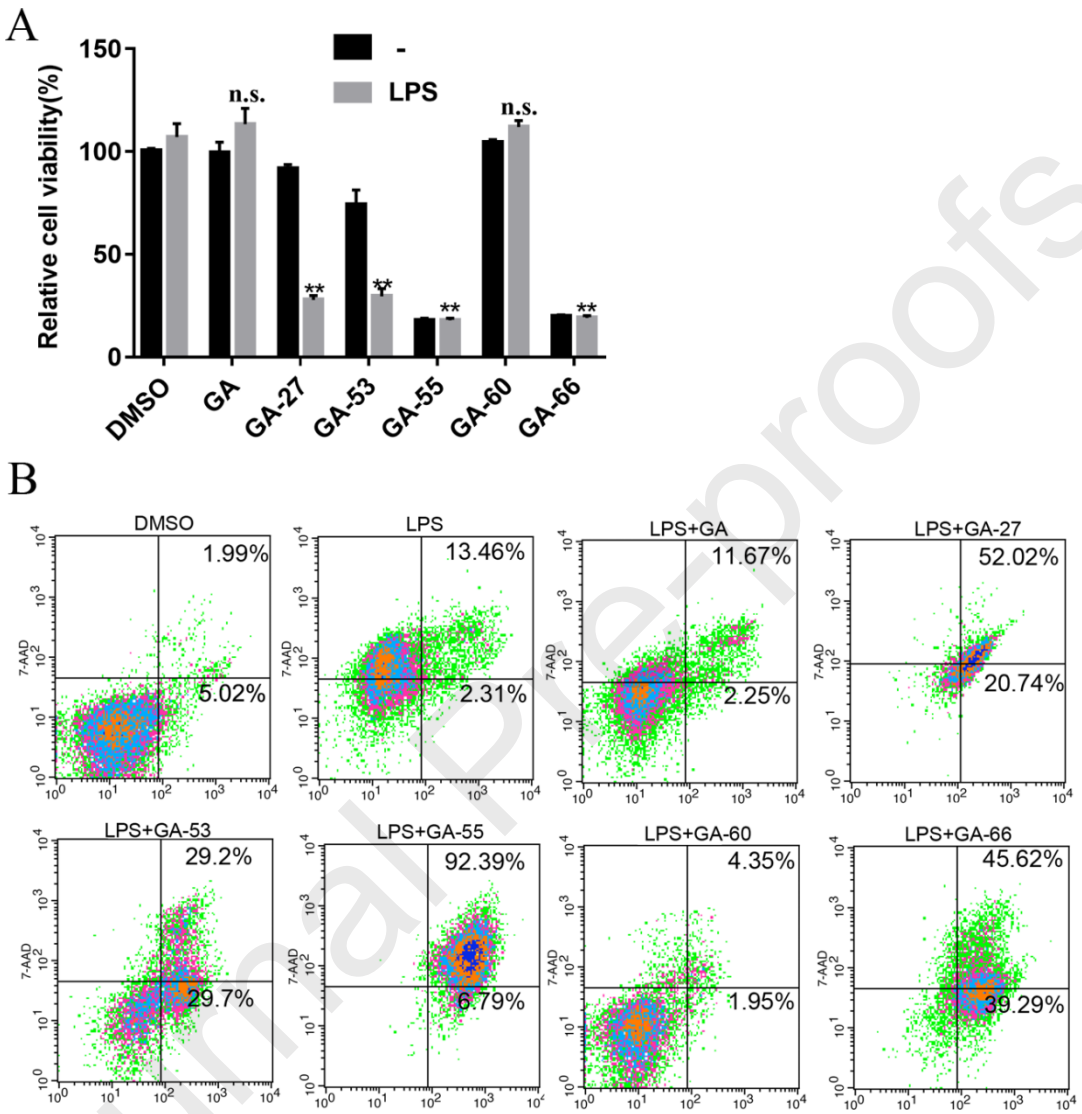

Figure 3. Relative cell viability and percentage apoptosis in the presence of LPS upon the treatment of **GA-27**, **GA-53**, **GA-55**, **GA-60**, and **GA-66** (10 μM). (A) Relative cell viability (%) (means ± SD) in the presence of LPS upon the treatment with **GA-27, GA-53, GA-55, GA-60**, and **GA-66** (10 μM) are shown. (** $P < 0.01$ versus LPS simulation following Analysis of Variance; n.s., not significant.) (B) Rate of apoptosis (%) in the presence of LPS upon the treatment with **GA-27**, **GA-53**, **GA-55**, **GA-60**, and **GA-66** (10 μM).

2.6 GA-60 has a strong binding effect on HMGB1

To investigate and predict the binding mode of candidate compound **GA-60** and HMGB1 (PDB code: 1HMF), we further performed the docking simulation using Maestro software (Schrödinger, version 2018-4). Based on the proposed binding mode (**Figure 2**), it can be found that **GA** and **GA-60** both possibly establish favorable hydrogen bond interactions with Arg109 (green). The docking result also suggested that the carbonyl group at C11 of **GA** forms one a stable hydrogen bond with the guanidinium group of Arg109 (green). However, the carbonyl group of **GA-60** forms more stable bidentate hydrogen bond with the guanidinium group of Arg109 (green). On the other hand, **GA-60** establishes favorable cation-pi interaction with Lys113 (green). These results further confirmed that **GA-60** has a stronger binding effect on HMGB1 than the parent **GA** (**Figure 4 and 5**). From the docking results, it can be found that the appropriate modification of ring A in **GA** is beneficial to enhance the interaction between the candidate compound **GA-60** and HMGB1.

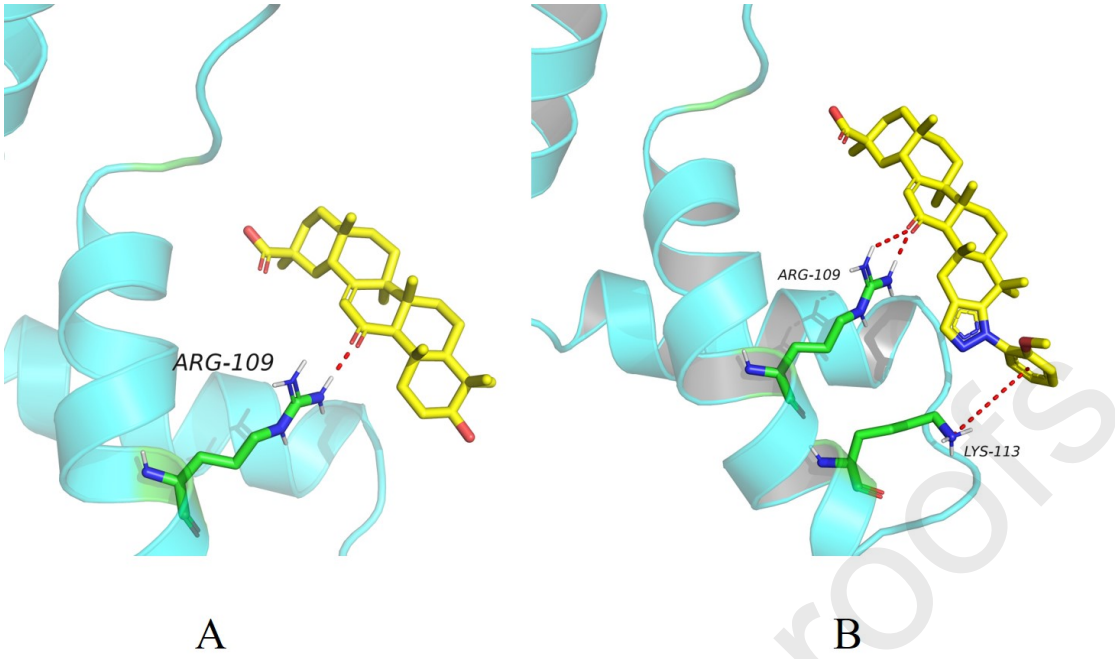

Figure 4. (A) Proposed binding mode of **GA** (yellow) and HMGB1 (PDB: 1HMF) (light blue). The carbonyl group of GA form one stable hydrogen bond with the guanidinium group of Arg109 (green). Oxygen and nitrogen atoms are shown in red and blue, respectively. (B) Proposed binding mode of **GA-60** (yellow) and HMGB1 (PDB: 1HMF) (light blue). **GA-60** establishes favorable cation-pi interaction with Lys113 (green). The carbonyl group of **GA-60** form two stable hydrogen bonds with the guanidinium group of Arg109 (green). Oxygen and nitrogen atoms are shown in red and blue, respectively.

2.7 GA-60 could bind to HMGB1.

Surface plasmon resonance (SPR) was used to verify the binding of GA analogues with HMGB1. Results showed that surface plasmon resonance was rapidly increased in response units (RU), indicating binding of **GA** (**Figure 5A**) and **GA-60** (**Figure 5B**) to the immobilized HMGB1, concentration-dependent manner. Glycyrrhizin was reported to bind directly to HMGB1 (K_d = ~150 μM) [25]. The affinity constant (K_d)

value for **GA** was determined to be 73.3 μM while **GA-60** had a binding ability for HMGB1 with a K_d value of 12.5 μM.

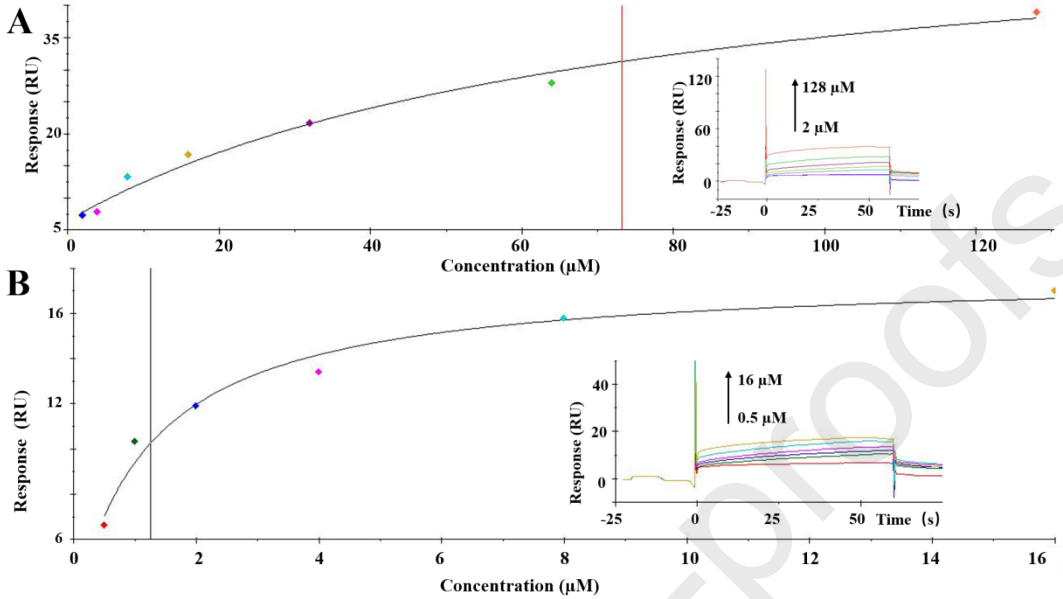

Figure 5. GA and **GA-60** were binding to HMGB1 *in vitro*. SPR analysis of the binding between GA (A) / GA-60 (B) and HMGB1.

2.8 GA-60 possesses enhanced *in vivo* therapeutic effects in LPS/CLP induced mouse models of sepsis than GA.

Previous researches reported that **GL** might protect rats from sepsis by blocking the interaction of HMGB1 with receptor for advanced glycation end products (RAGE) and TLR-4 and suppressing the downstream signaling pathway[32]. In the current study, we hypothesized that **GA-60** could result in efficient treatment of sepsis. We, therefore, first evaluated effects of **GA-60** treatment in LPS induced endotoxin shock *in vivo* (**Figure 6A**), by subjecting LPS induced mice to **GA-60** (10 mg/kg) twice a day thorough intraperitoneally (i.p.) injection, and including **GA** (10 mg/kg) as a positive control. The survival rate of mice treated by **GA-60** was 60%, which was higher than

that of **GA** (10%), while the vehicle-treated mice almost died in 72 hours. We then performed a murine CLP model, which is considered the gold standard model for *in vivo* sepsis[33], and found that all mice with vehicle or **GA** (10 mg/kg) died within 60 hours, while those under **GA-60** (10 mg/kg) had a 55% survival rate (**Figure 6B**). To further evaluate the anti-inflammatory effects of **GA-60** *in vivo*, we measured plasma TNF-α (**Figure 6C**) and HMGB1 (**Figure 6D**). Since HMGB1 peaks in plasma between 18-36 hours after LPS stimulation[9], we collected plasma 24 hours after LPS stimulation. As expected, we found a significant decrease of TNF-α, and HMGB1 in plasma from mice treated with **GA-60**, compared to those under **GA**. These results were consistent with the findings from our *in vitro* experiments.

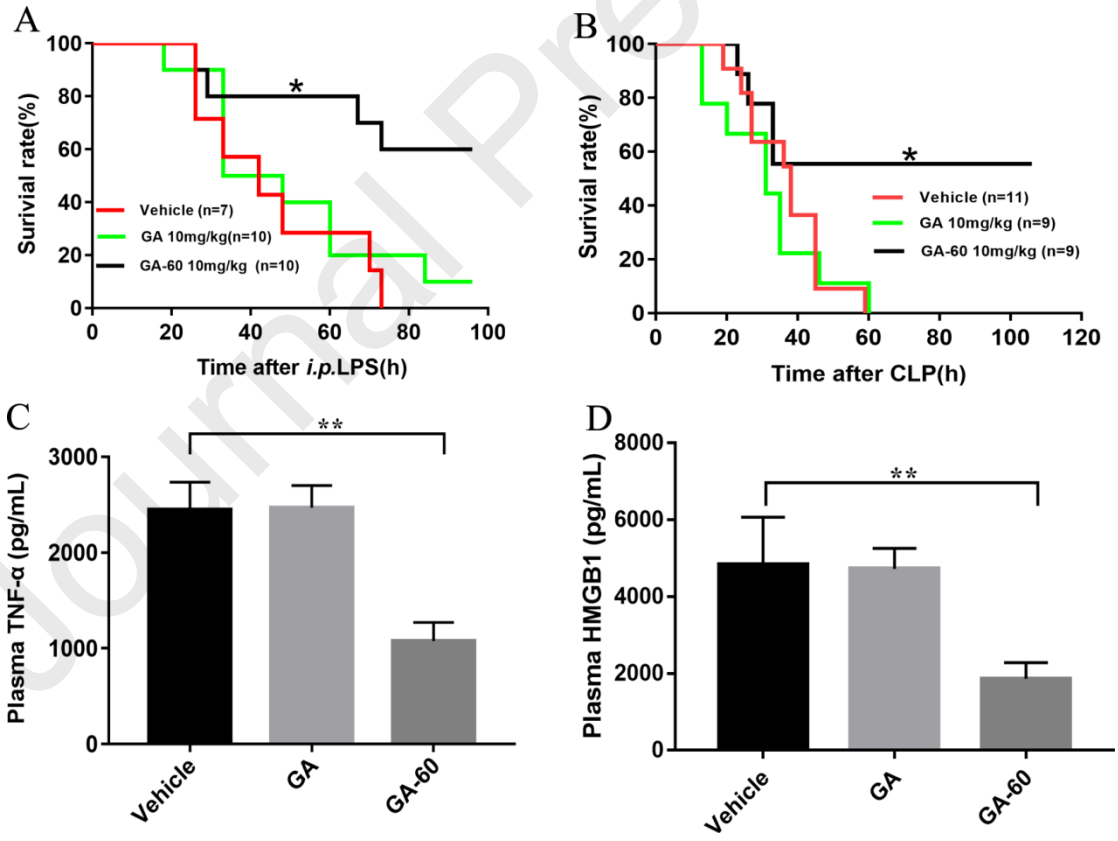

Figure 6. *In vivo* therapeutic effect of **GA-60** in LPS/CLP induced sepsis mouse model. Vehicle, **GA**, and **GA-60** was administered intraperitoneally at a dose of 10 mg/kg

every 12 h for 100 h, starting from 30min before LPS i.p. or CLP surgery. The survival curve of the vehicle, **GA**, and **GA-60** treated LPS (A) /CLP (B) induced sepsis are shown. (* $P < 0.05$; by Kaplan-Meier Survival Analysis). After LPS stimulation 24 h, plasma TNF-α (C) and HMGB1 (D) level *in vivo* after treatement with vehicle, **GA** and **GA-60** following ELISA. Data are means ± SD from three independent experiments (** $P < 0.01$ following Analysis of Variance).

2.9 GA-60 effectively inhibits inflammatory signaling pathway

HMGB1 interacts with at least 14 different receptor systems to transduce cellular signals[34, 35]. Mitogen-activated protein kinase (MAPK) and nuclear factor-κB (NF-κB) are the most common signal pathways stimulated by LPS[36] or HMGB1[37, 38]. The MAPKs constitute c-Jun N terminal kinase (JNK), extracellular signal-regulated kinases (ERKs), and p38 MAPK[39]. Interestingly, the interaction between HMGB1 and TLR can induce MyD88 signaling cascade and creat a cross-talk directly with p38 MAPK signaling[40, 41]. Furthermore, activation of MAPK has been shown to be related to RAGE activation or TLR-4 phosphorylation. NF-κB, a key regulator of inflammatory response, modulates the expression level of inflammatory mediators, cytokines, and chemokine genes in activated macrophages[42]. The activation of NF-κB is initiated by the phosphorylation, ubiquitination and degradation of inhibitory κB (IκB) proteins, which comprise IκB kinase α (IKKα) and IKKβ[41]. Since all the complex signaling pathways involved in HMGB1 seem to affect NF-κB activity[43], targeting the NF-κB signal pathway is considerd to be a promising strategy for

controlling sepsis-related inflammation. As excepted, **GA-60** (10 μM) inhibited the phosphorylation of JNK, p38, and ERK of MAPK (**Figure 7A**), as well as that of NF-κB, including p65 and IKKα/β (**Figure 7B**). Moreover, the inhibition was better than that of **GA** at a same concentration.

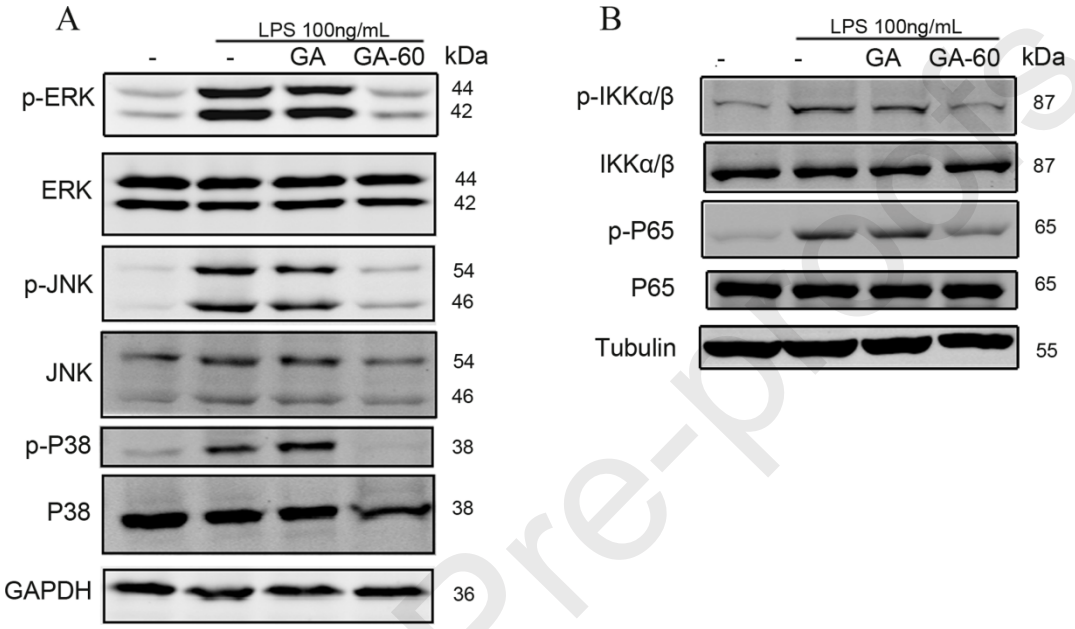

Figure 7. Inhibition of inflammatory signaling pathways in RAW264.7 cells. Western blot analysis relative to the phosphorylation (p) of p38, JNK, and ERK (**A**) and p65 and IKKα/β (**B**) after treatment with 10 μM **GA** and **GA-60** in Raw264.7 cells, followed by 100 ng/mL LPS treatment.

2.10 GA-60 inhibits release of HMGB1

A recent study reported that **GL** could inhibit the release of HMGB1 induced by LPS[44]. We, therefore, investigated whether **GA-60** inhibits the release of preformed or total HMGB1 in cells. We found that **GA-60** (10 μM) significantly inhibited release of HMGB1 (**Figure 8A**), while did not influence total intracellular HMGB1 protein levels (**Figure 8C**), and this was similar to GL. HMGB1 is a highly preserved nuclear

protein, with studies indicating that its transfer from the nucleus to cytoplasm, after LPS stimulation, and **GL** exhibits inhibitory functions[44]. In the current study, we also investigated whether **GA-60** could inhibit HMGB1 migration from the nucleus to the cytoplasm after LPS treatment. The cytoplasmic protein and nuclear protein were extracted respectively, and HMGB1 was detected by Western blot analysis. We found HMGB1 increase in the cytoplasm and its decrease in the nucleus following LPS stimulation in RAW264.7 cells. However, HMGB1 distribution was not affected by **GA** or **GA-60** (**Figure 8B**). These results suggest that **GA-60** can specifically prevent the release of HMGB1 without reducing its levels or affecting the levels in steady-state cells.

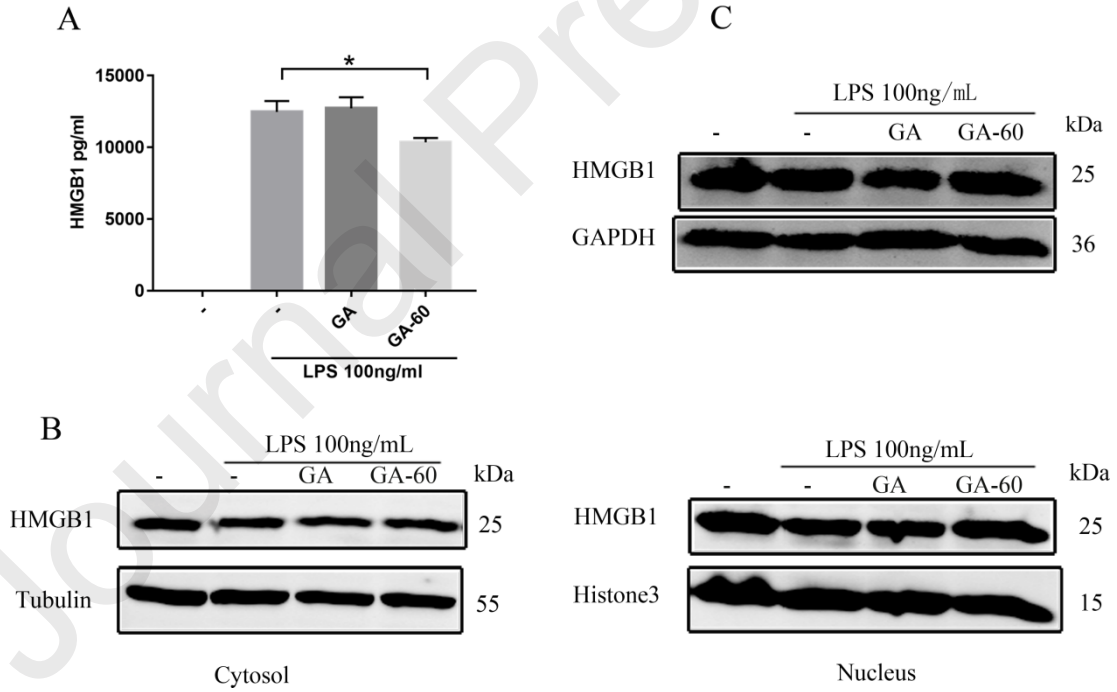

Figure 8. GA-60 inhibit HMGB1 release but not the translocation of HMGB1 in the cell. (A) RAW264.7 cells were stimulated by LPS (100ng/ml) and treated with **GA** or **GA-60** (10 μM). The release of HMGB1 was determined by ELISA assay (* $P < 0.05$ by Analysis of Variance). (B) RAW264.7 cells were stimulated by LPS (100 ng/mL)

and treated with **GA** or **GA-60** (10 μM). The cytoplasmic and nuclear protein was extracted separately, and HMGB1 was detected by Western blot. (C) Western blot analysis of HMGB1 after treatment with 10 μM **GA** and **GA-60** in RAW264.7 cells, followed by 100 ng/mL LPS treatment.

3. Conclusion and discussion

In the last decades, numerous basic and clinical studies have been conducted to identify and validate effective therapeutic drugs. However, limited success has been achieved and many diseases, such as sepsis, remain a big challenge to human health. Research seeking to explore new agents that are capable of inhibiting clinically accessible late mediators is dramatically rising. In the current study, we describe HMGB1, a late inflammatory mediator that can be exploited to widen the therapy window for sepsis. However, HMGB1 binds to multiple receptors, and is difficult to target multiple receptors for anti-inflammation. For this reason, it is more reasonable to directly target HMGB1 rather than its receptors. Glycyrrhizin is the first small-molecule that combined HMGB1 in the literature[45, 46].

In this article, substituted pyrazole rings, substituted indole rings and isooxazole rings were introduced into ring A of **GA** by structure-based design, through esterification, oxidation, nucleophilic substitution, cyclization and hydrolysis, getting 16 **GA** derivatives firstly. Using GA, GL and CBX as positive controls, the inhibitory effects of target compounds on TNF-α and IL-6 released by RAW264.7 cells were detected by flow cytometry. And the effect of the target compounds on the release

ability of NO was also detected. The results showed that the derivatives of N-phenyl-substituted pyrazole had better anti-inflammatory activities at 10 μM. According to this result, "N-phenyl substituted pyrazole" was further selected as the preferred structure to be modified. By introducing substituents of different properties into the ortho position of the phenyl group, **GA-27**, **GA-53**, **GA-55**, **GA-60**, and **GA-66** were obtained.

GA is considered a pan-assay-interference-compounds (PAINS) compound due to presence of the Michael receptor. Basically, a PAINS-like compound cannot obtain analogues with apparent structure-activity relationship (SAR)[47]. In this study, a clear cell-based structure-activity relationship of the GA analogues led to find the best compound **GA-60**. Then, we screened our analogues (**GA-60**) through the PAINS compound databases [ZINC (http://zinc15.docking.org/) and False Positive Remover (https://www.cbligand.org/PAINS/)], and found that they both passed the filter (Supporting information Figure S3). We used molecular docking and SPR assay to demonstrate the binding affinity with HMGB1, and the affinity constant (Kd) of GA-60 to HMGB1 was 12.5 μM. What's more, the therapeutic effect of **GA-60** in two different sepsis mice models was evaluated: **GA-60** significantly increased the survival rate at the dose of 10 mg/kg and inhibited TNF-α and HMGB1 levels in plasma.

Since hyperinflammation has been extensively implicated in the sepsis progression, we chose the classical inflammatory cell model, named LPS-stimulated RAW264.7 cells, to verify the anti-inflammatory activity of **GA** derivatives[48-50]. Stimulated macrophages to release HMGB1 and other cytokines involve MAPK and NF-κB signal

pathway[36-38]. Particularly, MAPK constitutes ERK, JNK, and p38 MAPK. In addition, IKKα and IKKβ subunits are responsible for phosphorylation of inducible IκB[41]. Since activation of NF-κB requires phosphorylation, ubiquitination and degradation of IκB proteins, we evaluated the effect of **GA-60** in MAPK and NF-κB pathway in order to clarify the mechanism of **GA-60** action.

To verify whether **GA-60** inhibits HMGB1 release, we used ELISA to measure HMGB1 levels in the cell supernatant following LPS stimulation. Here, we found that **GA-60** inhibited the HMGB1 release, but did not influence its distribution from the nucleus to the cytoplasm. However, the precise mechanism of how **GA-60** influences the release of HMGB1 remains to be studied.

Overall, these findings demonstrated the combination of **GA** and HMGB1 using the molecular docking and SPR assay, and application of a **GA** derivative **GA-60** in treatment of sepsis. The work provides a new candidate for targeted sepsis treatment in future.

4. Experimental Section

4.1 Chemistry materials and methods

Unless otherwise noted, all materials were obtained from commercial suppliers. Anhydrous organic solvents were purchased from J&K under N_2 in Sure/Seal bottles and used directly. All solvents and reagents were of analytically pure grade, and no further purification was needed. Petroleum ether describes a mixture of hexanes in the bp range of 60 to 90 °C. Analytical thin-layer chromatography was performed on Yantai Huanghai HSGF254 silica gel plates and visualized by fluorescence quenching under

UV light. Flash column chromatography was performed using silica gel (200–300 mesh). Nuclear magnetic resonance (NMR) spectra were recorded using TMS as the internal standard in $CDCl_3$, Acetone-d_6 or CD_3OD with a Bruker BioSpin GmbH spectrometer at 300 MHz or 500 MHz. When peak multiplicities are reported, the following abbreviations are used: s = singlet, d = doublet, t = triplet, m = multiplet, and dd = doublet of doublets. HRMS was recorded on an Agilent-6520 Q-TOF mass spectrometer (Agilent Technologies, Palo Alto, CA, USA). All the final compounds were tested by HPLC and the purities were higher than 95%. The reverse phase HPLC was conducted on Agilent Technologies 1260 Infinity, which was equipped with C18 column (Aglilent Eclipse XDB-C18, 5 μm, 4.6 mm × 250 mm). The mobile phase A was 0.1% formic acid in water and mobile phase B was acetonitrile. The gradient of 20 – 95% B was run at a flow rate of 1.0 mL/min over 30 min.

4.1.1 Methyl (2S,4aS,6aS,6bR,8aR,10S,12aS,12bR,14bR)-10-hydroxy-2,4a,6a,6b,9,9,12a-heptamethyl-13-oxo-1,2,3,4,4a,5,6,6a,6b,7,8,8a,9,10,11,12,12a,12b,13,14b-icosahydropicene-2-carboxylate **(GA-1)**

To a solution of **GA** (2.062 g, 4.38 mmol, 1.0 eq.) and K_2CO_3 (0.605 g, 4.38 mmol, 1.0 eq.) in anhydrous acetone (50 mL) was added dropwise CH_3I (0.4 mL, 6.42 mmol, 1.5 eq.) at room temperature. The mixture was stirred at room temperature for 12 h. The reaction mixture was poured into H_2O (30 mL) and extracted with $CHCl_3$ (3×50 mL). The organic layer was dried over anhydrous Na_2SO_4 and concentrated. The residue was purified by silica gel chromatography (petroleum ether/AcOEt, 6/1−4/1 v/v) to give **GA-1** (2.015 g, 95%) as a white solid. ^{1}H NMR (500 MHz, $CDCl_3$) δ 5.66 (s, 1H), 3.68 (s, 3H), 3.22 (dd, J = 5.2, 10.9 Hz, 1H), 2.79 (d, J = 13.5 Hz, 1H), 2.34 (s, 1H), 2.11 – 1.96 (m, 3H), 1.95 – 1.77 (m, 2H), 1.70 – 1.56 (m, 7H), 1.41 (dd, J = 9.8, 21.2 Hz, 3H),

1.36 (s, 3H), 1.31 (d, *J* = 9.5 Hz, 2H), 1.14 (d, *J* = 4.5 Hz, 5H), 1.12 (s, 3H), 1.00 (s, 5H), 0.80 (s, 6H), 0.69 (d, *J* = 11.3 Hz, 1H); ^{13}C NMR (125 MHz, $CDCl_3$) δ 200.2, 176.9, 169.2, 128.5, 78.7, 61.8, 54.9, 51.8, 48.4, 45.4, 44.0, 43.2, 41.1, 39.1 (2×C), 37.7, 37.1, 32.7, 31.8, 31.1, 28.5, 28.3, 28.1, 27.3, 26.5, 26.4, 23.4, 18.7, 17.5, 16.3, 15.5. HRMS (ESI): m/z calcd for $C_{31}H_{49}O_4$ $[M+H]^+$: 485.3625, found 485.3623.

4.1.2 Methyl (2S,4aS,6aS,6bR,8aR,12aS,12bR,14bR)-2,4a,6a,6b,9,9,12a-heptamethyl-10,13-dioxo-1,2,3,4,4a,5,6,6a,6b,7,8,8a,9,10,11,12,12a,12b,13,14b-icosahydropicene-2-carboxylate **(GA-2)**

PCC (69 mg, 0.318 mmol, 1.5 eq.) was added to the solution of **GA-1** (102 mg, 0.212 mmol, 1.0 eq.) in anhydrous dichloromethane (15 mL) and stirred for 4 h at room temperature. Solvent was evaporated under reduced pressure and reaction mixture was purified by silica gel column chromatography (petroleum ether/EtOAc, 6/1−4/1−2/1 v/v) to afford compound **GA-2** (87 mg, 85% yield) as colourless crystals. ^{1}H NMR (500 MHz, $CDCl_3$) δ 5.67 (s, 1H), 3.66 (s, 3H), 2.92 (dq, *J* = 3.6, 4.1, 11.2 Hz, 1H), 2.66 – 2.52 (m, 1H), 2.41 (s, 1H), 2.37 – 2.29 (m, 1H), 2.08 (dd, *J* = 3.1, 13.4 Hz, 1H), 2.04 – 1.93 (m, 2H), 1.92 – 1.76 (m, 2H), 1.66 (td, *J* = 5.7, 12.1 Hz, 1H), 1.61 – 1.54 (m, 1H), 1.45 – 1.35 (m, 3H), 1.34 (s, 3H), 1.28 (dt, *J* = 4.3, 7.2 Hz, 3H), 1.23 (s, 3H), 1.22 (s, 3H), 1.13 (s, 3H), 1.11 (s, 3H), 1.07 (s, 3H), 1.03 (s, 3H), 0.84 (t, *J* = 6.9 Hz, 1H), 0.78 (s, 3H); ^{13}C NMR (125 MHz, $CDCl_3$) δ 217.1, 199.4, 176.8, 169.7, 128.4, 61.0, 55.4, 51.7, 48.3, 47.7, 45.2, 44.0, 43.3, 41.1, 39.7, 37.7, 36.6, 34.2, 32.1, 31.8, 31.1, 28.5, 28.2, 26.5, 26.4, 26.3, 23.3, 21.4, 18.8, 18.5, 15.6. HRMS (ESI): m/z calcd for $C_{31}H_{46}O_4Na$ $[M+Na]^+$: 505.3288, found 505.3289.

4.1.3 Methyl (2S,4aS,6aS,6bR,8aR,12aS,12bR,14bR)-2,4a,6a,6b,9,9,12a-

heptamethyl-10,13-dioxo-11-(2,2,2-trifluoroacetyl)-,2,3,4,4a,5,6,6a,6b,7,8,8a,9,10, 11,12,12a,12b,13,14b-icosahydropicene-2-carboxylate **(GA-3)**

NaH (5 mg, 0.125 mmol, 2.5 eq.) was added slowly to a solution of **GA-2** (24 mg, 0.05 mmol, 1.0 eq.) in THF (10 mL). The mixture was stirred at room temperature for 10 min and then added ethyl trifluoroacetate (14.9 μL, 0.125 mmol, 2.5 eq.) rapidly, kept stirring for another 8h. The reaction was quenched slowly with the addition of saturated ammonium chloride solution. The mixture was poured into saturated salt solution (15 mL) and extracted with CH_2Cl_2 (3×15 mL). The organic layer was evaporated in vacuum and purified on a silica gel column chromatography (petroleum ether/AcOEt, 8/1−6/1−4/1 v/v) to give **GA-3** (20.3 mg, 70% yield) as a brownish red solid. ^{1}H NMR (500 MHz, $CDCl_3$) δ 5.73 (s, 1H), 3.87 – 3.78 (m, 1H), 3.69 (s, 3H), 2.44 (s, 1H), 2.17 (d, J = 3.6 Hz, 1H), 2.12 (dd, J = 3.3, 13.6 Hz, 1H), 2.08 – 1.90 (m, 5H), 1.85 (d, J = 4.4 Hz, 1H), 1.75 – 1.55 (m, 3H), 1.50 (td, J = 5.0, 12.2, 13.2 Hz, 3H), 1.38 (s, 4H), 1.34 – 1.29 (m, 3H), 1.22 (d, J = 4.6 Hz, 4H), 1.18 (s, 3H), 1.14 (d, J = 5.6 Hz, 6H), 1.07 – 1.01 (m, 1H), 0.88 (t, J = 6.8 Hz, 1H), 0.83 (s, 3H); ^{13}C NMR (125 MHz, $CDCl_3$) δ 199.0, 194.9, 176.8, 169.7, 128.5, 118.6, 102.2, 59.2, 52.0, 51.8, 48.4, 44.9, 44.0, 43.3, 41.2, 40.5, 37.7, 35.5, 31.8, 31.5, 31.1, 29.7, 29.2, 29.0, 28.6, 28.3, 26.5, 26.4, 23.2, 21.3, 18.8, 18.2, 14.6. HRMS (ESI): m/z calcd for $C_{33}H_{45}F_3O_5Na$ $[M+Na]^+$: 601.3111, found 601.3112.

4.1.4 Methyl (2S,4aS,6aS,6bR,8aR,12aS,12bR,14bR)-11-formyl-2,4a,6a,6b,9,9,12a-heptam-ethyl-10,13-dioxo-1,2,3,4,4a,5,6,6a,6b,7,8,8a,9,10,11,12,12a,12b,13,14b-icosahydropice-ne-2-carboxylate **(GA-4)**

NaH (5 mg, 0.125 mmol, 2.5 eq.) was added slowly to a solution of **GA-2** (24 mg, 0.05 mmol, 1.0 eq.) in THF (10 mL). The mixture was stirred at room temperature for

10 min and then added ethyl formate (10 μL, 0.125 mmol, 2.5 eq.) rapidly, kept stirring for another 8h. The reaction was quenched slowly with the addition of saturated ammonium chloride solution. The mixture was poured into saturated salt solution (15 mL) and extracted with CH_2Cl_2 (3×15 mL). The organic layer was evaporated in vacuum and purified on a silica gel column chromatography (petroleum ether/AcOEt, 8/1−6/1−4/1 v/v) to afford **GA-4** (20.4 mg, 80% yield) as a pale yellow solid. ^{1}H NMR (500 MHz, $CDCl_3$) δ 8.63 (d, J = 3.2 Hz, 1H), 5.74 (s, 1H), 3.71 (s, 3H), 3.47 (d, J = 14.8 Hz, 1H), 2.44 (s, 1H), 2.20 – 2.11 (m, 1H), 2.05 – 1.99 (m, 2H), 1.98 – 1.91 (m, 2H), 1.86 (td, J = 4.4, 13.6 Hz, 1H), 1.68 (dd, J = 4.0, 13.3 Hz, 1H), 1.62 (t, J = 13.5 Hz, 2H), 1.55 – 1.46 (m, 3H), 1.38 (s, 3H), 1.32 (d, J = 10.1 Hz, 3H), 1.21 (s, 3H), 1.18 (s, 3H), 1.15 (d, J = 4.6 Hz, 6H), 1.14 (s, 3H), 1.07 – 1.01 (m, 1H), 0.88 (t, J = 6.9 Hz, 2H), 0.83 (s, 3H).;^{13}C NMR (125 MHz, $CDCl_3$) δ 199.5, 189.5, 188.9, 176.3, 128.5, 105.8, 60.3, 59.6, 52.2, 48.4, 45.0, 43.8, 43.3, 41.2, 40.0, 39.7, 37.7, 36.2, 31.8, 31.1, 29.7, 28.6, 28.4, 28.3, 26.5, 26.4, 23.2, 20.9, 18.8, 18.3, 14.7, 14.3. HRMS (ESI): m/z calcd for $C_{32}H_{46}O_5Na$ $[M+Na]^+$: 533.3237, found 533.3237.

4.1.5 Methyl (2S,4aS,6aS,6bR,8aR,13aS,13bR,15bR)-2,4a,6a,6b,9,9,13a-heptamethyl -14-ox-o-12-(trifluoromethyl)-2,3,4,4a,5,6,6a,6b,7,8,8a,9,11,13,13a,13b,14,15b-octadecah-ydr-o-1H-chryseno[1,2-f]indazole-2-carboxylate **(GA-5)**

To a solution of **GA-3** (35 mg, 0.06 mmol, 1.0 eq.) in ethanol (10 mL) was added phenylhydrazine hydrochloride (17.3 mg, 0.12 mmol, 2 eq.) at room temperature. The reaction mixture was heated under reflux for 4 h. After cooling to room temperature, the mixture was concentrated. The residue was purified by silica gel chromatography (petroleum ether/AcOEt, 8/1−6/1−4/1 v/v) to give **GA-8** (27.2 mg, 70%) as a pale yellow solid. ^{1}H NMR (500 MHz, $CDCl_3$) δ 5.75 (s, 1H), 3.89 (d, J = 16.0 Hz, 1H),

3.70 (s, 3H), 2.69 – 2.40 (m, 2H), 2.15 – 1.77 (m, 9H), 1.76 – 1.48 (m, 8H), 1.39 (s, 5H), 1.19 (s, 4H), 1.16 (s, 3H), 1.13 (s, 3H), 1.05 (d, J = 23.0 Hz, 2H), 0.85 (d, J = 15.1 Hz, 3H); ^{13}C NMR (125 MHz, $CDCl_3$) δ 199.1, 196.6, 176.9, 170.5, 169.8, 169.4, 164.0, 128.6, 60.0, 52.4, 51.8, 48.4, 45.3, 44.0, 43.3, 41.2, 38.0, 37.7, 33.0, 31.9, 31.1, 31.0, 30.9, 29.2, 28.6, 28.3, 26.5, 26.4, 23.8, 23.2, 18.2, 18.1, 15.7. HRMS (ESI): m/z calcd for $C_{33}H_{46}F_3N_2O_3$ $[M+H]^+$: 575.3455, found 575.3442.

4.1.6 Methyl (2S,4aS,6aS,6bR,8aR,13aS,13bR,15bR)-2,4a,6a,6b,9,9,13a-eptamethyl -14-ox-o-2,3,4,4a,5,6,6a,6b,7,8,8a,9,11,13,13a,13b,14,15b-octadecahydro-1H-chryseno[1,2-f]i-ndazole-2-carboxylate **(GA-6)**

To a solution of **GA-4** (20 mg, 0.04 mmol, 1.0 eq.) in ethanol (10 mL) was added hydrazine dihydrochloride (6.5 mg, 0.06 mmol, 1.5 eq.) at room temperature. The reaction mixture was heated under reflux for 3 h. After cooling, the mixture was concentrated. The residue was purified by silica gel chromatography (petroleum ether/AcOEt, 8/1−6/1−4/1 v/v) to give **GA-6** (15.2 mg, 75%) as a white solid. ^{1}H NMR (500 MHz, $CDCl_3$) δ 7.37 (s, 1H), 5.74 (s, 1H), 3.70 (s, 3H), 2.54 (s, 1H), 2.17 – 1.81 (m, 7H), 1.79 – 1.43 (m, 8H), 1.39 (s, 4H), 1.34 (s, 5H), 1.23 (s, 1H), 1.19 (s, 3H), 1.15 (s, 3H), 1.09 (s, 3H), 1.07 – 1.00 (m, 1H), 0.91 – 0.79 (m, 4H); ^{13}C NMR (125 MHz, $CDCl_3$) δ 199.6, 176.9, 176.3, 169.4, 128.7, 122.0, 113.2, 60.1, 53.1, 51.8, 48.4, 45.3, 44.0, 43.3, 41.2, 38.2, 37.8, 33.5, 31.9, 31.8, 31.2, 31.1, 29.7, 28.6, 28.3, 26.6, 26.4, 24.1, 23.2, 18.4, 18.2, 15.5; HRMS (ESI): m/z calcd for $C_{32}H_{47}N_2O_3$ $[M+H]^+$: 507.3581, found 507.3574.

4.1.7 Methyl (2S,4aS,6aS,6bR,8aR,13aS,13bR,15bR)-2,4a,6a,6b,9,9,13a -heptamethyl-14-o-xo-1,2,3,4,4a,5,6,6a,6b,7,8,8a,9,13,13a,13b,14,15b

-octadecahydropiceno[2,3-d]isoxazole-2-carboxylate **(GA-7)**

To a solution of **GA-4** (50 mg, 0.1 mmol, 1.0 eq.) in anhydrous pyridine (15 mL) was added hydroxylamine hydrochloride (21 mg， 0.3 mmol, 3.0 eq.) at room temperature. The reaction mixture was heated under reflux for 5 h. After cooling, the mixture was concentrated. The residue was purified by silica gel chromatography (petroleum ether/AcOEt, 8/1−6/1−4/1 v/v) to give **GA-7** (38.0 mg, 75%) as a pale yellow solid. ^{1}H NMR (500 MHz, $CDCl_3$) δ 8.05 (s, 1H), 5.75 (s, 1H), 3.70 (s, 3H), 2.52 (s, 2H), 2.08 – 1.97 (m, 4H), 1.97 – 1.92 (m, 3H), 1.87 (td, J = 4.5, 13.7 Hz, 2H), 1.78 – 1.70 (m, 2H), 1.69 – 1.56 (m, 5H), 1.55 – 1.50 (m, 2H), 1.19 (s, 5H), 1.15 (d, J = 2.5 Hz, 5H), 1.08 (s, 5H), 0.83 (s, 5H); ^{13}C NMR (125 MHz, $CDCl_3$) δ 199.4, 176.9, 170.0, 167.4, 153.7, 128.5, 113.2, 59.7, 53.2, 51.8, 48.4, 45.2, 44.0, 43.8, 43.3, 41.2, 37.8, 37.7, 34.6, 33.8, 31.8, 31.5, 31.1, 28.6, 28.3, 26.6, 26.4, 24.8, 23.2, 18.3, 18.2, 15.2; HRMS (ESI): m/z calcd for $C_{32}H_{45}NO_4Na$ $[M+Na]^+$: 530.3241, found 530.3267.

4.1.8 Methyl (2S,4aS,6aS,6bR,8aR,13aS,13bR,15bR)-2,4a,6a,6b,9,9,13a-heptamethyl-14-ox-o-10-phenyl-12-(trifluoromethyl)-,3,4,4a,5,6,6a,6b,7,8,8a,9,10,13,13a,13b,14,15b-oct-adecahydro-1H-chryseno[1,2-f]indazole-2-carboxylate **(GA-8)**

Compound **GA-8** was synthesized in the same procedure as that of **GA-5** (yield 70%); pale yellow solid. ^{1}H NMR (500 MHz, $CDCl_3$) δ 7.49 – 7.43 (m, 3H), 7.40 (dd, J = 1.6, 8.1 Hz, 2H), 5.76 (s, 1H), 3.96 (d, J = 16.0 Hz, 1H), 3.71 (s, 3H), 2.57 (s, 1H), 2.21 (s, 1H), 2.16 – 2.11 (m, 1H), 2.09 – 1.91 (m, 4H), 1.87 (dt, J = 6.6, 13.5 Hz, 1H), 1.76 – 1.67 (m, 1H), 1.66 – 1.54 (m, 3H), 1.53 – 1.47 (m, 2H), 1.44 – 1.40 (m, 1H), 1.39 (s, 3H), 1.35 – 1.31 (m, 2H), 1.20 (d, J = 7.1 Hz, 6H), 1.16 (s, 3H), 1.08 (d, J = 6.5 Hz, 6H), 0.84 (s, 4H); ^{13}C NMR (125 MHz, $CDCl_3$) δ 199.0, 176.9, 169.3, 147.7, 141.4, 139.7, 129.6, 129.0 (2×C), 128.6 (2×C), 123.0, 120.9, 113.0, 60.2, 53.8, 51.8, 48.4, 45.2,

44.0, 43.3, 41.2, 37.7, 37.5, 36.5, 34.8, 31.9, 31.9, 31.1, 29.2, 28.6, 28.3, 26.5, 26.4, 23.1, 22.4, 18.3, 18.2, 15.8; HRMS (ESI): m/z calcd for $C_{39}H_{49}F_3N_2O_3Na$ $[M+Na]^+$: 673.3587, found 673.3600.

4.1.9 Methyl (2S,4aS,6aS,6bR,8aR,13aS,13bR,15bR)-10-(4-fluorophenyl)-2,4a,6a,6b, 9,9,13a-heptamethyl-14-oxo-12-(trifluoromethyl)2,3,4,4a,5,6,6a,6b,7,8,8a,9,10,13, 13a,13b, 14,15b-octadecahydro-1H-chryseno[1,2-f]indazole-2-carboxylate **(GA-9)**

Compound **GA-9** was synthesized in the same procedure as that of **GA-5** (yield 70%); pale yellow solid. ^{1}H NMR (500 MHz, $CDCl_3$) δ 7.39 (dd, J = 4.8, 8.9 Hz, 2H), 7.14 (t, J = 8.5 Hz, 2H), 5.76 (s, 1H), 3.71 (s, 3H), 2.60 (d, J = 35.7 Hz, 2H), 2.28 – 2.10 (m, 6H), 2.09 – 1.98 (m, 2H), 1.97 – 1.92 (m, 1H), 1.86 (d, J = 4.6 Hz, 1H), 1.71 (d, J = 3.6 Hz, 1H), 1.63 (t, J = 13.5 Hz, 1H), 1.58 – 1.47 (m, 3H), 1.39 (s, 4H), 1.35 – 1.28 (m, 3H), 1.26 (s, 4H), 1.16 (s, 3H), 1.07 (d, J = 1.9 Hz, 6H), 0.84 (s, 3H); ^{13}C NMR (125 MHz, $CDCl_3$) δ 199.0, 176.8, 169.3, 165.2, 161.9, 148.0, 137.4, 130.9, 130.8, 128.6, 120.0, 115.7, 115.6, 113.2, 60.2, 53.7, 51.8, 48.4, 45.1, 44.0, 43.3, 41.2, 37.7, 37.5, 36.4, 34.8, 31.9, 31.1, 29.2, 29.2, 28.6, 28.3, 26.5, 26.4, 23.1, 22.4, 18.3, 18.2, 15.8; HRMS (ESI): m/z calcd for $C_{39}H_{48}F_4N_2O_3Na$ $[M+Na]^+$: 691.3493, found 691.3507.

4.1.10 Methyl (2S,4aS,6aS,6bR,8aR,13aS,13bR,15bR)-10-(4-chlorophenyl)-2,4a,6a, 6b,9,9,13a-heptamethyl-14-oxo-12-(trifluoromethyl)-2,3,4,4a,5,6,6a,6b,7,8,8a,9,10,13,13a, 13b,14,15b-octadecahydro-1H-chryseno[1,2-f]indazole-2-carboxylate **(GA-10)**

Compound **GA-10** was synthesized in the same procedure as that of **GA-5** to obtain a pale yellow oil, which was used to hydrolysis reaction without further purification. HRMS (ESI): m/z calcd for $C_{39}H_{48}ClF_3N_2O_3Na$ $[M+Na]^+$: 707.3198,

found 707.3214.

4.1.11 Methyl (2S,4aS,6aS,6bR,8aR,13aS,13bR,15bR)-10-(4-bromophenyl)-2,4a,6a, 6b,9,9,13a-heptamethyl-14-oxo-12-(trifluoromethyl)-2,3,4,4a,5,6,6a,6b,7,8,8a,9,10,13,13a, 13b,14,15b-octadecahydro-1H-chryseno[1,2-f]indazole-2-carboxylate **(GA-11)**

Compound **GA-11** was synthesized in the same procedure as that of **GA-5** to obtain a pale yellow oil, which was used to hydrolysis reaction without further purification. HRMS (ESI): m/z calcd for $C_{39}H_{48}BrF_3N_2O_3Na$ $[M+Na]^+$: 751.2693, found 751.2705.

4.1.12 Methyl (2S,4aS,6aS,6bR,8aR,13aS,13bR,15bR)-2,4a,6a,6b,9,9,13a-eptamethyl -14-ox-o-10-phenyl-2,3,4,4a,5,6,6a,6b,7,8,8a,9,10,13,13a,13b,14,15b-octadecahydro -1H-chrys-eno[1,2-f]indazole-2-carboxylate **(GA-12)**

Compound **GA-12** was synthesized in the same procedure as that of **GA-6** (yield 70%); pale yellow solid. ^{1}H NMR (500 MHz, $CDCl_3$) δ 7.50 – 7.32 (m, 5H), 5.76 (s, 1H), 3.71 (s, 3H), 2.59 (d, J = 41.3 Hz, 2H), 2.22 – 2.09 (m, 5H), 2.03 (dd, J = 6.5, 19.0 Hz, 4H), 1.86 (dt, J = 6.8, 13.5 Hz, 1H), 1.74 – 1.58 (m, 3H), 1.54 – 1.44 (m, 3H), 1.39 (s, 4H), 1.33 (d, J = 9.4 Hz, 2H), 1.27 (d, J = 15.6 Hz, 5H), 1.05 (d, J = 17.0 Hz, 8H), 0.87 (d, J = 8.0 Hz, 1H), 0.84 (s, 3H); ^{13}C NMR (125 MHz, $CDCl_3$) δ 199.6, 176.9, 169.4, 145.5, 141.7, 138.5, 129.1 (2×C), 128.8, 128.7, 128.4 (2×C), 114.2, 60.4, 54.4, 51.8, 48.4, 45.2, 44.0, 43.3, 41.2, 38.0, 37.8, 34.8, 32.0, 31.9, 31.1, 29.7, 29.4, 28.6, 28.3, 26.5, 26.4, 23.2, 22.5, 18.4, 18.2, 15.6; HRMS (ESI): m/z calcd for $C_{38}H_{51}N_2O_3$ $[M+H]^+$: 583.3894, found 583.3892.

4.1.13 Methyl (2S,4aS,6aS,6bR,8aR,13aS,13bR,15bR)-10-(4-fluorophenyl)-,4a,6a,6b,

9,9,13a-heptamethyl-14-oxo-2,3,4,4a,5,6,6a,6b,7,8,8a,9,10,13,13a,13b,14,15b -octadecahydro-1H-chryseno[1,2-f]indazole-2-carboxylate **(GA-13)**

Compound **GA-13** was synthesized in the same procedure as that of **GA-6** (yield 75%); yellow solid. ^{1}H NMR (500 MHz, Acetone-d_6) δ 7.49 – 7.41 (m, 2H), 7.30 – 7.22 (m, 3H), 5.62 (s, 1H), 3.70 (s, 3H), 2.65 (s, 2H), 2.17 (dd, J = 5.8, 14.3 Hz, 3H), 1.98 – 1.86 (m, 3H), 1.81 (d, J = 13.4 Hz, 2H), 1.60 (d, J = 2.9 Hz, 2H), 1.51 (d, J = 13.1 Hz, 2H), 1.46 (s, 3H), 1.40 (t, J = 3.0 Hz, 1H), 1.38 – 1.32 (m, 2H), 1.19 (s, 3H), 1.15 (d, J = 4.0 Hz, 6H), 1.09 (s, 3H), 1.04 (s, 4H), 0.87 (s, 1H), 0.84 (s, 3H); ^{13}C NMR (125 MHz, Acetone-d_6) δ 198.3, 176.2, 169.2, 163.3, 138.1, 131.4, 131.3, 128.1, 118.5, 115.2 (2×C), 115.0 (2×C), 60.1, 54.1, 53.7, 51.0, 48.3, 44.9, 43.8, 43.2, 41.1, 37.8, 37.7, 37.2, 34.5, 31.7, 31.7, 30.7, 28.1, 27.4, 26.4, 26.1, 22.7, 22.1, 18.2, 17.7, 15.0; HRMS (ESI): m/z calcd for $C_{38}H_{50}FN_2O_3$ $[M+H]^+$: 601.3800, found 601.3803.

4.1.14 Methyl (2S,4aS,6aS,6bR,8aR,13aS,13bR,15bR)-10-(4-chlorophenyl)-,4a,6a,6b, 9,9,13a-heptamethyl-14-oxo-2,3,4,4a,5,6,6a,6b,7,8,8a,9,10,13,13a,13b,14,15b -ctadecahydro-1H-chryseno[1,2-f]indazole-2-carboxylate **(GA-14)**

Compound **GA-14** was synthesized in the same procedure as that of **GA-6** (yield 70%); yellow solid. ^{1}H NMR (500 MHz, Acetone-d_6) δ 7.54 (d, J = 8.6 Hz, 2H), 7.46 – 7.40 (m, 2H), 7.29 (s, 1H), 5.62 (s, 1H), 3.70 (s, 3H), 2.81 (s, 2H), 1.98 – 1.86 (m, 3H), 1.84 – 1.76 (m, 2H), 1.64 – 1.49 (m, 4H), 1.48 – 1.41 (m, 5H), 1.40 (s, 1H), 1.36 (dd, J = 3.1, 10.1 Hz, 1H), 1.32 (d, J = 3.8 Hz, 1H), 1.30 – 1.24 (m, 4H), 1.15 (d, J = 5.3 Hz, 6H), 1.09 (s, 3H), 1.04 (d, J = 7.9 Hz, 4H), 0.84 (s, 4H); ^{13}C NMR (125 MHz, Acetone-d_6) δ 198.3, 176.2, 169.2, 145.5, 141.7, 138.2, 134.1, 130.9 (2×C), 128.5 (2×C), 128.1, 114.3, 60.1, 54.1, 51.1, 48.3, 44.9, 43.8, 43.2, 41.1, 37.8, 37.7, 37.3, 34.5, 31.7, 31.7, 30.7, 29.5, 28.1, 27.4, 26.4, 26.1, 22.7, 22.2, 18.2, 17.7, 15.0; HRMS (ESI): m/z calcd

for $C_{38}H_{50}ClN_2O_3$ $[M+H]^+$: 617.3504, found 617.3496.

4.1.15 Methyl (2S,4aS,6aS,6bR,8aR,13aS,13bR,15bR)-10-(4-bromophenyl)-2,4a,6a,6b,9,9,13a-heptamethyl-14-oxo-2,3,4,4a,5,6,6a,6b,7,8,8a,9,10,13,13a,13b,14,15b-octadecahydro-1H-chryseno[1,2-f]indazole-2-carboxylate **(GA-15)**

Compound **GA-15** was synthesized in the same procedure as that of **GA-6** (yield 75%); yellow solid. ^{1}H NMR (500 MHz, Acetone-d_6) δ 7.69 (d, J = 8.6 Hz, 2H), 7.37 (d, J = 8.6 Hz, 2H), 7.29 (s, 1H), 5.62 (s, 1H), 3.70 (s, 3H), 2.80 (s, 2H), 2.21 – 2.14 (m, 3H), 1.99 – 1.86 (m, 3H), 1.84 – 1.76 (m, 2H), 1.60 (td, J = 3.2, 11.8, 12.9 Hz, 2H), 1.56 – 1.47 (m, 3H), 1.46 (s, 3H), 1.41 (d, J = 13.8 Hz, 2H), 1.36 (dd, J = 3.2, 10.5 Hz, 1H), 1.19 (s, 3H), 1.15 (d, J = 5.5 Hz, 6H), 1.09 (s, 3H), 1.05 (s, 3H), 0.87 (t, J = 6.9 Hz, 1H), 0.84 (s, 3H); ^{13}C NMR (125 MHz, Acetone-d_6) δ 198.3, 176.2, 169.2, 145.5, 138.3, 131.6 (2×C), 131.2 (2×C), 128.1, 124.1, 122.2, 114.3, 60.1, 54.1, 51.1, 48.3, 44.9, 43.8, 43.2, 41.1, 37.8, 37.7, 37.2, 34.5, 31.7, 31.7, 30.7, 29.5, 28.1, 27.4, 26.4, 26.1, 22.7, 22.2, 18.2, 17.7, 15.0; HRMS (ESI): m/z calcd for $C_{38}H_{50}BrN_2O_3$ $[M+H]^+$: 661.2999, found 661.2989.

4.1.16 Methyl (2S,4aS,6aS,6bR,8aR,15aS,15bR,17bR)-2,4a,6a,6b,9,9,15a-heptamethyl-16-oxo-2,3,4,4a,5,6,6a,6b,7,8,8a,9,10,15,15a,15b,16,17b-octadecahydro-1H-chryseno[2,1-b]carbazole-2-carboxylate **(GA-16)**

Compound **GA-16** was synthesized in the same procedure as that of **GA-18** to obtain a colorless oil, which was used to hydrolysis reaction without further purification. HRMS (ESI): m/z calcd for $C_{37}H_{49}NO_3Na$ $[M+Na]^+$: 578.3605, found 578.3616.

4.1.17 Methyl (2S,4aS,6aS,6bR,8aR,15aS,15bR,17bR)-13-fluoro-2,4a,6a,6b,9,9,15a-heptam-e-thyl-16-oxo-2,3,4,4a,5,6,6a,6b,7,8,8a,9,10,15,15a,15b,16,17b-

octadecahydro-1H-chrys-eno[2,1-b]carbazole-2-carboxylate **(GA-17)**

Compound **GA-17** was synthesized in the same procedure as that of **GA-18** to obtain a colorless oil, which was used to hydrolysis reaction without further purification. HRMS (ESI): m/z calcd for $C_{37}H_{48}FNO_3Na$ $[M+Na]^+$: 596.3510, found 596.3528.

4.1.18 Methyl (2S,4aS,6aS,6bR,8aR,15aS,15bR,17bR)-13-chloro-2,4a,6a,6b,9,9,15a-heptame-thyl-16-oxo-2,3,4,4a,5,6,6a,6b,7,8,8a,9,10,15,15a,15b,16,17b-ctadecahydro-1H-chrys-eno[2,1-b]carbazole-2-carboxylate **(GA-18)**

To a solution of **GA-2** (48 mg, 0.1 mmol, 1.0 eq.) in acetic acid (10 mL) was added 4-chlorophenylhydrazine hydrochloride (22 mg, 0.12 mmol, 1.2 eq.) at 118 °C for 4 h. After cooling to room temperature, the solvents were removed and the residue was purified by a column chromatography (petroleum ether/AcOEt, 8/1−6/1−4/1, v/v) to give **GA-18** (47.1 mg, 80%) as a light red solid. ^{1}H NMR (500 MHz, $CDCl_3$) δ 7.45 (d, J = 1.9 Hz, 1H), 7.18 (d, J = 8.5 Hz, 1H), 7.05 (dd, J = 2.0, 8.5 Hz, 1H), 5.77 (s, 1H), 3.72 (s, 3H), 2.63 (s, 3H), 2.18 (d, J = 3.0 Hz, 6H), 1.69 – 1.61 (m, 4H), 1.42 (s, 4H), 1.37 (d, J = 20.2 Hz, 4H), 1.32 (d, J = 4.5 Hz, 4H), 1.22 (s, 3H), 1.19 (d, J = 6.4 Hz, 2H), 1.17 (s, 5H), 0.88 (s, 2H), 0.85 (s, 3H); ^{13}C NMR (125 MHz, $CDCl_3$) δ 210.8, 199.6, 176.9, 169.2, 141.7, 134.5, 128.7, 124.6, 121.1, 118.1, 111.0, 107.2, 69.5, 60.4, 53.8, 52.9, 51.8, 48.4, 45.3, 44.0, 43.3, 41.2, 38.0, 37.8, 37.4, 34.1, 31.7, 31.0, 29.7, 29.2, 28.6, 28.3, 26.5, 23.4, 23.3, 18.3, 16.0; HRMS (ESI): m/z calcd for $C_{37}H_{49}ClNO_3$ $[M+H]^+$: 590.3395, found 590.3372.

4.1.19 Methyl (2S,4aS,6aS,6bR,8aR,15aS,15bR,17bR)-13-bromo-2,4a,6a,6b,9,9,15a-heptame-thyl-16-oxo-2,3,4,4a,5,6,6a,6b,7,8,8a,9,10,15,15a,15b,16,17b-ctadecahydro-1H-chrys-eno[2,1-b]carbazole-2-carboxylate **(GA-19)**

Compound **GA-19** was synthesized in the same procedure as that of **GA-18** (yield

75%); brownish red solid. ^{1}H NMR (500 MHz, $CDCl_3$) δ 7.61 (s, 1H), 7.20 – 7.12 (m, 2H), 5.77 (s, 1H), 3.72 (s, 3H), 2.63 (s, 5H), 1.63 (d, J = 13.5 Hz, 4H), 1.53 (d, J = 12.5 Hz, 2H), 1.42 (s, 5H), 1.32 (d, J = 5.1 Hz, 6H), 1.23 – 1.18 (m, 6H), 1.17 (d, J = 1.7 Hz, 6H), 0.88 (t, J = 6.9 Hz, 3H), 0.85 (s, 3H); ^{13}C NMR (125 MHz, $CDCl_3$) δ 210.8, 199.6, 176.9, 169.2, 141.5, 134.8, 130.1, 128.7, 123.6, 121.1, 111.5, 107.1, 60.4, 53.8, 52.9, 51.8, 48.4, 45.3, 44.0, 43.3, 41.2, 38.0, 34.1, 31.9, 31.7, 31.2, 31.0, 29.7, 29.2, 28.6, 28.3, 26.6, 23.3, 22.7, 18.3, 16.0, 14.1; HRMS (ESI): m/z calcd for $C_{37}H_{48}BrNO_3Na$ $[M+Na]^+$: 656.2710, found 656.2702.

4.1.20 (2S,4aS,6aS,6bR,8aR,13aS,13bR,15bR)-2,4a,6a,6b,9,9,13a-heptamethyl-14 -oxo-12-(tr-ifluoromethyl)-2,3,4,4a,5,6,6a,6b,7,8,8a,9,11,13,13a,13b,14,15b-octadecahydro-1H-ch-ryseno[1,2-f]indazole-2-carboxylic acid **(GA-20)**

To a solution of **GA-5** (57.4 mg, 0.1 mmol, 1.0 eq.) in MeOH (20 mL) was added NaOH (20.0 mg, 0.5 mmol, 5.0 eq.) at room temperature for 72 h. After the reaction, dilute hydrochloric acid was added to neutralize (pH = 5). The solvents which had been neutralized were removed and the residue was purified by a column chromatography (petroleum ether/AcOEt, 4/1−2/1−1/1 v/v) to get **GA-20** (33.6 mg, 60%) as a pale yellow solid. ^{1}H NMR (500 MHz, $CDCl_3$) δ 5.78 (s, 1H), 2.64 (s, 1H), 2.57 (s, 1H), 2.25 (d, J = 13.4 Hz, 1H), 2.11 (d, J = 16.4 Hz, 1H), 2.04 (dd, J = 7.2, 15.6 Hz, 2H), 1.95 (d, J = 12.3 Hz, 1H), 1.91 – 1.83 (m, 1H), 1.74 (d, J = 11.1 Hz, 1H), 1.68 – 1.60 (m, 3H), 1.58 – 1.49 (m, 3H), 1.44 (d, J = 7.9 Hz, 2H), 1.40 (s, 3H), 1.34 (s, 4H), 1.23 (s, 3H), 1.20 (d, J = 5.0 Hz, 4H), 1.13 (s, 3H), 1.07 (t, J = 10.8 Hz, 2H), 0.92 (t, J = 7.5 Hz, 1H), 0.86 (s, 3H); ^{13}C NMR (125 MHz, $CDCl_3$) δ 199.0, 180.7, 169.4, 148.6, 128.6, 122.5, 120.1, 114.3, 59.9, 53.8, 52.3, 48.1, 45.3, 43.7, 43.3, 38.0, 37.7, 33.1, 31.9, 31.0, 29.7, 29.3, 29.2, 28.6, 28.4, 26.4, 23.8, 23.2, 22.7, 18.2, 15.7, 14.1. HRMS (ESI): m/z

calcd for $C_{32}H_{43}F_3N_2O_3Na$ $[M+Na]^+$: 583.3118, found 583.3144.

4.1.21 (2S,4aS,6aS,6bR,8aR,13aS,13bR,15bR)-2,4a,6a,6b,9,9,13a-heptamethyl-14-oxo-2,3,4,4a,5,6,6a,6b,7,8,8a,9,11,13,13a,13b,14,15b-octadecahydro-1H-chryseno [1,2-f]indazole-2-carboxylic acid **(GA-21)**

Compound **GA-21** was synthesized in the same procedure as that of **GA-20** (yield 55%); pale yellow solid. ^{1}H NMR (500 MHz, $CDCl_3$) δ 7.54 (s, 1H), 6.17 (s, 1H), 2.64 – 2.58 (m, 1H), 2.35 (t, J = 7.5 Hz, 1H), 2.05 – 1.96 (m, 4H), 1.86 (d, J = 11.1 Hz, 2H), 1.74 (s, 3H), 1.66 (s, 4H), 1.42 (s, 3H), 1.39 (s, 4H), 1.10 (s, 4H), 1.08 (s, 1H), 0.99 (s, 3H), 0.94 (s, 3H), 0.88 (t, J = 6.9 Hz, 7H); ^{13}C NMR (125 MHz, $CDCl_3$) δ 198.5, 178.9, 165.2, 162.7, 132.4, 123.1, 87.5, 59.4, 50.2, 45.4, 44.6, 43.8, 36.5, 34.9, 32.6, 31.9, 31.3, 30.9, 29.4, 29.3, 29.2, 29.1, 27.1, 24.7, 23.1, 22.7, 22.1, 20.6, 18.1, 15.5, 14.1; HRMS (ESI): m/z calcd for $C_{31}H_{45}N_2O_3$ $[M+H]^+$: 493.3425, found 493.3430.

4.1.22 (2S,4aS,6aS,6bR,8aR,13aS,13bR,15bR)-2,4a,6a,6b,9,9,13a-heptamethyl-14-oxo-1,2,3,4,4a,5,6,6a,6b,7,8,8a,9,13,13a,13b,14,15b-octadecahydropiceno[2,3-d]isoxazole-2-car-boxylic acid **(GA-22)**

Compound **GA-22** was synthesized in the same procedure as that of **GA-20** (yield 65%); white solid. ^{1}H NMR (500 MHz, CD_3OD) δ 8.07 (d, J = 13.7 Hz, 1H), 5.70 (s, 1H), 3.80 (d, J = 15.5 Hz, 1H), 2.54 (d, J = 11.1 Hz, 1H), 2.29 – 2.11 (m, 3H), 2.10 – 1.81 (m, 6H), 1.79 – 1.59 (m, 4H), 1.55 (d, J = 19.8 Hz, 3H), 1.40 – 1.37 (m, 4H), 1.36 – 1.33 (m, 4H), 1.16 (d, J = 6.4 Hz, 6H), 1.04 (s, 4H), 0.82 (d, J = 5.5 Hz, 4H); ^{13}C NMR (125 MHz, CD_3OD) δ 200.3, 179.2, 167.5, 153.9, 151.4, 128.0, 113.3, 59.6, 53.0, 45.2, 43.6, 43.4, 41.2, 37.7, 37.6, 34.4, 33.7, 31.8, 31.6, 31.1, 30.9, 29.5, 28.4, 28.1, 26.5, 26.2, 24.5, 23.0, 18.2, 18.0, 15.0; HRMS (ESI): m/z calcd for $C_{31}H_{43}NO_4Na$

$[M+Na]^+$: 516.3084, found 516.3123.

4.1.23 (2S,4aS,6aS,6bR,8aR,13aS,13bR,15bR)-2,4a,6a,6b,9,9,13a-heptamethyl-14-oxo-10-ph-enyl-12-(trifluoromethyl)-,3,4,4a,5,6,6a,6b,7,8,8a,9,10,13,13a,13b,14,15b-octadecahy-dro-1H-chryseno[1,2-f]indazole-2-carboxylic acid **(GA-23)**

Compound **GA-23** was synthesized in the same procedure as that of **GA-20** (yield 60%); pale yellow solid. ^{1}H NMR (500 MHz, CD_3OD) δ 7.49 (dt, J = 7.0, 14.2 Hz, 5H), 5.62 (s, 1H), 3.77 (d, J = 15.8 Hz, 1H), 2.53 (s, 1H), 2.30 (d, J = 11.3 Hz, 1H), 2.16 (t, J = 9.4 Hz, 3H), 2.06 – 1.81 (m, 4H), 1.71 (d, J = 12.0 Hz, 3H), 1.64 – 1.53 (m, 6H), 1.47 (dd, J = 11.7, 21.5 Hz, 6H), 1.37 (s, 3H), 1.35 (s, 1H), 1.07 (s, 7H), 0.84 (d, J = 8.5 Hz, 1H), 0.74 (s, 3H); ^{13}C NMR (125 MHz, CD_3OD) δ 199.9, 181.1, 167.7, 148.4, 140.9, 139.4, 129.9, 129.2, 128.8 (2×C), 128.7 (2×C), 123.7, 113.0, 59.1, 53.7, 45.1, 43.6, 42.1, 40.4, 37.3, 36.2, 35.9, 35.6, 34.7, 32.8, 31.7, 29.5, 28.8, 28.6, 28.4, 26.6, 22.1, 20.3, 18.2, 17.9, 15.7, 15.7; HRMS (ESI): m/z calcd for $C_{38}H_{47}F_3N_2O_3Na$ $[M+Na]^+$: 659.3431, found 659.3428.

4.1.24 (2S,4aS,6aS,6bR,8aR,13aS,13bR,15bR)-10-(4-fluorophenyl)-2,4a,6a,6b,9,9,13a-hepta-methyl-14-oxo-12-(trifluoromethyl)-,3,4,4a,5,6,6a,6b,7,8,8a,9,10,13,13a,13b,14,15b-octadecahydro-1H-chryseno[1,2-f]indazole-2-carboxylic acid **(GA-24)**

Compound **GA-24** was synthesized in the same procedure as that of **GA-20** (yield 60%); pale yellow solid. ^{1}H NMR (500 MHz, CD_3OD) δ 7.41 (d, J = 7.2 Hz, 2H), 7.21 – 7.15 (m, 2H), 5.62 (s, 1H), 3.77 (d, J = 15.9 Hz, 1H), 2.53 (s, 1H), 2.30 (d, J = 10.6 Hz, 1H), 2.20 – 2.12 (m, 3H), 2.05 – 1.86 (m, 3H), 1.70 (t, J = 12.7 Hz, 3H), 1.64 – 1.54 (m, 5H), 1.48 (dd, J = 13.1, 21.7 Hz, 5H), 1.17 (d, J = 8.4 Hz, 5H), 1.07 (s, 7H), 0.93 – 0.80 (m, 3H), 0.74 (s, 3H); ^{13}C NMR (125 MHz, CD_3OD) δ 199.8, 181.0, 167.7, 162.1, 148.6, 136.9, 136.9, 130.9, 130.8, 123.7, 115.7, 115.5, 113.2, 113.2, 59.1, 53.7,

45.1, 43.6, 42.1, 40.4, 37.3, 36.2, 35.9, 35.6, 34.7, 32.8, 31.7, 30.3, 29.5, 28.9, 28.6, 28.4, 26.6, 22.1, 20.3, 18.2, 17.9, 15.7; HRMS (ESI): m/z calcd for $C_{38}H_{46}F_4N_2O_3Na$ $[M+Na]^+$: 677.3337, found 677.3351.

4.1.25 (2S,4aS,6aS,6bR,8aR,13aS,13bR,15bR)-10-(4-chlorophenyl)-,4a,6a,6b,9,9,13a-hepta-methyl-14-oxo-12-(trifluoromethyl)-2,3,4,4a,5,6,6a,6b,7,8,8a,9,10,13,13a,13b, 14,15b-o-ctadecahydro-1H-chryseno[1,2-f]indazole-2-carboxylic acid **(GA-25)**

Compound **GA-25** was synthesized in the same procedure as that of **GA-20** (yield 60%); pale yellow solid. ^{1}H NMR (500 MHz, CD_3OD) δ 7.47 (s, 2H), 7.38 (s, 2H), 5.62 (s, 1H), 3.77 (d, J = 15.8 Hz, 1H), 2.53 (s, 1H), 2.30 (d, J = 10.8 Hz, 1H), 2.16 (s, 4H), 2.08 – 1.84 (m, 3H), 1.77 – 1.67 (m, 3H), 1.64 – 1.55 (m, 5H), 1.48 (d, J = 12.2 Hz, 5H), 1.38 (s, 3H), 1.31 (d, J = 10.9 Hz, 3H), 1.08 (s, 7H), 0.85 (d, J = 16.6 Hz, 1H), 0.74 (s, 3H); ^{13}C NMR (125 MHz, CD_3OD) δ 199.8, 181.0, 167.8, 148.6, 139.4, 135.9, 130.3, 128.9, 125.8, 123.6, 120.6, 113.3, 59.1, 53.7, 45.1, 43.6, 42.1, 40.4, 37.3, 36.2, 35.8, 35.6, 34.7, 32.8, 31.7, 30.3, 29.5, 28.9, 28.4, 26.6, 22.2, 20.3, 18.2, 17.9, 15.7, 15.6; HRMS (ESI): m/z calcd for $C_{38}H_{46}ClF_3N_2O_3Na$ $[M+Na]^+$: 693.3041, found 693.3059.

4.1.26 (2S,4aS,6aS,6bR,8aR,13aS,13bR,15bR)-10-(4-bromophenyl)-,4a,6a,6b,9,9, 13a-hepta-methyl-14-oxo-12-trifluoromethyl)-,3,4,4a,5,6,6a,6b,7,8,8a,9,10,13,13a, 13b, 14,15b-o-ctadecahydro-1H-chryseno[1,2-f]indazole-2-carboxylic acid **(GA-26)**

Compound **GA-26** was synthesized in the same procedure as that of **GA-20** (yield 60%); pale yellow solid. ^{1}H NMR (500 MHz, CD_3OD) δ 7.68 – 7.59 (m, 2H), 7.33 – 7.27 (m, 2H), 5.62 (s, 1H), 3.77 (d, J = 15.9 Hz, 1H), 2.53 (s, 1H), 2.30 (d, J = 11.6 Hz, 1H), 2.15 (d, J = 22.8 Hz, 5H), 2.06 – 1.86 (m, 3H), 1.70 (t, J = 12.5 Hz, 2H), 1.59 (t, J = 12.5 Hz, 5H), 1.52 – 1.43 (m, 5H), 1.37 (s, 4H), 1.31 (d, J = 8.8 Hz, 2H), 1.07 (s,

7H), 0.89 – 0.79 (m, 1H), 0.74 (s, 3H); ^{13}C NMR (125 MHz, CD_3OD) δ 199.8, 181.0, 167.7, 148.6, 139.9, 132.0 (2×C), 130.5 (2×C), 124.0, 123.7, 122.7, 120.6, 113.3, 59.1, 53.7, 45.1, 43.6, 42.1, 40.4, 37.3, 36.2, 35.9, 35.6, 34.7, 32.8, 31.7, 29.5, 28.9, 28.6, 28.4, 26.6, 22.2, 20.3, 18.2, 17.9, 15.7, 15.7; HRMS (ESI): m/z calcd for $C_{38}H_{46}BrF_3N_2O_3Na$ $[M+Na]^+$: 737.2536, found 737.2555.

4.1.27 (2S,4aS,6aS,6bR,8aR,13aS,13bR,15bR)-2,4a,6a,6b,9,9,13a-heptamethyl-14-oxo-10-ph-enyl-2,3,4,4a,5,6,6a,6b,7,8,8a,9,10,13,13a,13b,14,15b-octadecahydro-1H-chryseno[1,2-f]indazole-2-carboxylic acid **(GA-27)**

Compound **GA-27** was synthesized in the same procedure as that of **GA-20** (yield 65%); pale yellow solid. ^{1}H NMR (500 MHz, CD_3OD) δ 7.49 – 7.41 (m, 3H), 7.36 (d, J = 4.0 Hz, 2H), 7.30 (s, 1H), 5.71 (s, 1H), 3.70 (d, J = 15.4 Hz, 1H), 2.60 (d, J = 8.3 Hz, 1H), 2.23 (d, J = 11.6 Hz, 1H), 2.19 – 2.11 (m, 2H), 2.06 (s, 1H), 1.93 (dd, J = 15.0, 20.8 Hz, 3H), 1.77 – 1.54 (m, 4H), 1.51 (d, J = 7.3 Hz, 2H), 1.40 (d, J = 3.9 Hz, 5H), 1.17 (s, 6H), 1.13 (s, 3H), 1.08 – 1.04 (m, 4H), 1.02 (s, 3H), 0.83 (s, 4H); ^{13}C NMR (125 MHz, CD_3OD) δ 200.6, 179.2, 171.5, 146.4, 141.5, 138.0, 129.3, 129.1 (2×C), 128.5 (2×C), 128.1, 114.4, 60.3, 54.3, 45.2, 43.6, 43.4, 41.2, 37.9, 37.7, 37.4, 34.7, 31.8, 30.9, 29.5, 29.1, 28.4, 28.1, 28.0, 26.4, 26.3, 23.0, 22.2, 18.2, 18.0, 15.3; HRMS (ESI): m/z calcd for $C_{37}H_{49}N_2O_3$ $[M+H]^+$: 569.3738, found 569.3742.

4.1.28 (2S,4aS,6aS,6bR,8aR,13aS,13bR,15bR)-10-(4-fluorophenyl)-2,4a,6a,6b,9,9,13a-hepta-methyl-14-oxo-2,3,4,4a,5,6,6a,6b,7,8,8a,9,10,13,13a,13b,14,15b-octadecahydro-1H-chryseno[1,2-f]indazole-2-carboxylic acid **(GA-28)**

Compound **GA-28** was synthesized in the same procedure as that of **GA-20** (yield 55%); pale yellow solid. ^{1}H NMR (500 MHz, Acetone-d_6) δ 10.72 (s, 1H), 7.45 (dd, J = 4.9, 8.8 Hz, 2H), 7.34 (s, 1H), 7.24 (t, J = 8.7 Hz, 2H), 5.62 (s, 1H), 3.71 (d, J = 15.4

Hz, 1H), 2.66 (s, 1H), 2.31 – 2.10 (m, 4H), 1.99 – 1.85 (m, 4H), 1.79 (t, *J* = 13.4 Hz, 2H), 1.65 – 1.58 (m, 2H), 1.56 – 1.48 (m, 3H), 1.47 (s, 3H), 1.20 (d, *J* = 3.8 Hz, 6H), 1.15 (s, 3H), 1.09 (d, *J* = 4.6 Hz, 3H), 1.04 (s, 4H), 0.90 (d, *J* = 7.4 Hz, 1H), 0.86 (s, 3H); ^{13}C NMR (125 MHz, Acetone-d_6) δ 198.2, 177.0, 169.5, 163.7, 138.6, 137.6, 131.8, 128.1, 115.2 (2×C), 115.0 (2×C), 114.4, 70.2, 60.0, 54.0, 48.4, 44.9, 43.4, 43.3, 41.2, 37.8, 37.1, 34.6, 31.7, 31.6, 30.7, 28.2, 27.5, 26.4, 26.2, 22.7, 21.9, 19.1, 18.2, 17.7, 15.0; HRMS (ESI): m/z calcd for $C_{37}H_{48}FN_2O_3$ $[M+H]^+$: 587.3643, found 587.3649.

4.1.29 (2S,4aS,6aS,6bR,8aR,13aS,13bR,15bR)-10-(4-chlorophenyl)-2,4a,6a,6b,9,9,13a-hepta-methyl-14-oxo-2,3,4,4a,5,6,6a,6b,7,8,8a,9,10,13,13a,13b,14,15b-octadecahydro-1H-ch-ryseno[1,2-f]indazole-2-carboxylic acid **(GA-29)**

Compound **GA-29** was synthesized in the same procedure as that of **GA-20** (yield 60%); yellow solid. ^{1}H NMR (500 MHz, Acetone-d_6) δ 10.67 (s, 1H), 7.53 (d, *J* = 8.7 Hz, 2H), 7.43 (d, *J* = 8.7 Hz, 2H), 7.33 (s, 1H), 5.62 (s, 1H), 3.70 (d, *J* = 15.4 Hz, 1H), 2.66 (s, 1H), 2.29 – 2.16 (m, 3H), 1.90 (ddd, *J* = 6.2, 8.7, 17.9 Hz, 3H), 1.79 (t, *J* = 13.4 Hz, 2H), 1.60 (ddd, *J* = 7.9, 12.7, 17.6 Hz, 2H), 1.55 – 1.48 (m, 2H), 1.46 (s, 3H), 1.42 (dd, *J* = 2.9, 9.8 Hz, 4H), 1.20 (d, *J* = 3.0 Hz, 6H), 1.15 (s, 3H), 1.09 (s, 3H), 1.05 (s, 3H), 0.89 (s, 1H), 0.86 (s, 3H); ^{13}C NMR (125 MHz, Acetone-d_6) δ 198.2, 192.4, 169.4, 138.4, 134.3, 133.0, 131.1 (2×C), 128.5 (2×C), 128.1, 121.7, 120.0, 60.0, 54.1, 48.4, 44.9, 44.4, 43.3, 43.3, 41.2, 37.8, 37.2, 34.5, 31.7, 31.7, 31.7, 30.7, 28.2, 27.5, 26.4, 26.2, 22.7, 22.1, 18.2, 17.7, 15.0; HRMS (ESI): m/z calcd for $C_{37}H_{48}ClN_2O_3$ $[M+H]^+$: 603.3348, found 603.3341.

4.1.30 (2S,4aS,6aS,6bR,8aR,13aS,13bR,15bR)-10-(4-bromophenyl)-2,4a,6a,6b,9,9,13a-hepta-methyl-14-oxo-2,3,4,4a,5,6,6a,6b,7,8,8a,9,10,13,13a,13b,14,15b-octadecahydro-1H-ch-ryseno[1,2-f]indazole-2-carboxylic acid **(GA-30)**

Compound **GA-30** was synthesized in the same procedure as that of **GA-20** (yield 60%); yellow solid. ^{1}H NMR (500 MHz, Acetone-d_6) δ 10.66 (s, 1H), 7.71 – 7.66 (m, 2H), 7.39 – 7.32 (m, 3H), 5.62 (s, 1H), 3.71 (d, J = 15.4 Hz, 1H), 2.66 (s, 1H), 2.19 (d, J = 15.5 Hz, 3H), 1.94 – 1.87 (m, 3H), 1.79 (t, J = 13.4 Hz, 3H), 1.64 – 1.57 (m, 3H), 1.52 (d, J = 12.8 Hz, 3H), 1.46 (s, 4H), 1.20 (d, J = 3.3 Hz, 6H), 1.15 (s, 3H), 1.10 (s, 3H), 1.05 (s, 3H), 0.86 (s, 4H); ^{13}C NMR (125 MHz, Acetone-d_6) δ 198.2, 189.1, 176.9, 169.4, 161.5, 137.9, 136.4, 131.6 (2×C), 131.4 (2×C), 128.1, 120.0, 60.0, 56.7, 54.1, 51.8, 48.4, 44.9, 43.4, 43.3, 41.2, 37.8, 37.1, 34.5, 31.7, 30.7, 28.2, 27.5, 26.4, 26.2, 22.7, 22.4, 22.1, 18.2, 17.7, 15.0; HRMS (ESI): m/z calcd for $C_{37}H_{48}BrN_2O_3$ $[M+H]^+$: 647.2843, found 647.2841.

4.1.31 (2S,4aS,6aS,6bR,8aR,15aS,15bR,17bR)-2,4a,6a,6b,9,9,15a-heptamethyl-16-oxo-2,3,4,4a,5,6,6a,6b,7,8,8a,9,10,15,15a,15b,16,17b-octadecahydro-1H-hryseno[2,1-b]carbazo-le-2-carboxylic acid **(GA-31)**

Compound **GA-31** was synthesized in the same procedure as that of **GA-20** (yield 60%); pale yellow solid. ^{1}H NMR (500 MHz, CD_3OD) δ 7.37 (d, J = 7.6 Hz, 1H), 7.27 (d, J = 7.9 Hz, 1H), 7.01 (t, J = 7.4 Hz, 1H), 6.95 (d, J = 7.4 Hz, 1H), 5.62 (s, 1H), 3.75 (d, J = 15.3 Hz, 1H), 2.62 (s, 1H), 2.31 (d, J = 11.2 Hz, 1H), 2.27 – 2.11 (m, 4H), 2.09 – 1.99 (m, 1H), 1.93 (t, J = 12.6 Hz, 1H), 1.77 (dd, J = 12.5, 24.2 Hz, 1H), 1.73 – 1.66 (m, 2H), 1.60 (t, J = 11.8 Hz, 5H), 1.31 (d, J = 7.2 Hz, 4H), 1.23 (s, 9H), 1.21 (s, 6H), 0.88 – 0.80 (m, 1H), 0.75 (s, 3H); ^{13}C NMR (125 MHz, CD_3OD) δ 200.8, 181.1, 167.4, 140.7, 136.5, 127.8, 123.8, 120.2, 117.9, 117.5, 110.3, 105.6, 59.5, 53.2, 45.1, 43.9, 42.2, 40.4, 37.8, 37.5, 37.4, 35.9, 35.5, 34.0, 33.1, 31.7, 30.4, 29.5, 28.4, 26.6, 22.7, 20.3, 18.4, 18.0, 15.8, 15.7;HRMS (ESI): m/z calcd for $C_{36}H_{47}NO_3Na$ $[M+Na]^+$: 564.3448, found 564.3477.

4.1.32 (2S,4aS,6aS,6bR,8aR,15aS,15bR,17bR)-13-fluoro-2,4a,6a,6b,9,9,15a-heptamethyl-16-oxo-2,3,4,4a,5,6,6a,6b,7,8,8a,9,10,15,15a,15b,16,17b-octadecahydro-1H-chryseno[2,1-b]carbazole-2-carboxylic acid **(GA-32)**

Compound **GA-32** was synthesized in the same procedure as that of **GA-20** (yield 60%); pale yellow solid. ^{1}H NMR (500 MHz, CD_3OD) δ 7.16 (dd, J = 4.4, 8.7 Hz, 1H), 6.99 (dd, J = 2.4, 9.8 Hz, 1H), 6.74 (td, J = 2.5, 9.2 Hz, 1H), 2.60 (d, J = 6.7 Hz, 1H), 2.33 – 2.22 (m, 2H), 2.20 – 2.13 (m, 2H), 2.07 – 1.87 (m, 3H), 1.82 – 1.64 (m, 4H), 1.64 – 1.54 (m, 5H), 1.47 (d, J = 10.2 Hz, 4H), 1.40 – 1.32 (m, 7H), 1.30 (s, 3H), 1.19 (d, J = 3.2 Hz, 6H), 0.84 (t, J = 6.9 Hz, 1H), 0.74 (s, 3H); ^{13}C NMR (125 MHz, CD_3OD) δ 201.1, 179.2, 171.3, 158.2, 156.4, 142.8, 133.0, 128.1, 110.7, 108.1, 102.4, 60.5, 53.0, 45.4, 43.6, 43.4, 41.2, 38.0, 37.7, 37.5, 34.2, 32.0, 31.8, 30.9, 30.4, 29.5, 28.7, 28.4, 28.1, 26.5, 26.3, 23.0, 22.8, 18.4, 18.1, 15.7; HRMS (ESI): m/z calcd for $C_{36}H_{46}FNO_3Na$ $[M+Na]^+$: 582.3354, found 582.3385.

4.1.33 (2S,4aS,6aS,6bR,8aR,15aS,15bR,17bR)-13-chloro-2,4a,6a,6b,9,9,15a-heptamethyl-16-oxo-2,3,4,4a,5,6,6a,6b,7,8,8a,9,10,15,15a,15b,16,17b-octadecahydro-1H-chryseno[2,1-b]carbazole-2-carboxylic acid **(GA-33)**

Compound **GA-33** was synthesized in the same procedure as that of **GA-20** (yield 55%); pale yellow solid. ^{1}H NMR (500 MHz, CD_3OD) δ 7.53 – 7.48 (m, 2H), 6.98 (dd, J = 2.0, 8.5 Hz, 1H), 5.62 (s, 1H), 3.63 (s, 1H), 2.61 (s, 1H), 2.34 – 2.22 (m, 2H), 2.17 (s, 1H), 2.09 – 1.86 (m, 4H), 1.84 – 1.69 (m, 4H), 1.64 (d, J = 10.0 Hz, 4H), 1.58 (t, J = 11.2 Hz, 4H), 1.48 (d, J = 10.1 Hz, 4H), 1.41 (s, 3H), 1.33 (s, 5H), 1.10 (s, 3H), 0.79 (d, J = 4.1 Hz, 1H), 0.75 (s, 3H); ^{13}C NMR (125 MHz, CD_3OD) δ 201.7, 181.2, 167.7, 144.7, 134.8, 129.7, 124.4, 123.8, 120.5, 117.4, 111.5, 106.8, 54.5, 50.6, 45.8, 45.4,

43.4, 42.2, 40.4, 37.5, 35.9, 35.5, 34.1, 32.6, 31.6, 30.0, 29.5, 29.2, 28.7, 26.7, 23.2, 22.5, 20.7, 18.3, 15.9, 13.7; HRMS (ESI): m/z calcd for $C_{36}H_{46}ClNO_3Na$ $[M+Na]^+$: 598.3058, found 598.3063.

4.1.34 (2S,4aS,6aS,6bR,8aR,15aS,15bR,17bR)-13-bromo-2,4a,6a,6b,9,9,15a-heptamethyl-16-oxo-2,3,4,4a,5,6,6a,6b,7,8,8a,9,10,15,15a,15b,16,17b-octadecahydro-1H-chryseno[2,1-b]carbazole-2-carboxylic acid **(GA-34)**

Compound **GA-34** was synthesized in the same procedure as that of **GA-20** (yield 55%); light brown solid. ^{1}H NMR (500 MHz, CD_3OD) δ 7.50 – 7.47 (m, 1H), 7.14 (d, J = 8.5 Hz, 1H), 7.07 (dd, J = 1.9, 8.5 Hz, 1H), 5.71 (s, 1H), 3.79 (d, J = 15.4 Hz, 1H), 2.67 (s, 1H), 2.28 – 2.19 (m, 2H), 2.16 (d, J = 9.4 Hz, 3H), 2.07 (td, J = 4.1, 13.6 Hz, 1H), 1.98 – 1.83 (m, 4H), 1.82 – 1.74 (m, 1H), 1.65 (q, J = 13.5, 14.5 Hz, 3H), 1.61 – 1.49 (m, 4H), 1.42 (s, 3H), 1.40 – 1.36 (m, 3H), 1.19 (s, 3H), 1.16 (s, 3H), 1.11 (s, 4H), 0.84 (d, J = 5.0 Hz, 4H); ^{13}C NMR (125 MHz, CD_3OD) δ 201.0, 179.2, 171.3, 142.3, 135.2, 129.7, 128.1, 122.8, 120.2, 111.7, 111.1, 105.6, 60.5, 53.0, 45.4, 43.6, 43.4, 41.2, 37.9, 37.7, 37.4, 34.1, 31.8, 30.9, 30.3, 29.5, 28.7, 28.4, 28.1, 26.5, 26.3, 23.0, 22.7, 18.4, 18.1, 15.6; HRMS (ESI): m/z calcd for $C_{36}H_{46}BrNO_3Na$ $[M+Na]^+$: 642.2553, found 642.2566.

4.1.35 Methyl (2S,4aS,6aS,6bR,8aR,13aS,13bR,15bR)-10-(3-fluorophenyl)-,4a,6a,6b, 9,9, 13a-heptamethyl-14-oxo-2,3,4,4a,5,6,6a,6b,7,8,8a,9,10,13,13a,13b,14,15b-octade cahydro-1H-chryseno[1,2-f]indazole-2-carboxylate **(GA-35)**

Compound **GA-35** was synthesized in the same procedure as that of **GA-6** (yield 70%); pale yellow solid. ^{1}H NMR (500 MHz, Acetone-d_6) δ 7.59 – 7.50 (m, 1H), 7.34 – 7.26 (m, 3H), 7.22 (dt, J = 2.2, 9.5 Hz, 1H), 5.62 (s, 1H), 3.70 (s, 3H), 2.78 (d, J = 16.9 Hz, 2H), 2.20 – 2.13 (m, 3H), 1.97 – 1.86 (m, 3H), 1.84 – 1.76 (m, 2H), 1.60 (dd,

J = 2.8, 11.1 Hz, 2H), 1.57 – 1.49 (m, 2H), 1.46 (s, 3H), 1.44 – 1.37 (m, 3H), 1.20 (s, 4H), 1.15 (d, *J* = 2.5 Hz, 6H), 1.11 (s, 3H), 1.07 (s, 3H), 0.84 (s, 4H); ^{13}C NMR (125 MHz, Acetone-d_6) δ 198.3, 176.2, 169.2, 162.9, 138.3, 129.9, 129.8, 128.1, 125.4, 116.7, 115.8, 115.7, 114.3, 60.1, 54.1, 51.0, 48.3, 44.9, 43.8, 43.2, 41.1, 37.8, 37.7, 37.2, 34.5, 31.7, 31.7, 30.7, 29.6, 28.1, 27.4, 26.4, 26.1, 22.7, 22.1, 18.2, 17.7, 15.0; HRMS (ESI): m/z calcd for $C_{38}H_{50}FN_2O_3$ $[M+H]^+$: 601.3800, found 601.3822.

4.1.26 Methyl (2S,4aS,6aS,6bR,8aR,13aS,13bR,15bR)-10-(2-fluorophenyl)-,4a,6a,6b, 9,9,13a-heptamethyl-14-oxo-2,3,4,4a,5,6,6a,6b,7,8,8a,9,10,13,13a,13b,14,15b-octadecahydro-1H-chryseno[1,2-f]indazole-2-carboxylate **(GA-36)**

Compound **GA-36** was synthesized in the same procedure as that of **GA-6** (yield 70%); pale yellow solid. ^{1}H NMR (500 MHz, Acetone-d_6) δ 7.63 – 7.56 (m, 1H), 7.53 (td, *J* = 1.6, 7.7 Hz, 1H), 7.38 – 7.29 (m, 3H), 5.62 (s, 1H), 3.70 (s, 3H), 2.80 (s, 1H), 2.66 (s, 1H), 2.24 – 2.15 (m, 3H), 2.08 (s, 3H), 1.99 – 1.86 (m, 3H), 1.84 – 1.76 (m, 2H), 1.66 – 1.55 (m, 2H), 1.54 – 1.48 (m, 2H), 1.46 (s, 3H), 1.42 (ddt, *J* = 3.7, 7.0, 13.7 Hz, 3H), 1.34 (dd, *J* = 3.8, 14.1 Hz, 1H), 1.30 – 1.24 (m, 2H), 1.20 (s, 3H), 1.15 (s, 6H), 1.09 (s, 1H), 1.04 (s, 1H), 0.84 (s, 3H); ^{13}C NMR (125 MHz, Acetone-d_6) δ 198.3, 176.2, 169.2, 159.8, 157.8, 138.7, 131.7, 128.1, 124.1, 124.1, 116.2, 116.0, 114.1, 60.0, 51.1, 48.3, 44.9, 43.8, 43.6, 43.2, 41.1, 37.9, 37.7, 37.2, 34.3, 31.7, 31.7, 30.7, 29.7, 28.1, 28.1, 27.4, 26.4, 26.2, 22.7, 19.0, 18.2, 17.7; HRMS (ESI): m/z calcd for $C_{38}H_{50}FN_2O_3$ $[M+H]^+$: 601.3800, found 601.3817.

4.1.37 Methyl (2S,4aS,6aS,6bR,8aR,13aS,13bR,15bR)-10-(3-chlorophenyl)-,4a,6a,6b, 9,9,13a-heptamethyl-14-oxo-2,3,4,4a,5,6,6a,6b,7,8,8a,9,10,13,13a,13b,14,15b-octadecahydro-1H-chryseno[1,2-f]indazole-2-carboxylate **(GA-37)**

Compound **GA-37** was synthesized in the same procedure as that of **GA-6** (yield

72%); pale yellow solid. ^{1}H NMR (500 MHz, Acetone-d_6) δ 7.61 – 7.49 (m, 2H), 7.46 (t, J = 1.8 Hz, 1H), 7.40 (dt, J = 1.7, 7.4 Hz, 1H), 7.29 (d, J = 4.9 Hz, 1H), 5.62 (s, 1H), 3.70 (s, 3H), 2.77 (s, 1H), 2.65 (s, 1H), 2.22 – 2.14 (m, 3H), 1.98 – 1.86 (m, 3H), 1.85 – 1.75 (m, 2H), 1.60 (ddd, J = 3.0, 13.0, 23.8 Hz, 2H), 1.54 – 1.48 (m, 2H), 1.46 (s, 3H), 1.44 – 1.37 (m, 3H), 1.36 – 1.31 (m, 1H), 1.27 (d, J = 10.5 Hz, 3H), 1.15 (d, J = 2.9 Hz, 6H), 1.10 (s, 3H), 1.07 (s, 3H), 0.84 (s, 4H); ^{13}C NMR (125 MHz, Acetone-d_6) δ 198.3, 176.2, 169.2, 138.4, 133.3, 129.8, 129.3, 128.9, 128.1, 127.9, 120.5, 118.3, 114.4, 60.1, 54.1, 51.0, 48.3, 44.9, 43.8, 43.2, 41.1, 37.8, 37.7, 37.2, 34.5, 31.7, 31.7, 30.7, 29.6, 28.1, 27.4, 26.4, 26.1, 22.7, 22.2, 18.2, 17.7, 15.0; HRMS (ESI): m/z calcd for $C_{38}H_{50}ClN_2O_3$ $[M+H]^+$: 617.3504, found 617.3522.

4.1.38 Methyl (2S,4aS,6aS,6bR,8aR,13aS,13bR,15bR)-10-(2-chlorophenyl)-,4a,6a,6b,9,9,13a-heptamethyl-14-oxo-2,3,4,4a,5,6,6a,6b,7,8,8a,9,10,13,13a,13b,14,15b-octadecahydro-1H-chryseno[1,2-f]indazole-2-carboxylate **(GA-38)**

Compound **GA-38** was synthesized in the same procedure as that of **GA-6** (yield 70%); pale yellow solid. ^{1}H NMR (500 MHz, Acetone-d_6) δ 7.65 – 7.46 (m, 4H), 7.34 (d, J = 3.1 Hz, 1H), 5.62 (s, 1H), 3.70 (s, 3H), 2.77 (s, 2H), 2.23 – 2.13 (m, 3H), 1.98 – 1.86 (m, 3H), 1.85 – 1.77 (m, 2H), 1.65 – 1.49 (m, 4H), 1.47 (d, J = 1.9 Hz, 3H), 1.44 – 1.39 (m, 2H), 1.34 (dd, J = 3.7, 14.1 Hz, 1H), 1.30 – 1.21 (m, 4H), 1.20 (d, J = 1.8 Hz, 3H), 1.18 (d, J = 1.8 Hz, 3H), 1.15 (s, 3H), 1.12 (s, 1H), 1.08 – 1.01 (m, 1H), 1.00 (s, 1H), 0.92 (s, 1H), 0.84 (s, 3H); ^{13}C NMR (125 MHz, Acetone-d_6) δ 200.6, 198.3, 197.6, 176.2, 164.6, 160.2, 143.0, 138.7, 131.6, 129.9, 128.1, 127.1, 114.1, 60.1, 59.9, 54.1, 53.9, 51.0, 48.3, 44.9, 44.9, 43.8, 43.2, 41.1, 38.0, 37.7, 37.3, 34.4, 31.7, 30.7, 28.1, 27.4, 26.2, 22.7, 22.4, 19.9, 17.7, 14.5; HRMS (ESI): m/z calcd for $C_{38}H_{50}ClN_2O_3$ $[M+H]^+$: 617.3504, found 617.3532.

4.1.39 Methyl (2S,4aS,6aS,6bR,8aR,13aS,13bR,15bR)-10-(3-bromophenyl)-,4a,6a,6b, 9,9,13a-heptamethyl-14-oxo-2,3,4,4a,5,6,6a,6b,7,8,8a,9,10,13,13a,13b,14,15b-octadecahydro-1H-chryseno[1,2-f]indazole-2-carboxylate **(GA-39)**

Compound **GA-39** was synthesized in the same procedure as that of **GA-6** (yield 75%); yellow solid. ^{1}H NMR (500 MHz, $CDCl_3$) δ 7.61 – 7.55 (m, 2H), 7.36 (d, J = 12.2 Hz, 2H), 7.31 (t, J = 7.8 Hz, 1H), 5.75 (s, 1H), 3.77 (d, J = 15.6 Hz, 1H), 3.70 (s, 3H), 2.54 (s, 1H), 2.15 (s, 1H), 2.12 (d, J = 3.6 Hz, 1H), 2.09 – 1.92 (m, 4H), 1.85 (td, J = 4.3, 13.6 Hz, 1H), 1.75 – 1.67 (m, 1H), 1.62 (t, J = 13.5 Hz, 1H), 1.56 (dt, J = 5.8, 9.9 Hz, 1H), 1.53 – 1.46 (m, 2H), 1.32 (d, J = 9.4 Hz, 2H), 1.28 (dd, J = 2.7, 11.6 Hz, 2H), 1.25 (s, 3H), 1.18 (s, 3H), 1.15 (d, J = 2.2 Hz, 6H), 1.08 (s, 3H), 1.04 (s, 3H), 1.02 (d, J = 2.2 Hz, 1H), 0.83 (s, 3H); ^{13}C NMR (125 MHz, $CDCl_3$) δ 199.5, 176.9, 169.5, 145.8, 143.5, 138.9, 132.4, 132.1, 129.7, 128.7, 127.8, 121.8, 114.7, 60.4, 54.4, 51.8, 48.3, 45.1, 44.0, 43.3, 41.2, 37.9, 37.8, 37.5, 34.8, 32.0, 31.9, 31.1, 30.9, 29.7, 28.6, 28.3, 26.4, 23.2, 22.6, 18.4, 18.2, 15.6; HRMS (ESI): m/z calcd for $C_{38}H_{50}BrN_2O_3$ $[M+H]^+$: 661.2999, found 661.3029.

4.1.40 Methyl (2S,4aS,6aS,6bR,8aR,13aS,13bR,15bR)-10-(2-bromophenyl)-,4a,6a,6b, 9,9,13a-heptamethyl-14-oxo-2,3,4,4a,5,6,6a,6b,7,8,8a,9,10,13,13a,13b,14,15b-octadecahydro-1H-chryseno[1,2-f]indazole-2-carboxylate **(GA-40)**

Compound **GA-40** was synthesized in the same procedure as that of **GA-6** (yield 75%); yellow solid. ^{1}H NMR (500 MHz, CD_3OD) δ 7.72 (td, J = 1.3, 7.8 Hz, 1H), 7.59 – 7.39 (m, 3H), 7.36 (d, J = 2.9 Hz, 1H), 5.69 (d, J = 3.4 Hz, 1H), 4.25 – 4.09 (m, 1H), 3.75 – 3.67 (m, 3H), 2.63 (t, J = 8.1 Hz, 1H), 2.30 – 2.04 (m, 4H), 2.01 – 1.83 (m, 3H), 1.79 – 1.66 (m, 2H), 1.62 – 1.47 (m, 4H), 1.43 (d, J = 3.8 Hz, 3H), 1.35 (d, J = 12.4 Hz, 2H), 1.19 (s, 3H), 1.18 (s, 1H), 1.16 (d, J = 6.3 Hz, 6H), 1.12 (s, 1H), 1.06 (d, J = 16.1

Hz, 3H), 0.94 (s, 2H), 0.87 (s, 1H), 0.84 (s, 3H); ^{13}C NMR (125 MHz, CD_3OD) δ 200.5, 177.3, 168.7, 146.1, 145.9, 140.7, 138.6, 133.2, 131.1, 128.0, 124.9, 114.8, 60.3, 54.3, 51.3, 45.1, 44.0, 43.4, 41.1, 37.9, 34.5, 34.4, 31.7, 30.8, 29.7, 29.4, 28.1, 27.5, 27.1, 26.3, 26.1, 22.7, 19.9, 18.2, 17.7, 15.3, 14.5, 13.6; HRMS (ESI): m/z calcd for $C_{38}H_{50}BrN_2O_3$ $[M+H]^+$: 661.2999, found 661.3024.

4.1.41 Methyl (2S,4aS,6aS,6bR,8aR,13aS,13bR,15bR)-10-(4-methoxyphenyl)-,4a,6a, 6b,9, 9,13a-heptamethyl-14-oxo-2,3,4,4a,5,6,6a,6b,7,8,8a,9,10,13,13a,13b,14,15b-octadecahydro-1H-chryseno[1,2-f]indazole-2-carboxylate **(GA-41)**

Compound **GA-41** was synthesized in the same procedure as that of **GA-6** (yield 75%); white solid. ^{1}H NMR (500 MHz, $CDCl_3$) δ 7.38 (s, 1H), 7.30 (d, J = 8.4 Hz, 2H), 6.92 (d, J = 8.7 Hz, 2H), 5.75 (s, 1H), 3.85 (s, 3H), 3.78 (s, 1H), 3.71 (s, 3H), 2.54 (s, 1H), 2.12 (d, J = 4.5 Hz, 1H), 2.08 – 1.92 (m, 4H), 1.85 (td, J = 4.2, 13.6 Hz, 1H), 1.77 – 1.58 (m, 3H), 1.57 – 1.45 (m, 4H), 1.25 (s, 5H), 1.20 (d, J = 7.7 Hz, 1H), 1.18 (s, 3H), 1.16 (s, 6H), 1.08 (s, 3H), 1.03 (s, 3H), 0.89 (dt, J = 7.3, 13.9 Hz, 1H), 0.83 (s, 3H); ^{13}C NMR (125 MHz, $CDCl_3$) δ 199.5, 176.9, 169.4, 159.8, 149.8, 145.9, 137.9, 130.2, 130.2, 128.7, 128.7, 114.3, 113.6, 60.4, 55.5, 54.4, 51.8, 48.4, 45.1, 44.0, 43.3, 41.2, 38.0, 37.8, 34.8, 32.0, 31.9, 31.1, 30.9, 29.7, 29.3, 28.6, 28.3, 26.4, 23.2, 22.4, 18.4, 18.2, 15.6; HRMS (ESI): m/z calcd for $C_{39}H_{52}N_2O_4Na$ $[M+Na]^+$: 635.3819, found 635.3831.

4.1.42 Methyl (2S,4aS,6aS,6bR,8aR,13aS,13bR,15bR)-10-(3-methoxyphenyl)-,4a,6a, 6b,9,9,13a-heptamethyl-14-oxo-2,3,4,4a,5,6,6a,6b,7,8,8a,9,10,13,13a,13b,14,15b-octadecahydro-1H-chryseno[1,2-f]indazole-2-carboxylate **(GA-42)**

Compound **GA-42** was synthesized in the same procedure as that of **GA-6** (yield 75%); white solid. ^{1}H NMR (500 MHz, CD_3OD) δ 7.40 – 7.31 (m, 1H), 7.29 (s, 1H), 7.01 (d, J = 7.8 Hz, 1H), 6.95 (d, J = 7.5 Hz, 1H), 6.92 – 6.87 (m, 1H), 5.70 (s, 1H),

3.80 (d, *J* = 2.6 Hz, 3H), 3.70 (d, *J* = 2.7 Hz, 4H), 2.66 – 2.48 (m, 1H), 2.19 – 2.01 (m, 4H), 1.99 – 1.84 (m, 3H), 1.78 – 1.62 (m, 2H), 1.54 (d, *J* = 24.9 Hz, 4H), 1.40 (d, *J* = 4.3 Hz, 5H), 1.17 (d, *J* = 3.5 Hz, 3H), 1.14 (d, *J* = 4.7 Hz, 6H), 1.10 (d, *J* = 3.6 Hz, 3H), 1.05 (d, *J* = 3.1 Hz, 4H), 0.82 (d, *J* = 3.1 Hz, 4H); ^{13}C NMR (125 MHz, CD_3OD) δ 200.5, 177.4, 173.8, 159.5, 146.2, 142.6, 138.0, 129.1, 128.1, 121.3, 114.9, 114.4, 102.7, 60.4, 59.8, 55.2, 54.3, 45.2, 44.0, 43.4, 41.1, 37.8, 37.7, 37.4, 34.7, 31.8, 30.9, 29.5, 29.1, 29.0, 28.4, 27.8, 26.4, 26.2, 22.9, 22.2, 18.2, 17.9, 15.3; HRMS (ESI): m/z calcd for $C_{39}H_{53}N_2O_4$ $[M+H]^+$: 613.4000, found 613.4011.

4.1.43 Methyl (2S,4aS,6aS,6bR,8aR,13aS,13bR,15bR)-10-(2-methoxyphenyl)-2,4a,6a, 6b,9,9,13a-heptamethyl-14-oxo-2,3,4,4a,5,6,6a,6b,7,8,8a,9,10,13,13a,13b,14,15b-octadecahyd-ro-1H-chryseno[1,2-f]indazole-2-carboxylate **(GA-43)**

Compound **GA-43** was synthesized in the same procedure as that of **GA-6** (yield 75%); white solid. ^{1}H NMR (500 MHz, CD_3OD) δ 7.46 (t, *J* = 7.1 Hz, 1H), 7.31 (s, 2H), 7.10 – 6.93 (m, 2H), 5.69 (d, *J* = 4.2 Hz, 1H), 4.30 – 4.00 (m, 1H), 3.77 – 3.60 (m, 6H), 2.60 (s, 1H), 2.14 (d, *J* = 17.5 Hz, 5H), 2.07 – 1.81 (m, 4H), 1.68 (dd, *J* = 15.5, 29.5 Hz, 2H), 1.58 – 1.46 (m, 3H), 1.40 (s, 4H), 1.18 (s, 3H), 1.14 (d, *J* = 6.7 Hz, 6H), 1.11 (s, 1H), 1.05 (s, 3H), 0.96 (s, 2H), 0.85 (d, *J* = 23.9 Hz, 5H); ^{13}C NMR (125 MHz, CD_3OD) δ 200.5, 177.4, 176.9, 171.1, 156.5, 138.3, 138.2, 131.1, 130.7, 128.1, 119.8, 114.1, 111.8, 60.4, 55.1, 54.3, 51.5, 45.2, 44.0, 43.8, 43.4, 41.1, 37.9, 37.7, 34.6, 31.8, 30.9, 30.2, 29.3, 28.3, 27.8, 26.8, 26.4, 26.2, 22.9, 22.1, 17.9, 15.4, 14.9; HRMS (ESI): m/z calcd for $C_{39}H_{53}N_2O_4$ $[M+H]^+$: 613.4000, found 613.4023.

4.1.44 Methyl (2S,4aS,6aS,6bR,8aR,13aS,13bR,15bR)-2,4a,6a,6b,9,9,13a-heptamethyl-14-o-xo-10-(4-(trifluoromethyl)phenyl)-2,3,4,4a,5,6,6a,6b,7,8,8a,9,10, 13,13a,13b,14,15b-octa-decahydro-1H-chryseno[1,2-f]indazole-2-carboxylate **(GA-44)**

Compound **GA-44** was synthesized in the same procedure as that of **GA-6** (yield 75%); pale yellow solid. ^{1}H NMR (500 MHz, CD_3OD) δ 7.76 (d, J = 8.3 Hz, 2H), 7.63 – 7.52 (m, 3H), 5.70 (s, 1H), 3.70 (s, 4H), 2.61 (s, 1H), 2.20 – 2.12 (m, 3H), 2.08 (d, J = 4.2 Hz, 1H), 2.01 – 1.81 (m, 4H), 1.78 – 1.63 (m, 3H), 1.54 (dd, J = 12.9, 25.3 Hz, 5H), 1.41 (s, 3H), 1.18 (s, 3H), 1.15 (d, J = 2.6 Hz, 6H), 1.08 (s, 3H), 1.04 (s, 3H), 0.86 (s, 1H), 0.83 (s, 3H); ^{13}C NMR (125 MHz, CD_3OD) δ 200.5, 177.4, 171.3, 146.6, 145.0, 138.7, 131.5, 131.2, 129.7, 128.1, 125.7, 124.7, 122.5, 114.9, 60.3, 54.2, 51.5, 45.2, 44.0, 43.4, 41.1, 37.8, 37.6, 37.2, 34.6, 31.7, 30.8, 29.5, 29.2, 28.2, 27.7, 26.4, 26.2, 22.8, 22.4, 22.3, 18.2, 17.8, 15.2; HRMS (ESI): m/z calcd for $C_{39}H_{49}F_3N_2O_3Na$ $[M+Na]^+$: 673.3587, found 673.3589.

4.1.45 Methyl (2S,4aS,6aS,6bR,8aR,13aS,13bR,15bR)-2,4a,6a,6b,9,9,13a-heptamethyl-14-o-xo-10-(3-(trifluoromethyl)phenyl)-2,3,4,4a,5,6,6a,6b,7,8,8a,9,10, 13,13a,13b,14,15b-octa-decahydro-1H-chryseno[1,2-f]indazole-2-carboxylate **(GA-45)**

Compound **GA-45** was synthesized in the same procedure as that of **GA-6** (yield 75%); pale yellow solid. ^{1}H NMR (500 MHz, CD_3OD) δ 7.78 (s, 1H), 7.71 – 7.58 (m, 4H), 5.70 (d, J = 5.2 Hz, 1H), 3.75 – 3.66 (m, 4H), 2.60 (d, J = 13.6 Hz, 1H), 2.22 – 2.11 (m, 4H), 2.09 – 1.76 (m, 5H), 1.66 (d, J = 13.3 Hz, 3H), 1.41 (d, J = 6.6 Hz, 5H), 1.18 (s, 3H), 1.14 (s, 6H), 1.06 (d, J = 5.3 Hz, 4H), 1.02 (d, J = 4.3 Hz, 4H), 0.83 (d, J = 3.5 Hz, 4H); ^{13}C NMR (125 MHz, CD_3OD) δ 200.4, 177.4, 160.4, 146.7, 142.3, 138.7, 132.6, 129.5, 128.1, 126.1, 124.4, 122.3, 120.0, 115.0, 60.3, 54.2, 51.6, 45.2, 44.0, 43.4, 42.2, 41.1, 37.8, 37.7, 37.2, 34.7, 31.8, 30.9, 29.5, 29.2, 28.3, 27.9, 26.4, 26.2, 22.9, 22.3, 18.2, 17.9, 15.3; HRMS (ESI): m/z calcd for $C_{39}H_{50}F_3N_2O_3$ $[M+H]^+$: 651.3768, found 651.3792.

4.1.46 Methyl (2S,4aS,6aS,6bR,8aR,13aS,13bR,15bR)-2,4a,6a,6b,9,9,13a-

heptamethyl-14-ox-o-10-(2-(trifluoromethyl)phenyl)-,3,4,4a,5,6,6a,6b,7,8,8a,9,10,13, 13a,13b,14,15b-octa-decahydro-1H-chryseno[1,2-f]indazole-2-carboxylate **(GA-46)**

Compound **GA-46** was synthesized in the same procedure as that of **GA-6** (yield 75%); pale yellow solid. ^{1}H NMR (500 MHz, CD_3OD) δ 7.82 – 7.76 (m, 1H), 7.70 (td, J = 2.3, 5.9, 6.5 Hz, 2H), 7.59 (dd, J = 1.4, 7.4 Hz, 2H), 5.70 (d, J = 2.3 Hz, 1H), 3.70 (s, 3H), 2.65 – 2.57 (m, 2H), 2.23 – 2.09 (m, 4H), 2.00 – 1.82 (m, 4H), 1.78 – 1.63 (m, 3H), 1.41 (d, J = 6.8 Hz, 5H), 1.22 (s, 2H), 1.19 – 1.17 (m, 5H), 1.15 (d, J = 4.9 Hz, 5H), 1.07 (s, 3H), 0.90 (s, 2H), 0.83 (s, 3H), 0.80 (s, 2H); ^{13}C NMR (125 MHz, CD_3OD) δ 200.5, 177.4, 171.2, 146.7, 138.6, 138.6, 131.9, 131.6, 130.2, 130.1, 128.1, 127.7, 115.1, 114.9, 60.1, 54.4, 51.5, 45.1, 44.0, 43.4, 41.1, 37.9, 37.7, 37.3, 34.8, 34.6, 31.7, 30.8, 30.3, 29.5, 28.6, 28.3, 27.7, 26.2, 22.8, 20.7, 17.8, 15.5, 14.2; HRMS (ESI): m/z calcd for $C_{39}H_{49}F_3N_2O_3Na$ $[M+Na]^+$: 673.3587, found 673.3600.

4.1.47 Methyl (2S,4aS,6aS,6bR,8aR,13aS,13bR,15bR)-2,4a,6a,6b,9,9,13a-heptamethyl-14-o-xo-10-(p-tolyl)-2,3,4,4a,5,6,6a,6b,7,8,8a,9,10,13,13a,13b,14,15b-octadecahydro-1H-chr-yseno[1,2-f]indazole-2-carboxylate **(GA-47)**

Compound **GA-47** was synthesized in the same procedure as that of **GA-6** to obtain a colorless oil, which was used to hydrolysis reaction without further purification. HRMS (ESI): m/z calcd for $C_{39}H_{53}N_2O_3$ $[M+H]^+$: 597.4051, found 597.4015.

4.1.48 Methyl (2S,4aS,6aS,6bR,8aR,13aS,13bR,15bR)-2,4a,6a,6b,9,9,13a-heptamethyl-14-o-xo-10-(m-tolyl)-2,3,4,4a,5,6,6a,6b,7,8,8a,9,10,13,13a,13b,14,15b-octadecahydro-1H-chr-yseno[1,2-f]indazole-2-carboxylate **(GA-48)**

Compound **GA-48** was synthesized in the same procedure as that of **GA-14** to obtain a colorless oil, which was used to hydrolysis reaction without further purification. HRMS (ESI): m/z calcd for $C_{39}H_{53}N_2O_3$ $[M+H]^+$: 597.4051, found 597.4013.

4.1.49 Methyl (2S,4aS,6aS,6bR,8aR,13aS,13bR,15bR)-2,4a,6a,6b,9,9,13a-heptamethyl-14-o-xo-10-(o-tolyl)-2,3,4,4a,5,6,6a,6b,7,8,8a,9,10,13,13a,13b,14,15b-octadecahydro-1H-chr-yseno[1,2-f]indazole-2-carboxylate **(GA-49)**

Compound **GA-49** was synthesized in the same procedure as that of **GA-14** to obtain a colorless oil, which was used to hydrolysis reaction without further purification. HRMS (ESI): m/z calcd for $C_{39}H_{53}N_2O_3$ $[M+H]^+$: 597.4051, found 597.4003.

4.1.50 Methyl (2S,4aS,6aS,6bR,8aR,13aS,13bR,15bR)-2,4a,6a,6b,9,9,13a-heptamethyl-10-(4-(methylsulfonyl)phenyl)-14-oxo-2,3,4,4a,5,6,6a,6b,7,8,8a,9,10,13,13a,13b,14,15b-octa-decahydro-1H-chryseno[1,2-f]indazole-2-carboxylate **(GA-50)**

Compound **GA-50** was synthesized in the same procedure as that of **GA-6** to obtain a pale yellow oil, which was used to hydrolysis reaction without further purification. HRMS (ESI): m/z calcd for $C_{39}H_{53}N_2O_5S$ $[M+H]^+$: 661.3670, found 661.3697.

4.1.51 Methyl (2S,4aS,6aS,6bR,8aR,13aS,13bR,15bR)-2,4a,6a,6b,9,9,13a-heptamethyl-14-oxo-10-(4-sulfamoylphenyl)-2,3,4,4a,5,6,6a,6b,7,8,8a,9,10,13,13a,13b,14,15b-octadecahy-dro-1H-chryseno[1,2-f]indazole-2-carboxylate **(GA-51)**

Compound **GA-51** was synthesized in the same procedure as that of **GA-14**. to obtain a pale yellow oil, which was used to hydrolysis reaction without further purification. HRMS (ESI): m/z calcd for $C_{38}H_{52}N_3O_5S$ $[M+H]^+$: 662.3622, found 662.3665.

4.1.52 (2S,4aS,6aS,6bR,8aR,13aS,13bR,15bR)-10-(3-fluorophenyl)-2,4a,6a,6b,9,9,13a-hepta-methyl-14-oxo-2,3,4,4a,5,6,6a,6b,7,8,8a,9,10,13,13a,13b,14,15b-

octadecahydro-1H-ch-ryseno[1,2-f]indazole-2-carboxylic acid **(GA-52)**

Compound **GA-52** was synthesized in the same procedure as that of **GA-20** (yield 67%); pale yellow solid. ^{1}H NMR (500 MHz, $CDCl_3$) δ 7.51 – 7.34 (m, 2H), 7.25 – 7.16 (m, 2H), 6.97 (s, 1H), 5.79 (s, 1H), 3.81 – 3.73 (m, 1H), 2.55 (s, 1H), 2.30 – 2.21 (m, 1H), 2.04 (ddd, J = 10.5, 21.2, 48.8 Hz, 5H), 1.90 – 1.82 (m, 1H), 1.75 – 1.60 (m, 3H), 1.53 (dd, J = 9.5, 28.2 Hz, 4H), 1.42 (d, J = 10.4 Hz, 5H), 1.35 (dd, J = 5.0, 12.5 Hz, 2H), 1.19 (s, 3H), 1.15 (s, 4H), 1.07 (s, 3H), 1.02 (s, 3H), 0.87 (s, 4H); ^{13}C NMR (125 MHz, $CDCl_3$) δ 199.3, 181.2, 169.9, 163.6, 143.0, 129.9, 129.5, 128.6, 127.9, 117.5, 116.4, 115.3, 105.9, 71.3, 60.2, 54.1, 48.2, 45.1, 43.3, 41.0, 37.7, 34.9, 31.9, 30.9, 29.7, 29.1, 28.6, 28.4, 26.5, 26.4, 23.2, 22.7, 22.2, 18.3, 18.2, 15.6, 14.1; HRMS (ESI): m/z calcd for $C_{37}H_{48}FN_2O_3$ $[M+H]^+$: 587.3643, found 587.3645.

4.1.53 (2S,4aS,6aS,6bR,8aR,13aS,13bR,15bR)-10-(2-fluorophenyl)-2,4a,6a,6b,9,9, 13a-hepta-methyl-14-oxo-2,3,4,4a,5,6,6a,6b,7,8,8a,9,10,13,13a,13b,14,15b-octadecahydro-1H-ch-ryseno[1,2-f]indazole-2-carboxylic acid **(GA-53)**

Compound **GA-53** was synthesized in the same procedure as that of **GA-20** (yield 66%); pale yellow solid. ^{1}H NMR (500 MHz, $CDCl_3$) δ 7.44 (s, 3H), 7.25 – 7.14 (m, 2H), 5.78 (s, 1H), 3.77 (d, J = 15.4 Hz, 1H), 2.56 (s, 1H), 2.23 (d, J = 12.9 Hz, 1H), 2.10 – 1.80 (m, 5H), 1.68 (dt, J = 14.5, 41.7 Hz, 3H), 1.51 (dd, J = 13.2, 23.3 Hz, 4H), 1.43 (d, J = 10.1 Hz, 2H), 1.39 (s, 3H), 1.37 – 1.28 (m, 4H), 1.25 (s, 4H), 1.22 (s, 4H), 1.19 (s, 4H), 0.86 (s, 4H); ^{13}C NMR (125 MHz, $CDCl_3$) δ 199.2, 193.3, 181.5, 169.6, 150.7, 139.5, 132.8, 131.4, 130.2, 128.7, 123.9, 123.8, 116.5, 60.4, 54.0, 48.2, 45.2, 43.8, 43.3, 41.0, 37.7, 34.5, 32.0, 31.9, 30.9, 29.7, 29.3, 28.6, 28.4, 26.5, 26.4, 23.2, 22.7, 18.4, 18.2, 14.1, 13.9; HRMS (ESI): m/z calcd for $C_{37}H_{48}FN_2O_3$ $[M+H]^+$: 587.3643, found 587.3663.

4.1.54 (2S,4aS,6aS,6bR,8aR,13aS,13bR,15bR)-10-(3-chlorophenyl)-2,4a,6a,6b,9,9,13a-hepta-methyl-14-oxo-2,3,4,4a,5,6,6a,6b,7,8,8a,9,10,13,13a,13b,14,15b-octadecahydro-1H-ch-ryseno[1,2-f]indazole-2-carboxylic acid **(GA-54)**

Compound **GA-54** was synthesized in the same procedure as that of **GA-20** (yield 60%); pale yellow solid. ^{1}H NMR (500 MHz, CD_3OD) δ 7.53 – 7.46 (m, 2H), 7.41 (dd, J = 8.9, 16.9 Hz, 2H), 7.31 (d, J = 8.0 Hz, 1H), 5.71 (s, 1H), 3.71 (d, J = 15.5 Hz, 1H), 2.60 (d, J = 13.9 Hz, 1H), 2.28 – 2.19 (m, 2H), 2.18 – 2.01 (m, 4H), 1.90 (ddd, J = 10.7, 16.2, 38.5 Hz, 4H), 1.73 (t, J = 12.4 Hz, 2H), 1.66 – 1.55 (m, 4H), 1.54 – 1.48 (m, 3H), 1.17 (d, J = 5.2 Hz, 6H), 1.12 (s, 3H), 1.08 (s, 3H), 1.03 (s, 3H), 0.89 (dd, J = 6.0, 8.8 Hz, 1H), 0.83 (s, 3H); ^{13}C NMR (125 MHz, CD_3OD) δ 200.5, 179.3, 171.6, 147.1, 142.1, 138.8, 134.0, 129.8, 129.7, 129.5, 128.0, 127.7, 114.9, 60.3, 54.2, 45.2, 43.6, 43.4, 41.2, 37.8, 37.7, 37.2, 34.7, 31.8, 30.9, 29.5, 29.1, 28.4, 28.1, 26.4, 26.2, 22.9, 22.5, 22.2, 18.2, 17.9, 15.3; HRMS (ESI): m/z calcd for $C_{37}H_{48}ClN_2O_3$ $[M+H]^+$: 603.3348, found 603.3354.

4.1.55 (2S,4aS,6aS,6bR,8aR,13aS,13bR,15bR)-10-(2-chlorophenyl)-2,4a,6a,6b,9,9,13a-hepta-methyl-14-oxo-2,3,4,4a,5,6,6a,6b,7,8,8a,9,10,13,13a,13b,14,15b-octadecahydro-1H-ch-ryseno[1,2-f]indazole-2-carboxylic acid **(GA-55)**

Compound **GA-55** was synthesized in the same procedure as that of **GA-20** (yield 62%); pale yellow solid. ^{1}H NMR (500 MHz, $CDCl_3$) δ 7.58 – 7.31 (m, 5H), 5.77 (s, 1H), 3.77 (d, J = 15.3 Hz, 1H), 2.56 (d, J = 10.3 Hz, 1H), 2.26 – 2.19 (m, 1H), 2.09 – 1.91 (m, 3H), 1.90 – 1.79 (m, 1H), 1.71 (t, J = 11.1 Hz, 1H), 1.62 (t, J = 13.9 Hz, 1H), 1.58 – 1.45 (m, 4H), 1.38 (d, J = 6.9 Hz, 3H), 1.36 – 1.28 (m, 3H), 1.24 (d, J = 3.7 Hz, 3H), 1.20 (s, 3H), 1.18 (s, 3H), 1.15 (d, J = 5.9 Hz, 3H), 1.09 (s, 2H), 1.00 (s, 2H), 0.91 (s, 2H), 0.85 (s, 3H); ^{13}C NMR (125 MHz, $CDCl_3$) δ 199.7, 181.3, 169.7, 139.7, 139.3,

135.0, 131.3, 130.5, 130.1, 130.1, 128.6, 126.7, 114.4, 60.4, 54.4, 53.8, 48.2, 45.2, 43.8, 43.3, 41.0, 38.0, 37.7, 34.5, 31.9, 30.9, 30.1, 29.7, 29.2, 28.6, 28.4, 26.4, 23.2, 18.4, 18.2, 15.8, 15.1; HRMS (ESI): m/z calcd for $C_{37}H_{48}ClN_2O_3$ $[M+H]^+$: 603.3348, found 603.3362.

4.1.56 (2S,4aS,6aS,6bR,8aR,13aS,13bR,15bR)-10-(3-bromophenyl)-2,4a,6a,6b,9,9,13a-hepta-methyl-14-oxo-2,3,4,4a,5,6,6a,6b,7,8,8a,9,10,13,13a,13b,14,15b-octadecahydro-1H-ch-ryseno[1,2-f]indazole-2-carboxylic acid **(GA-56)**

Compound **GA-56** was synthesized in the same procedure as that of **GA-20** (yield 55%); yellow solid. ^{1}H NMR (500 MHz, $CDCl_3$) δ 7.61 (d, J = 7.7 Hz, 2H), 7.45 – 7.29 (m, 3H), 5.79 (s, 1H), 3.78 (d, J = 15.6 Hz, 1H), 2.55 (s, 1H), 2.28 – 2.22 (m, 1H), 2.01 (ddt, J = 8.6, 16.9, 25.7 Hz, 4H), 1.92 – 1.82 (m, 2H), 1.76 – 1.61 (m, 4H), 1.26 (s, 4H), 1.25 (s, 3H), 1.23 (s, 3H), 1.19 (s, 3H), 1.16 (s, 3H), 1.09 (s, 3H), 1.05 (s, 4H), 0.94 – 0.90 (m, 1H), 0.87 (s, 3H); ^{13}C NMR (125 MHz, $CDCl_3$) δ 199.5, 180.5, 169.6, 156.6, 139.8, 138.8, 134.0, 132.4, 130.8, 129.8, 128.7, 127.9, 121.8, 60.3, 53.7, 48.2, 45.2, 43.7, 43.3, 41.0, 37.7, 34.8, 31.9, 30.9, 29.7, 29.3, 29.2, 28.6, 28.4, 26.5, 26.4, 23.2, 22.7, 18.4, 18.2, 15.6, 14.1; HRMS (ESI): m/z calcd for $C_{37}H_{48}BrN_2O_3$ $[M+H]^+$: 647.2843, found 647.2868.

4.1.57 (2S,4aS,6aS,6bR,8aR,13aS,13bR,15bR)-10-(2-bromophenyl)-2,4a,6a,6b,9,9,13a-hepta-methyl-14-oxo-2,3,4,4a,5,6,6a,6b,7,8,8a,9,10,13,13a,13b,14,15b-octadecahydro-1H-ch-ryseno[1,2-f]indazole-2-carboxylic acid **(GA-57)**

Compound **GA-57** was synthesized in the same procedure as that of **GA-20** (yield 50%); yellow solid. ^{1}H NMR (500 MHz, CD_3OD) δ 7.68 (td, J = 1.3, 8.0 Hz, 1H), 7.51 (ddd, J = 1.6, 7.8, 17.9 Hz, 1H), 7.46 – 7.41 (m, 1H), 7.37 (q, J = 4.9, 5.8 Hz, 2H), 5.70 (s, 1H), 3.70 (dd, J = 2.5, 15.4 Hz, 1H), 2.59 (d, J = 8.9 Hz, 1H), 2.28 – 2.01 (m, 4H),

2.00 – 1.81 (m, 4H), 1.72 (t, *J* = 12.1 Hz, 1H), 1.65 – 1.46 (m, 6H), 1.39 (d, *J* = 5.9 Hz, 5H), 1.16 (d, *J* = 4.7 Hz, 7H), 1.14 (d, *J* = 4.6 Hz, 3H), 1.10 (s, 1H), 1.03 (d, *J* = 12.2 Hz, 3H), 0.85 (d, *J* = 6.8 Hz, 1H), 0.82 (s, 3H); ^{13}C NMR (125 MHz, CD_3OD) *δ* 200.6, 179.3, 171.5, 146.3, 140.6, 138.9, 133.3, 131.1, 128.1, 127.5, 125.0, 114.8, 60.2, 54.3, 45.2, 43.6, 43.4, 41.2, 37.9, 37.7, 37.4, 34.6, 34.5, 31.8, 30.9, 30.0, 29.5, 28.4, 28.1, 27.3, 26.3, 23.0, 22.7, 20.2, 18.0, 15.6, 14.7; HRMS (ESI): m/z calcd for $C_{37}H_{48}BrN_2O_3$ $[M+H]^+$: 647.2843, found 647.2854.

4.1.58 (2S,4aS,6aS,6bR,8aR,13aS,13bR,15bR)-10-(4-methoxyphenyl)-2,4a,6a,6b,9,9,13a-hep-tamethyl-14-oxo-2,3,4,4a,5,6,6a,6b,7,8,8a,9,10,13,13a,13b,14,15b-octadecahydro-1H-chryseno[1,2-f]indazole-2-carboxylic acid **(GA-58)**

Compound **GA-58** was synthesized in the same procedure as that of **GA-20** (yield 55%); white solid. ^{1}H NMR (500 MHz, $CDCl_3$) *δ* 7.37 (s, 1H), 7.30 (d, *J* = 8.0 Hz, 2H), 6.92 (d, *J* = 8.5 Hz, 2H), 5.78 (s, 1H), 3.85 (s, 3H), 3.76 (d, *J* = 15.2 Hz, 1H), 2.55 (s, 1H), 2.25 – 2.20 (m, 1H), 2.09 – 1.92 (m, 4H), 1.87 (dt, *J* = 6.8, 13.4 Hz, 1H), 1.76 – 1.59 (m, 3H), 1.58 – 1.46 (m, 4H), 1.25 (d, *J* = 1.9 Hz, 6H), 1.22 (s, 3H), 1.19 (s, 3H), 1.16 (s, 3H), 1.07 (s, 3H), 1.03 (s, 3H), 0.87 (d, *J* = 7.8 Hz, 4H); ^{13}C NMR (125 MHz, $CDCl_3$) *δ* 210.8, 199.7, 180.8, 169.5, 159.8, 145.9, 138.0, 134.8, 130.3, 128.7, 120.0, 114.2, 113.5, 60.4, 55.5, 54.4, 53.7, 48.2, 45.2, 43.7, 43.3, 41.0, 38.0, 37.7, 34.8, 31.9, 30.9, 29.7, 29.2, 28.6, 28.4, 26.4, 23.2, 22.7, 22.4, 18.2, 15.6, 14.1; HRMS (ESI): m/z calcd for $C_{38}H_{51}N_2O_4$ $[M+H]^+$: 599.3843, found 599.3850.

4.1.59 (2S,4aS,6aS,6bR,8aR,13aS,13bR,15bR)-10-(3-methoxyphenyl)-2,4a,6a,6b,9,9,13a-hep-tamethyl-14-oxo-2,3,4,4a,5,6,6a,6b,7,8,8a,9,10,13,13a,13b,14,15b-octadecahydro-1H-chryseno[1,2-f]indazole-2-carboxylic acid **(GA-59)**

Compound **GA-59** was synthesized in the same procedure as that of **GA-20** (yield

55%); white solid. ^{1}H NMR (500 MHz, CD_3OD) δ 7.39 – 7.28 (m, 2H), 7.06 – 7.00 (m, 1H), 6.98 – 6.93 (m, 1H), 6.91 (d, J = 2.2 Hz, 1H), 5.71 (d, J = 3.5 Hz, 1H), 3.81 (d, J = 1.6 Hz, 3H), 3.70 (dd, J = 3.0, 15.4 Hz, 1H), 2.60 (q, J = 4.8, 6.3 Hz, 1H), 2.27 – 2.20 (m, 1H), 2.16 (d, J = 3.3 Hz, 4H), 2.00 – 1.85 (m, 3H), 1.72 (d, J = 11.1 Hz, 1H), 1.66 (d, J = 13.3 Hz, 1H), 1.59 (d, J = 10.2 Hz, 2H), 1.51 (d, J = 12.1 Hz, 2H), 1.41 (s, 3H), 1.31 (d, J = 11.6 Hz, 3H), 1.17 (d, J = 6.0 Hz, 6H), 1.13 (s, 3H), 1.10 (s, 3H), 1.06 (s, 3H), 0.84 (s, 3H); ^{13}C NMR (125 MHz, CD_3OD) δ 200.6, 179.3, 171.6, 159.6, 129.1, 128.1, 126.5, 124.0, 121.4, 115.2, 114.9, 114.9, 114.4, 60.3, 55.3, 54.3, 45.2, 43.6, 43.4, 41.2, 37.8, 37.7, 37.4, 34.8, 31.8, 31.8, 30.9, 29.5, 29.1, 28.4, 28.1, 27.0, 26.5, 26.3, 23.0, 22.9, 18.2, 15.3; HRMS (ESI): m/z calcd for $C_{38}H_{51}N_2O_4$ $[M+H]^+$: 599.3843, found 599.3845.

4.1.60 (2S,4aS,6aS,6bR,8aR,13aS,13bR,15bR)-10-(2-methoxyphenyl)-2,4a,6a,6b,9,9,13a-hep-tamethyl-14-oxo-2,3,4,4a,5,6,6a,6b,7,8,8a,9,10,13,13a,13b,14,15b-octadecahydro-1H-chryseno[1,2-f]indazole-2-carboxylic acid **(GA-60)**

Compound **GA-60** was synthesized in the same procedure as that of **GA-20** (yield 60%); white solid. ^{1}H NMR (500 MHz, CD_3OD) δ 7.61 – 7.59 (m, 1H), 7.48 (t, J = 8.1 Hz, 1H), 7.40 – 7.31 (m, 2H), 7.06 – 7.02 (m, 1H), 5.71 (s, 1H), 3.74 (d, J = 9.7 Hz, 3H), 2.61 (d, J = 4.2 Hz, 1H), 2.27 – 2.15 (m, 3H), 2.10 – 2.04 (m, 1H), 1.93 (d, J = 34.3 Hz, 3H), 1.73 (d, J = 13.2 Hz, 2H), 1.69 – 1.62 (m, 2H), 1.58 (dd, J = 8.0, 14.5 Hz, 3H), 1.51 (d, J = 12.8 Hz, 2H), 1.41 (d, J = 3.5 Hz, 4H), 1.39 – 1.34 (m, 3H), 1.18 (s, 3H), 1.17 (s, 3H), 1.14 (s, 2H), 1.12 (d, J = 4.6 Hz, 3H), 1.06 (s, 2H), 0.84 (s, 3H); ^{13}C NMR (125 MHz, CD_3OD) δ 200.7, 179.1, 171.6, 156.4, 156.4, 137.9, 131.3, 130.6, 128.0, 119.8, 115.4, 114.2, 111.8, 60.3, 55.0, 54.0, 45.2, 45.2, 43.6, 43.4, 41.2, 37.9, 37.9, 37.6, 34.6, 31.7, 30.8, 29.4, 28.3, 27.9, 26.2, 24.8, 22.8, 22.4, 19.9, 17.8, 15.3,

13.5; HRMS (ESI): m/z calcd for $C_{38}H_{51}N_2O_4$ $[M+H]^+$: 599.3843, found 599.3879.

4.1.61 (2S,4aS,6aS,6bR,8aR,13aS,13bR,15bR)-2,4a,6a,6b,9,9,13a-heptamethyl-14-oxo-10-(4-(trifluoromethyl)phenyl)-2,3,4,4a,5,6,6a,6b,7,8,8a,9,10,13,13a,13b,14,15b-octadecahy-dro-1H-chryseno[1,2-f]indazole-2-carboxylic acid **(GA-61)**

Compound **GA-61** was synthesized in the same procedure as that of **GA-20** (yield 55%); yellow solid. ^{1}H NMR (500 MHz, CD_3OD) δ 7.77 (d, J = 8.0 Hz, 2H), 7.57 (d, J = 7.9 Hz, 2H), 7.40 (s, 1H), 5.71 (s, 1H), 3.72 (d, J = 15.5 Hz, 1H), 2.61 (s, 1H), 2.25 (d, J = 7.8 Hz, 1H), 2.18 (s, 1H), 2.09 (s, 1H), 1.98 – 1.87 (m, 3H), 1.74 (d, J = 11.5 Hz, 1H), 1.65 (t, J = 13.5 Hz, 1H), 1.58 (s, 2H), 1.52 (d, J = 12.3 Hz, 2H), 1.42 (s, 3H), 1.39 (d, J = 4.8 Hz, 1H), 1.36 (d, J = 8.1 Hz, 3H), 1.18 (s, 3H), 1.17 (s, 3H), 1.14 (s, 3H), 1.08 (s, 3H), 1.04 (s, 3H), 0.86 (d, J = 6.1 Hz, 1H), 0.84 (s, 3H); ^{13}C NMR (125 MHz, CD_3OD) δ 200.5, 179.5, 171.8, 147.0, 144.6, 138.9, 131.7, 129.9 (2×C), 129.0, 128.0, 125.7 (2×C), 115.1, 60.3, 54.2, 45.2, 43.6, 43.4, 41.2, 37.8, 37.7, 37.2, 34.7, 31.7, 29.5, 29.1, 28.5, 28.3, 27.9, 26.4, 26.2, 22.8, 22.4, 22.2, 18.2, 17.8, 15.2; HRMS (ESI): m/z calcd for $C_{38}H_{48}F_3N_2O_3$ $[M+H]^+$: 637.3612, found 637.3625.

4.1.62 (2S,4aS,6aS,6bR,8aR,13aS,13bR,15bR)-2,4a,6a,6b,9,9,13a-heptamethyl-14-oxo-10-(3-(trifluoromethyl)phenyl)-2,3,4,4a,5,6,6a,6b,7,8,8a,9,10,13,13a,13b,14,15b-octadecahy-dro-1H-chryseno[1,2-f]indazole-2-carboxylic acid **(GA-62)**

Compound **GA-62** was synthesized in the same procedure as that of **GA-20** (yield 55%); yellow solid. ^{1}H NMR (500 MHz, CD_3OD) δ 7.79 (d, J = 7.7 Hz, 1H), 7.70 – 7.57 (m, 4H), 5.71 (s, 1H), 3.72 (d, J = 15.5 Hz, 1H), 2.61 (s, 1H), 2.27 – 2.23 (m, 1H), 2.18 (s, 1H), 2.08 (dt, J = 6.8, 13.7 Hz, 1H), 1.98 – 1.84 (m, 4H), 1.73 (d, J = 9.6 Hz, 1H), 1.65 (t, J = 13.4 Hz, 2H), 1.61 – 1.56 (m, 2H), 1.55 – 1.48 (m, 3H), 1.42 (s, 3H), 1.18 (s, 3H), 1.17 (s, 3H), 1.14 (s, 3H), 1.06 (d, J = 6.8 Hz, 4H), 1.03 (s, 3H), 0.86 (d,

J = 5.1 Hz, 1H), 0.84 (s, 3H); ^{13}C NMR (125 MHz, CD_3OD) δ 200.5, 171.7, 165.1, 146.7, 138.8, 132.7, 131.2, 129.5, 128.0, 127.3, 126.1, 123.7, 122.3, 115.0, 60.3, 54.2, 45.2, 43.6, 43.4, 41.2, 37.8, 37.6, 37.2, 34.6, 31.7, 30.8, 29.5, 29.1, 28.3, 27.9, 26.4, 26.2, 22.8, 22.4, 22.2, 18.2, 17.8, 15.2; HRMS (ESI): m/z calcd for $C_{38}H_{48}F_3N_2O_3$ $[M+H]^+$: 637.3612, found 637.3627.

4.1.63 (2S,4aS,6aS,6bR,8aR,13aS,13bR,15bR)-2,4a,6a,6b,9,9,13a-heptamethyl-14-oxo-10-(2-(trifluoromethyl)phenyl)-2,3,4,4a,5,6,6a,6b,7,8,8a,9,10,13,13a,13b,14,15b-octadecahy-dro-1H-chryseno[1,2-f]indazole-2-carboxylic acid **(GA-63)**

Compound **GA-63** was synthesized in the same procedure as that of **GA-20** (yield 60%); yellow solid. ^{1}H NMR (500 MHz, CD_3OD) δ 7.85 – 7.75 (m, 1H), 7.69 (td, *J* = 2.3, 6.1, 6.6 Hz, 2H), 7.57 (s, 1H), 7.34 (d, *J* = 3.4 Hz, 1H), 5.71 (d, *J* = 2.5 Hz, 1H), 3.73 – 3.67 (m, 1H), 2.61 (d, *J* = 8.0 Hz, 1H), 2.28 – 2.02 (m, 5H), 1.98 – 1.83 (m, 4H), 1.73 (s, 2H), 1.65 (t, *J* = 13.5 Hz, 2H), 1.60 – 1.55 (m, 3H), 1.51 (dd, *J* = 3.1, 12.9 Hz, 3H), 1.46 (s, 1H), 1.06 (s, 3H), 1.03 (s, 1H), 0.90 (s, 3H), 0.87 (s, 1H), 0.85 (s, 1H), 0.84 – 0.83 (m, 4H), 0.82 (d, *J* = 2.6 Hz, 1H), 0.79 (d, *J* = 9.7 Hz, 4H); ^{13}C NMR (125 MHz, CD_3OD) δ 200.6, 179.2, 171.6, 146.7, 146.4, 138.7, 138.6, 131.9, 131.6, 130.2, 128.0, 127.7, 115.1, 114.9, 60.1, 54.5, 45.1, 43.6, 43.4, 41.2, 37.9, 37.6, 34.7, 31.7, 30.8, 30.3, 29.5, 28.3, 28.0, 26.2, 24.8, 23.0, 22.8, 22.5, 17.9, 17.8, 14.3, 13.6; HRMS (ESI): m/z calcd for $C_{38}H_{48}F_3N_2O_3$ $[M+H]^+$: 637.3612, found 637.3643.

4.1.64 (2S,4aS,6aS,6bR,8aR,13aS,13bR,15bR)-2,4a,6a,6b,9,9,13a-heptamethyl-14-oxo-10-(p-tolyl)-2,3,4,4a,5,6,6a,6b,7,8,8a,9,10,13,13a,13b,14,15b-octadecahydro-1H-chryse- no[1,2-f]indazole-2-carboxylic acid **(GA-64)**

Compound **GA-64** was synthesized in the same procedure as that of **GA-20** (yield 65%); pale yellow solid. ^{1}H NMR (500 MHz, CD_3OD) δ 7.28 (s, 1H), 7.26 – 7.21 (m,

4H), 5.70 (s, 1H), 3.69 (d, *J* = 15.4 Hz, 1H), 2.59 (d, *J* = 6.4 Hz, 1H), 2.44 – 2.38 (m, 3H), 2.23 (d, *J* = 13.5 Hz, 1H), 2.17 (d, *J* = 9.8 Hz, 1H), 2.14 – 2.02 (m, 2H), 1.99 – 1.79 (m, 4H), 1.64 (d, *J* = 13.6 Hz, 2H), 1.50 (d, *J* = 10.0 Hz, 2H), 1.40 (d, *J* = 4.2 Hz, 6H), 1.17 (s, 6H), 1.13 (s, 3H), 1.10 – 1.05 (m, 4H), 1.03 – 1.01 (m, 3H), 0.87 – 0.80 (m, 4H); ^{13}C NMR (125 MHz, CD_3OD) δ 200.6, 179.2, 171.6, 146.3, 139.5, 139.0, 137.7, 129.0 (2×C), 128.8 (2×C), 128.0, 114.3, 60.3, 54.3, 45.2, 43.6, 43.4, 41.2, 37.9, 37.6, 37.3, 34.6, 31.8, 31.7, 30.8, 29.5, 28.9, 28.3, 27.9, 26.4, 26.2, 22.8, 22.0, 20.6, 18.2, 17.8, 15.1; HRMS (ESI): m/z calcd for $C_{38}H_{51}N_2O_3$ $[M+H]^+$: 583.3894, found 583.3930.

4.1.65 (2S,4aS,6aS,6bR,8aR,13aS,13bR,15bR)-2,4a,6a,6b,9,9,13a-heptamethyl-14-oxo-10-(m-tolyl)-2,3,4,4a,5,6,6a,6b,7,8,8a,9,10,13,13a,13b,14,15b-octadecahydro-1H-chryseno[1,2-f]indazole-2-carboxylic acid **(GA-65)**

Compound **GA-65** was synthesized in the same procedure as that of **GA-20** (yield 60%); pale yellow solid. ^{1}H NMR (500 MHz, CD_3OD) δ 7.30 (d, *J* = 17.3 Hz, 3H), 7.16 (s, 2H), 5.71 (s, 1H), 3.70 (d, *J* = 15.4 Hz, 1H), 2.58 (s, 1H), 2.37 (s, 3H), 2.22 (d, *J* = 11.3 Hz, 1H), 2.15 (s, 3H), 2.05 (s, 1H), 1.97 – 1.85 (m, 3H), 1.71 (s, 1H), 1.65 – 1.53 (m, 3H), 1.50 (s, 2H), 1.41 – 1.38 (m, 4H), 1.16 (s, 6H), 1.12 (s, 3H), 1.07 (s, 4H), 1.02 (s, 3H), 0.83 (s, 4H); ^{13}C NMR (125 MHz, CD_3OD) δ 200.6, 179.3, 152.9, 146.6, 138.6, 138.1, 130.1, 129.7, 128.2, 128.1, 128.0, 126.2, 114.4, 60.3, 54.3, 45.2, 43.6, 43.4, 41.2, 37.8, 37.7, 37.3, 34.7, 31.8, 30.9, 29.5, 29.5, 29.1, 28.4, 28.2, 28.1, 26.4, 26.3, 23.0, 22.1, 18.2, 18.0, 15.3; HRMS (ESI): m/z calcd for $C_{38}H_{51}N_2O_3$ $[M+H]^+$: 583.3894, found 583.3919.

4.1.66 (2S,4aS,6aS,6bR,8aR,13aS,13bR,15bR)-2,4a,6a,6b,9,9,13a-heptamethyl-14-oxo-10-(o-tolyl)-2,3,4,4a,5,6,6a,6b,7,8,8a,9,10,13,13a,13b,14,15b-octadecahydro-1H-

chryseno[1,2-f]indazole-2-carboxylic acid **(GA-66)**

Compound **GA-66** was synthesized in the same procedure as that of **GA-20** (yield 55%); pale yellow solid. ^{1}H NMR (500 MHz, CD_3OD) δ 7.32 (ddd, J = 6.4, 11.7, 25.9 Hz, 5H), 5.71 (s, 1H), 3.70 (dd, J = 6.3, 15.3 Hz, 1H), 2.61 (s, 1H), 2.24 (d, J = 14.3 Hz, 1H), 2.16 (s, 2H), 2.06 (s, 1H), 1.99 – 1.91 (m, 3H), 1.91 – 1.83 (m, 3H), 1.73 (s, 1H), 1.68 – 1.44 (m, 5H), 1.43 – 1.37 (m, 5H), 1.19 – 1.15 (m, 9H), 1.13 – 1.10 (m, 3H), 1.04 (d, J = 13.1 Hz, 1H), 0.94 (d, J = 3.0 Hz, 2H), 0.84 (s, 5H); ^{13}C NMR (125 MHz, CD_3OD) δ 200.6, 179.3, 171.5, 145.9, 140.4, 138.1, 137.6, 130.6, 129.6, 129.3, 128.0, 125.7, 114.4, 60.2, 54.3, 45.2, 43.6, 43.4, 41.2, 37.9, 37.7, 37.4, 34.7, 34.5, 31.8, 30.9, 29.7, 29.5, 28.3, 28.0, 27.0, 26.4, 26.2, 22.9, 22.5, 19.9, 18.2, 17.9; HRMS (ESI): m/z calcd for $C_{38}H_{51}N_2O_3$ $[M+H]^+$: 583.3894, found 583.3907.

4.1.67 (2S,4aS,6aS,6bR,8aR,13aS,13bR,15bR)-2,4a,6a,6b,9,9,13a-heptamethyl-10-(4-(methy-lsulfonyl)phenyl)-14-oxo-2,3,4,4a,5,6,6a,6b,7,8,8a,9,10,13,13a,13b,14,15b-octadecahy-ro-1H-chryseno[1,2-f]indazole-2-carboxylic acid **(GA-67)**

Compound **GA-67** was synthesized in the same procedure as that of **GA-20** (yield 60%); yellow solid. ^{1}H NMR (500 MHz, CD_3OD) δ 8.06 (d, J = 8.5 Hz, 2H), 7.63 (d, J = 8.5 Hz, 2H), 7.36 (s, 1H), 5.71 (s, 1H), 3.72 (d, J = 15.5 Hz, 1H), 3.16 (s, 3H), 2.59 (s, 1H), 2.23 (dd, J = 3.4, 13.3 Hz, 1H), 2.19 – 2.12 (m, 2H), 2.07 (td, J = 4.3, 13.5 Hz, 1H), 1.98 – 1.82 (m, 3H), 1.77 – 1.69 (m, 1H), 1.67 – 1.57 (m, 2H), 1.52 (t, J = 11.9 Hz, 2H), 1.40 (d, J = 5.4 Hz, 4H), 1.36 – 1.30 (m, 2H), 1.17 (d, J = 6.5 Hz, 6H), 1.14 (s, 3H), 1.07 (s, 3H), 1.04 (s, 4H), 0.83 (s, 4H); ^{13}C NMR (125 MHz, CD_3OD) δ 200.5, 179.2, 171.6, 146.8, 146.6, 141.2, 139.2, 130.1 (2×C), 128.0, 128.0 (2×C), 115.2, 60.3, 54.2, 45.2, 43.8, 43.6, 43.4, 41.2, 37.8, 37.6, 37.3, 34.7, 31.8, 31.8, 30.9, 29.5, 29.4, 28.3, 28.1, 26.4, 26.2, 22.9, 22.6, 18.2, 17.9, 15.3; HRMS (ESI): m/z calcd for

$C_{38}H_{50}N_2O_5SNa$ $[M+Na]^+$: 669.3333, found 669.3354.

4.1.68 (2S,4aS,6aS,6bR,8aR,13aS,13bR,15bR)-2,4a,6a,6b,9,9,13a-heptamethyl-14-oxo-10-(4-sulfamoylphenyl)-2,3,4,4a,5,6,6a,6b,7,8,8a,9,10,13,13a,13b,14,15b-octadecahydro-1H-chryseno[1,2-f]indazole-2-carboxylic acid **(GA-68)**

Compound **GA-68** was synthesized in the same procedure as that of **GA-20** (yield 60%); yellow solid. ^{1}H NMR (500 MHz, CD_3OD) δ 7.99 (d, J = 8.3 Hz, 2H), 7.50 (d, J = 8.2 Hz, 3H), 7.42 (s, 1H), 7.34 (s, 1H), 5.71 (s, 1H), 3.71 (d, J = 15.6 Hz, 1H), 2.59 (d, J = 20.7 Hz, 1H), 2.22 (d, J = 13.4 Hz, 1H), 2.18 – 2.09 (m, 2H), 2.04 (s, 1H), 1.97 – 1.81 (m, 3H), 1.71 (s, 1H), 1.58 (d, J = 29.1 Hz, 3H), 1.51 (s, 2H), 1.39 (d, J = 4.7 Hz, 5H), 1.16 (s, 6H), 1.12 (s, 3H), 1.05 (d, J = 4.2 Hz, 3H), 1.02 (d, J = 3.8 Hz, 4H), 0.82 (s, 4H); ^{13}C NMR (125 MHz, CD_3OD) δ 200.5, 179.2, 171.6, 146.7, 144.8, 144.2, 138.8, 129.6 (2×C), 128.0, 126.6 (2×C), 115.0, 60.3, 54.2, 45.2, 43.6, 43.4, 41.2, 37.8, 37.6, 37.3, 34.7, 31.8, 30.9, 29.5, 29.2, 28.6, 28.3, 28.0, 26.4, 26.2, 22.9, 22.4, 18.2, 17.9, 15.3; HRMS (ESI): m/z calcd for $C_{37}H_{50}N_3O_5S$ $[M+H]^+$: 648.3466, found 648.3452.

4.2 Cell Culture

Murine macrophage-like RAW264.7 cells were kindly provided by Stem Cell Bank, Chinese Academy of Sciences. RAW264.7 cells were cultured in Dulbecco Modified Eagle Medium (DMEM, GBICO) supplemented with 10% fetal bovine serum and 1% penicillin/streptomycin at 37℃, 95% humidity, and 5% CO_2.

4.3 Animals

All animal experiments were performed in accordance with the National Institutes of

Health guidelines and approved by the Animal Care and Use Committee of the Second Military Medical University. Male C57BL/6J mice (6-8 weeks) were purchased from BiKai biochemistry Co. (Shanghai, China). Mice were maintained under appropriate temperature and humidity and an automated 12-hour dark-light cycle, and free access to standard dry diet and tap water.

4.4 Cell Cytotoxicity

Cell cytotoxicity was evaluated by cell counting kit-8 (CCK-8, Dojindo Laboratories). RAW264.7 cells were incubated in 96-well plates at a density of 10,000 cells per well. Each group consisted of three wells. All compounds were dissolved in dimethyl sulfoxide (DMSO, WAK-Chemie Medical GmbH, Steinbach, Germany) and diluted to a concentration of 300 μM, 100 μM, 30 μM, 10 μM, and 3 μM. After a day's incubation, GA derivates were treated afterward and cultured for another 24 h. After the incubation, l0 μL CCK-8 was added into 100 μL of culture media, and cells were incubated for 2 h. The 450 nm wave-length absorption values were measured on an EnSpire multimode plate reader (PerkinElmer, MA, USA). The IC50 values were calculated using SPSS 20.0.

4.5 Griess Assay

The production of NO in living cells was assayed and calculated using the NO assay kit (Beyotime Institute of Biotechnology, Shanghai, China). RAW264.7 cells were incubated in 96-well plates at a density of 50,000 cells per well. Each group consisted of two wells. All compounds were dissolved in DMSO and diluted to a concentration

of 30 μM, 10 μM, 3 μM, 1 μM, and 0.3 μM. After a day's incubation, LPS and GA derivates were treated afterward and cultured for another 24 h. The cell supernatant was then harvested and processed according to the NO assay kit instructions. The 540 nm wave-length absorption values were measured on an EnSpire multimode plate reader (PerkinElmer, MA, USA).

4.6 Measurement of supernatant TNF-α, IL-6 levels

RAW264.7 cells were incubated in 96-well plates at a density of 50,000 cells per well. Each group consisted of two wells. All compounds were dissolved in DMSO and diluted to a concentration of 30 μM, 10 μM, 3 μM, 1 μM, and 0.3 μM. After a day's incubation, LPS and GA derivates were treated afterward and cultured for another 24 h. The supernatant was collected and stored at -80℃ before use. LEGENDplex bead-based immunoassays (Biolegend, San Diego, CA) were used to analyze the cell supernatant TNF-α and IL-6 levels according to the manufacturer's instructions. Briefly, 25 μL of the standard, cell supernatant, and buffer solutions were added. To each well, 25 μL of mixed beads were added. Then, the plate was covered with a plate sealer and shook at 500 rpm for 2 hours at room temperature. After three washes, 25 μL of detection antibodies were added to each well. The plate was then covered with a plate sealer and shook at 500 rpm for another 1h at room temperature. After three washes, 25 μL of SP-FA was added to each well. The plate was then covered with a plate sealer and shook at 500 rpm for 0.5 h at room temperature. After three washes, the samples were tested on a flow cytometer. Data were calculated and collected using the

LEGENDplex data analysis software (Biolegend, San Diego, CA).

4.7 Annexin V–FITC Apoptosis

RAW264.7 cells were incubated at $1*10^6$ per well in 6 wells for 24 h. The media was aspirated, and each well refilled with different compounds (10 μM) in serum-free DMEM. After 2 h, 100 ng/mL LPS was treated and cultured for 24 h. Detection Kit (MultiSciences Biotech, Hangzhou, China) was used to carry out the measurements. Cell were trypsinized and washed twice with PBS. Then, cells were stained with annexin V-FITC and propidium iodide (PI) for 15 min in the dark at room temperature. The analysis was performed on BD FACS-Calibur flow cytometer (BD Biosciences).

4.8 Western Blot

RAW264.7 cells were harvested in NP-40 Lysis Buffer (Beyotime Institute of Biotechnology, Shanghai, China). And the preparation of nuclear and cytoplasmic proteins was conducted using a Nuclear and Cytoplasmic Protein Extraction Kit (Beyotime Institute of Biotechnology, Shanghai, China). Protein concentration was normalized with a BCA protein assay kit (Beyotime Institute of Biotechnology, Shanghai, China). Prepared protein samples were resolved on 8-12% SDS-PAGE gel and transferred to nitrocellulose (NC) membrane (Millipore, Bedford, MA, USA). After blocking, the membrane was incubated overnight at 4℃ with various primary antibodies, respectively. After washing with TBST, HRP-conjugated secondary antibodies were treated for one hour at room temperature. The bands were visualized and quantified with the Odyssey Infrared Imaging System (LI-COR Biotechnology,

Germany).

4.9 SPR biosensor analysis

Analysis of GA-60 binding to HMGB1 was conducted using a BIAcore T200 system (GE Healthcare, Sweden). Glycyrrhetinic acid (GA) was used as a positive control. HMGB1 diluted by 10mM sodium acetate buffer (pH 4.5) was immobilized by the amine coupling method on a CM5 sensor chip, giving a response unit of 5537.5 RU, according to the manufacturer's instructions. GA and GA-60 were diluted in phosphate buffer saline (PBS, Wisent Inc., Quebec, Canada) with 5% DMSO (WAK-Chemie Medical GmbH, Steinbach, Germany) running buffer at concentrations ranging from 0.5 μM to 128 μM with a duplicate middle concentration at the end of each running to confirm the stability of the sensor surface. GA and GA-60 were injected at a flow rate of 30 μL/min. The association and dissociation times were the 60 s and the 120 s. The affinity fitting was calculated using BIAcore T200 evaluation software by global fitting with the steady-state affinity model.

4.10 Sepsis model

Sepsis was induced by a single intraperitoneal injection (i.p.) injection of LPS (15 mg/kg) or CLP, as described previously[33]. All mice had free access to food and water after recovery from anesthesia. GA and GA-60 were dissolved in 5% anhydrous ethanol, 5% Kolliphor HS15 (HS15) and 90% PBS. Mice were treated with GA, GA-60, or vehicle for a dose of 10 mg/kg 12 h once by i.p. injection, starting from 30 min before LPS injection or CLP induction.

4.11 ELISA assay

The supernatant was collected as described above. Each group consisted of three wells. For the quantification of plasma TNF-α and HMGB1 level in LPS-induced C57BL/6 mice, plasma was collected 24 h after LPS stimulation. TNF-α and HMGB1 concentrations were measured using mouse TNF-α ELISA kits (eBioscience; Thermo Fisher Scientific Inc., USA) and mouse HMGB1 ELISA kits (Elab Science Biotechnology Co., Ltd) respectively according to the manufacturer's instructions. All experiments were independently performed at least three times.

4.15 Statistical analysis

SPSS software and GraphPad Prism software were used to examine statistical analysis. Data were presented as mean ± Standard Deviation (SD). One-way analysis of variance (ANOVA) was performed to analyze significant differences among multiple study groups. Survival analysis was performed using the Kaplan-Meier method. The p-value less than 0.05 was indicated as statistical significance.

Associated content

Supporting Information. Inhibition rate of released NO, TNF-α, and IL-6 upon treatment with all derivatives in rage of 0.3~30 μM; The full bolts of western blots analysis; Results of PAINS and False Positive Remover; Chemical structure, ^{1}H NMR, ^{13}C NMR, and HR-MS spectrum spectra of All GA Derivatives; SMILES molecular formula strings (CSV).

Acknowledgement

The work was supported by Professor of Chang Jiang Scholars Program, NSFC

(81520108030), Shanghai Engineering Research Center for the Preparation of Bioactive Natural Products (16DZ2280200), National Key Research and Development Program of China (2017YFC1700200), National Natural Science Foundation of China (No 81872880), State Key Laboratory of Innovative Natural Medicine and TCM Injections.

Abbreviations

Arg, arginine**; CLP,** cecal ligation and puncture; **CBX,** carbenoxolone; **Cys,** cysteine; **CCK-8**, cell counting kit-8; **DMSO,** dimethylsulfoxide; **ESI,** electron spray ionization**; ERK,** extracellular signal-regulated kinase; **eq.,** Equivalent **; ELISA,** enzyme linked immunosorbent assay; **GA,** glycyrrhetinic acid; **GL,** glycyrrhizic acid**; HMGB1,** high mobility group box protein 1; **HRMS,** high resolution mass spectrum**; IκB,** inhibitory κB (IκB) proteins; **IKKα/β,** IκB kinase α/β; **i.p.,** intraperitoneal injection; **IL-6**, Interleukin-6; **IL-1β**, Interleukin-1β; **JNK,** jun N-terminal kinase; **Kd,** dissociation constant; **LPS,** lipopolysaccharide; **MAPK,** mitogen-activated protein kinases**; NO**, nitric oxide; **NF-κB**, nuclear factor-κB; **NMR**, nuclear magnetic resonance; **PAINS,** pan-assay-interference-compounds; **PCC**, pyridinium chlorochromate; **p38,** p38 MAPK; **RAGE,** receptor for advanced glycation end products; **RU,** response units; **SPR,** surface plasmon resonance**; SAR,** structure-activity relationship; **Ser,** serine; **Tyr,** tyrosine; **THF,** Tetrahydrofuran**; TMS,** Tetramethyl silane**; TNF-α**, tumor necrosis factor-α. **TLR-4,** toll-like receptor-4.

References:

[1] M. Singer, C.S. Deutschman, C.W. Seymour, M. Shankar-Hari, D. Annane, M. Bauer, R. Bellomo, G.R. Bernard, J.-D. Chiche, C.M. Coopersmith, R.S. Hotchkiss,

M.M. Levy, J.C. Marshall, G.S. Martin, S.M. Opal, G.D. Rubenfeld, T.v.d. Poll, J.-L. Vincent, D.C. Angus, The Third International Consensus Definitions for Sepsis and Septic Shock (Sepsis-3), JAMA. 315 (2016) 801-810.

[2] K.E. Rudd, S.C. Johnson, K.M. Agesa, K.A. Shackelford, D. Tsoi, D.R. Kievlan, D.V. Colombara, K.S. Ikuta, N. Kissoon, S. Finfer, C. Fleischmann-Struzek, F.R. Machado, K.K. Reinhart, K. Rowan, C.W. Seymour, R.S. Watson, T.E. West, F. Marinho, S.I. Hay, R. Lozano, A.D. Lopez, D.C. Angus, C.J.L. Murray, M. Naghavi, Global, Regional, and National Sepsis Incidence and Mortality, 1990–2017: Analysis for the Global Burden of Disease Study, Lancet. 395 (2020) 200-211.

[3] A. Rhodes, L.E. Evans, W. Alhazzani, M.M. Levy, M. Antonelli, R. Ferrer, A. Kumar, J.E. Sevransky, C.L. Sprung, M.E. Nunnally, B. Rochwerg, G.D. Rubenfeld, D.C. Angus, D. Annane, R.J. Beale, G.J. Bellinghan, G.R. Bernard, J.D. Chiche, C. Coopersmith, D.P. De Backer, C.J. French, S. Fujishima, H. Gerlach, J.L. Hidalgo, S.M. Hollenberg, A.E. Jones, D.R. Karnad, R.M. Kleinpell, Y. Koh, T.C. Lisboa, F.R. Machado, J.J. Marini, J.C. Marshall, J.E. Mazuski, L.A. McIntyre, A.S. McLean, S. Mehta, R.P. Moreno, J. Myburgh, P. Navalesi, O. Nishida, T.M. Osborn, A. Perner, C.M. Plunkett, M. Ranieri, C.A. Schorr, M.A. Seckel, C.W. Seymour, L. Shieh, K.A. Shukri, S.Q. Simpson, M. Singer, B.T. Thompson, S.R. Townsend, T. Van der Poll, J.L. Vincent, W.J. Wiersinga, J.L. Zimmerman, R.P. Dellinger, Surviving Sepsis Campaign: International Guidelines for Management of Sepsis and Septic Shock: 2016, Crit. Care Med. 45 (2017) 486-552.

[4] J.-L. Vincent, G. Slotman, P.A.V. Leeuwen, M. Shelly, G. Friedman, Il-1ra

Administration Does Not Improve Cardiac Function in Patients with Severe Sepsis, J. Crit. Care. 14 (1999) 69-72.

[5] G.R. Bernard, B. Francois, J.-P. Mira, J.-L. Vincent, R.P. Dellinger, J.A. Russell, S.P. Larosa, P.-F. Laterre, M.M. Levy, W. Dankner, N. Schmitt, J. Lindemann, X. Wittebole, Evaluating the Efficacy and Safety of Two Doses of the Polyclonal Anti-Tumor Necrosis Factor-A Fragment Antibody Azd9773 in Adult Patients with Severe Sepsis and/or Septic Shock: Randomized, Double-Blind, Placebo-Controlled Phase Iib Study, Crit. Care Med. 42 (2014) 504-511.

[6] S.M. Opal, P.F. Laterre, B. Francois, S.P. LaRosa, D.C. Angus, J.P. Mira, X. Wittebole, T. Dugernier, D. Perrotin, M. Tidswell, L. Jauregui, K. Krell, J. Pachl, T. Takahashi, C. Peckelsen, E. Cordasco, C.S. Chang, S. Oeyen, N. Aikawa, T. Maruyama, R. Schein, A.C. Kalil, M. Van Nuffelen, M. Lynn, D.P. Rossignol, J. Gogate, M.B. Roberts, J.L. Wheeler, J.L. Vincent, A.S. Group, Effect of Eritoran, an Antagonist of Md2-Tlr4, on Mortality in Patients with Severe Sepsis: The Access Randomized Trial, JAMA. 309 (2013) 1154-1162.

[7] A. López, J.A. Lorente, J. Steingrub, J. Bakker, A. McLuckie, S. Willatts, M. Brockway, A. Anzueto, L. Holzapfel, D. Breen, M.S. Silverman, J. Takala, J. Donaldson, C. Arneson, G. Grove, S. Grossman, R. Grover, Multiple-Center, Randomized, Placebo-Controlled, Double-Blind Study of the Nitric Oxide Synthase Inhibitor 546c88: Effect on Survival in Patients with Septic Shock, Crit. Care Med. 32 (2004) 21-30.

[8] S.B. Hu, A. Zider, J.C. Deng, When Host Defense Goes Awry: Modeling Sepsis-

Induced Immunosuppression, Drug Discov. Today Dis. Models. 9 (2012) e33-e38.

[9] H. Wang, O. Bloom, M. Zhang, J.M. Vishnubhakat, M. Ombrellino, J. Che, A. Frazier, H. Yang, S. Ivanova, L. Borovikova, K.R. Manogue, E. Faist, E. Abraham, J. Andersson, U. Andersson, P.E. Molina, N.N. Abumrad, A. Sama, K.J. Tracey, Hmg-1 as a Late Mediator of Endotoxin Lethality in Mice, Science. 285 (1999) 248-251.

[10] K. Suda, Y. Kitagawa, S. Ozawa, Y. Saikawa, M. Ueda, M. Ebina, S. Yamada, S. Hashimoto, S. Fukata, E. Abraham, I. Maruyama, M. Kitajima, A. Ishizaka, Anti-High-Mobility Group Box Chromosomal Protein 1 Antibodies Improve Survival of Rats with Sepsis, World J. Surg. 30 (2006) 1755-1762.

[11] S. Gaïni, S.S. Pedersen, O.G. Koldkjær, C. Pedersen, H.J. Møller, High Mobility Group Box-1 Protein in Patients with Suspected Community-Acquired Infections and Sepsis: A Prospective Study, Crit. Care. 11 (2007) R32.

[12] J. Sunden-Cullberg, A. Norrby-Teglund, A. Rouhiainen, H. Rauvala, G. Herman, K.J. Tracey, M.L. Lee, J. Andersson, L. Tokics, C.J. Treutiger, Persistent Elevation of High Mobility Group Box-1 Protein (Hmgb1) in Patients with Severe Sepsis and Septic Shock, Crit. Care Med. 33 (2005) 564-573.

[13] S.I. Valdes-Ferrer, M. Rosas-Ballina, P.S. Olofsson, B. Lu, M.E. Dancho, M. Ochani, J.H. Li, J.A. Scheinerman, D.A. Katz, Y.A. Levine, L.K. Hudson, H. Yang, V.A. Pavlov, J. Roth, L. Blanc, D.J. Antoine, S.S. Chavan, U. Andersson, B. Diamond, K.J. Tracey, Hmgb1 Mediates Splenomegaly and Expansion of Splenic Cd11b+ Ly-6c(High) Inflammatory Monocytes in Murine Sepsis Survivors, J. Intern. Med. 274 (2013) 381-390.

[14] S.S. Chavan, P.T. Huerta, S. Robbiati, S.I. Valdes-Ferrer, M. Ochani, M. Dancho, M. Frankfurt, B.T. Volpe, K.J. Tracey, B. Diamond, Hmgb1 Mediates Cognitive Impairment in Sepsis Survivors, Mol. Med. 18 (2012) 930-937.

[15] U. Andersson, H. Wang, K. Palmblad, A.C. Aveberger, O. Bloom, H. Erlandsson-Harris, A. Janson, R. Kokkola, M. Zhang, H. Yang, K.J. Tracey, High Mobility Group 1 Protein (Hmg-1) Stimulates Proinflammatory Cytokine Synthesis in Human Monocytes, J. Exp. Med. 192 (2000) 565-570.

[16] J.-S. Bae, Role of High Mobility Group Box 1 in Inflammatory Disease: Focus on Sepsis, Arch. Pharm. Res. 35 (2012) 1511-1523.

[17] N.E. Stevens, M.J. Chapman, C.K. Fraser, T.R. Kuchel, J.D. Hayball, K.R. Diener, Therapeutic Targeting of Hmgb1 During Experimental Sepsis Modulates the Inflammatory Cytokine Profile to One Associated with Improved Clinical Outcomes, Sci. Rep. 7 (2017) 5850.

[18] S. Qin, H. Wang, R. Yuan, H. Li, M. Ochani, K. Ochani, M. Rosas-Ballina, C.J. Czura, J.M. Huston, E. Miller, X. Lin, B. Sherry, A. Kumar, G. Larosa, W. Newman, K.J. Tracey, H. Yang, Role of Hmgb1 in Apoptosis-Mediated Sepsis Lethality, J. Exp. Med. 203 (2006) 1637-1642.

[19] S. Gibot, F. Massin, A. Cravoisy, D. Barraud, L. Nace, B. Levy, P.-E. Bollaert, High-Mobility Group Box 1 Protein Plasma Concentrations During Septic Shock, Intensive Care Med. 33 (2007) 1347-1353.

[20] D.J. Newman, G.M. Cragg, K.M. Snader, The Influence of Natural Products Upon Drug Discovery, Nat. Prod. Rep. 17 (2000) 215-234.

[21] D.J. Newman, G.M. Cragg, Natural Products as Sources of New Drugs over the 30 Years from 1981 to 2010, J. Nat. Prod. 75 (2012) 311-335.

[22] D.J. Newman, G.M. Cragg, Natural Products as Sources of New Drugs over the Last 25 Years, J. Nat. Prod. 70 (2007) 461-477.

[23] D.J. Newman, G.M. Cragg, K.M. Snader, Natural Products as Sources of New Drugs over the Period 1981-2002, J. Nat. Prod. 66 (2003) 1022-1037.

[24] J.Y. Li, H.Y. Cao, P. Liu, G.H. Cheng, M.Y. Sun, Glycyrrhizic Acid in the Treatment of Liver Diseases: Literature Review, Biomed Res Int. 2014 (2014) 872139.

[25] L. Mollica, F. De Marchis, A. Spitaleri, C. Dallacosta, D. Pennacchini, M. Zamai, A. Agresti, L. Trisciuoglio, G. Musco, M.E. Bianchi, Glycyrrhizin Binds to High-Mobility Group Box 1 Protein and Inhibits Its Cytokine Activities, Chem. Biol. 14 (2007) 431-441.

[26] L. Cavone, M. Muzzi, R. Mencucci, B. Sparatore, M. Pedrazzi, F. Moroni, A. Chiarugi, 18β-Glycyrrhetic Acid Inhibits Immune Activation Triggered by Hmgb1, a Pro-Inflammatory Protein Found in the Tear Fluid During Conjunctivitis and Blepharitis, Ocul. Immunol. Inflamm. 19 (2011) 180-185.

[27] H. Yamaguchi, Y. Kidachi, K. Kamiie, T. Noshita, H. Umetsu, Structural Insight into the Ligand-Receptor Interaction between Glycyrrhetinic Acid (Ga) and the High-Mobility Group Protein B1 (Hmgb1)-DNA Complex, Bioinformation. 8 (2012) 1147-1153.

[28] D. Du, J. Yan, J. Ren, H. Lv, Y. Li, S. Xu, Y. Wang, S. Ma, J. Qu, W. Tang, Z. Hu, S. Yu, Synthesis, Biological Evaluation, and Molecular Modeling of

Glycyrrhizin Derivatives as Potent High-Mobility Group Box-1 Inhibitors with Anti-Heart-Failure Activity in Vivo, J. Med. Chem. 56 (2013) 97-108.

[29] B. Meka, S.R. Ravada, M.M.K. Kumar, K.P. Nagasree, T. Golakoti, Synthesis of New Analogs of Akba and Evaluation of Their Anti-Inflammatory Activities, Bioorg. Med. Chem. 25 (2017) 1374-1388.

[30] G.S. Subba Rao, P. Kondaiah, S.K. Singh, P. Ravanan, M.B. Sporn, Chemical Modifications of Natural Triterpenes - Glycyrrhetinic and Boswellic Acids: Evaluation of Their Biological Activity, Tetrahedron. 64 (2008) 11541-11548.

[31] E. Cario, I.M. Rosenberg, S.L. Brandwein, P.L. Beck, H.C. Reinecker, D.K. Podolsky, Lipopolysaccharide Activates Distinct Signaling Pathways in Intestinal Epithelial Cell Lines Expressing Toll-Like Receptors, J. Immunol. 164 (2000) 966-972.

[32] F. Zhao, Y. Fang, S. Deng, X. Li, Y. Zhou, Y. Gong, H. Zhu, W. Wang, Glycyrrhizin Protects Rats from Sepsis by Blocking Hmgb1 Signaling, Biomed Res Int. 2017 (2017) 9719647.

[33] D. Rittirsch, M.S. Huber-Lang, M.A. Flierl, P.A. Ward, Immunodesign of Experimental Sepsis by Cecal Ligation and Puncture, Nat. Protoc. 4 (2009) 31-36.

[34] R. Kang, R. Chen, Q. Zhang, W. Hou, S. Wu, L. Cao, J. Huang, Y. Yu, X.G. Fan, Z. Yan, X. Sun, H. Wang, Q. Wang, A. Tsung, T.R. Billiar, H.J. Zeh, M.T. Lotze, D. Tang, Hmgb1 in Health and Disease, Mol. Aspects Med. 40 (2014) 1-116.

[35] U. Andersson, K.J. Tracey, Hmgb1 Is a Therapeutic Target for Sterile Inflammation and Infection, Annu. Rev. Immunol. 29 (2011) 139-162.

[36] M. Guha, N. Mackman, Lps Induction of Gene Expression in Human

Monocytes, Cell. Signal. 13 (2001) 85-94.

[37] M.T. Lotze, K.J. Tracey, High-Mobility Group Box 1 Protein (Hmgb1): Nuclear Weapon in the Immune Arsenal, Nat. Rev. Immunol. 5 (2005) 331-342.

[38] Y.H. Qin, S.M. Dai, G.S. Tang, J. Zhang, D. Ren, Z.W. Wang, Q. Shen, Hmgb1 Enhances the Proinflammatory Activity of Lipopolysaccharide by Promoting the Phosphorylation of Mapk P38 through Receptor for Advanced Glycation End Products, J. Immunol. 183 (2009) 6244-6250.

[39] Y. Liu, E.G. Shepherd, L.D. Nelin, Mapk Phosphatases--Regulating the Immune Response, Nat. Rev. Immunol. 7 (2007) 202-212.

[40] S. Akira, K. Takeda, Toll-Like Receptor Signalling, Nat. Rev. Immunol. 4 (2004) 499-511.

[41] T. Kawai, S. Akira, Signaling to Nf-Kappab by Toll-Like Receptors, Trends Mol. Med. 13 (2007) 460-469.

[42] P.A. Baeuerle, T. Henkel, Function and Activation of Nf-Kappa B in the Immune System, Annu. Rev. Immunol. 12 (1994) 141-179.

[43] J.R. van Beijnum, W.A. Buurman, A.W. Griffioen, Convergence and Amplification of Toll-Like Receptor (Tlr) and Receptor for Advanced Glycation End Products (Rage) Signaling Pathways Via High Mobility Group B1 (Hmgb1), Angiogenesis. 11 (2008) 91-99.

[44] C.X. Wu, L.X. He, H. Guo, X.X. Tian, Q. Liu, H. Sun, Inhibition Effect of Glycyrrhizin in Lipopolysaccharide-Induced High-Mobility Group Box 1 Releasing and Expression from Raw264.7 Cells, Shock. 43 (2015) 412-421.

[45] E. Venereau, F.D. Leo, R. Mezzapelle, G. Careccia, G. Musco, M.E. Bianchi, Hmgb1 as Biomarker and Drug Target, Pharmacol. Res. 111 (2016) 534-544.

[46] S. VanPatten, Y. Al-Abed, High Mobility Group Box-1 (Hmgb1): Current Wisdom and Advancement as a Potential Drug Target, J. Med. Chem. 61 (2018) 5093-5107.

[47] J.L. Dahlin, J. Inglese, M.A. Walters, Mitigating Risk in Academic Preclinical Drug Discovery, Nature Reviews Drug Discovery. 14 (2015) 279-294.

[48] S.C. Chun, S.Y. Jee, S.G. Lee, S.J. Park, J.R. Lee, S.C. Kim, Anti-Inflammatory Activity of the Methanol Extract of Moutan Cortex in Lps-Activated Raw264.7 Cells, Evid. Based Complement. Alternat. Med. 4 (2007) 327-333.

[49] D. Yang, J. Lin, Y. Chen, S. Liu, F. Lu, T. Chang, M. Wang, H. Lin, Y. Chang, Suppressive Effect of Carotenoid Extract of Dunaliella Salina Alga on Production of Lps-Stimulated Pro-Inflammatory Mediators in Raw264.7 Cells Via Nf-Kb and Jnk Inactivation, J. Funct. Foods. 5 (2013) 607-615.

[50] C.L. Lu, Y.F. Zhu, M.M. Hu, D.M. Wang, X.J. Xu, C.J. Lu, W. Zhu, Optimization of Astilbin Extraction from the Rhizome of Smilax Glabra, and Evaluation of Its Anti-Inflammatory Effect and Probable Underlying Mechanism in Lipopolysaccharide-Induced Raw264.7 Macrophages, Molecules. 20 (2015) 625-644.

Highlights:

1. Novel Glycyrrhetinic Acid (GA) derivatives with fused heterocycles on A ring were structure-based designed and synthesized.

2. Candidate compound GA-60 could bind to HMGB1.

3. Candidate compound GA-60 extended survival in LPS/CLP induced mouse models of sepsis.

4. Candidate compound GA-60 exhibited excellent inhibitory functions on NO, TNF-α, and IL-6.

5. Candidate compound GA-60 could interfere with phosphorylation of p38, ERK, JNK MAPKs, as well as that of NF-κB p65 and IKKα/β.

Declaration of interests

☒ The authors declare that they have no known competing financial interests or personal relationships that could have appeared to influence the work reported in this paper.

☐The authors declare the following financial interests/personal relationships which may be considered as potential competing interests:

Highlights:

1. Novel Glycyrrhetinic Acid (GA) derivatives with fused heterocycles on A ring were structure-based designed and synthesized.

2. Candidate compound GA-60 could bind to HMGB1.

3. Candidate compound GA-60 extended survival in LPS/CLP induced mouse models of sepsis.

4. Candidate compound GA-60 exhibited excellent inhibitory functions on NO, TNF-α, and IL-6.

5. Candidate compound GA-60 could interfere with phosphorylation of p38, ERK, JNK MAPKs, as well as that of NF-κB p65 and IKKα/β.